Diagnostic Radiology of the Rheumatic Diseases

Interpreting Musculoskeletal Radiographs, Ultrasound, and MRI

Robert S. Katz
Anupam Basu
Editors

Springer

Diagnostic Radiology of the Rheumatic Diseases

Robert S. Katz • Anupam Basu
Editors

Diagnostic Radiology of the Rheumatic Diseases

Interpreting Musculoskeletal Radiographs, Ultrasound, and MRI

Springer

Editors
Robert S. Katz
Rush University Medical Center
Section of Rheumatology
Department of Internal Medicine
Chicago, IL
USA

Anupam Basu
Cook County Health
Department of Radiology
Chicago, IL
USA

ISBN 978-3-030-25115-4 ISBN 978-3-030-25116-1 (eBook)
https://doi.org/10.1007/978-3-030-25116-1

This Springer imprint is published by the registered company Springer Nature Switzerland AG
The registered company address is: Gewerbestrasse 11, 6330 Cham, Switzerland

"The practice of medicine is an art, not a trade; a calling, not a business; a calling in which your heart will be exercised equally with your head."

Sir William Osler

We dedicate this book to our mentors, Dr. Mary Betty Stevens and Dr. Lawrence Shulman, at Johns Hopkins Hospital and to the previous coauthors of this book, Dr. Jerry Petasnick and Dr. Lawrence Layfer, from Rush Medical College. Their teaching, compassion, and wisdom serve as an inspiration.

I'd also like to dedicate this book to my family.

Preface

We designed this book primarily for non-radiologists who want to understand how to approach and read musculoskeletal X-rays, ultrasounds, and MRIs. It is an introductory book.

It is written as an approach to radiology of the musculoskeletal diseases for medical students, house staff, fellows, and doctors in different specialties. We hope you find it helpful.

We have seen enormous strides and advances in radiology, not only newer technologies such as MRI, ultrasound for musculoskeletal diseases, and CT scans but also telemedicine and teleradiology where images are put on computer and sent anywhere.

Concomitantly, there have been tremendous advances in the treatment of rheumatic diseases, especially inflammatory arthritis. New and older biologic modifiers are used to reduce inflammation significantly and protect against joint damage.

There have been very significant advances since our last edition, and so we wanted to update it.

We hope this is accessible to those wanting to understand musculoskeletal radiology and how to approach it.

Contents

Contributors

Anupam Basu Cook County Health, Department of Radiology, Chicago, IL, USA

Sobia Hassan Department of Rheumatology, Rush University Medical Center, Chicago, IL, USA

Robert S. Katz Rush University Medical Center, Section of Rheumatology, Department of Internal Medicine, Chicago, IL, USA

Mehmet Kocak Department of Radiology & Nuclear Medicine, Rush University Medical Center, Chicago, IL, USA

Merve Ozen Department of Radiology & Nuclear Medicine, Rush University Medical Center, Chicago, IL, USA

Ben Small Northwestern Memorial Hospital, Section of Rheumatology, Department of Medicine, Chicago, IL, USA

Chapter 1
Radiographic Approach to Arthropathy

Anupam Basu

Radiographs remain the initial and often only imaging method in diagnosis and management of musculoskeletal diseases, using techniques that have changed only minimally since Wilhelm Conrad Roentgen obtained a radiograph of his wife's hand in 1895. Other imaging modalities, particularly ultrasound and magnetic resonance imaging (MRI) have enhanced our understanding of pathogenesis, diagnosis, and management of joint diseases. Nonetheless, radiographic analysis of the hands in rheumatologic diseases remains a central pillar in evaluation of patients with joint pain and/or dysfunction, particularly inflammatory arthropathies.

Radiographs are relatively inexpensive, readily available, provide excellent spatial resolution, and allow rapid assessment of multiple joints. As with all image interpretation, evaluation of radiographs in the setting of arthropathies should be approached in a systematic fashion to ensure that subtle abnormalities are not overlooked in favor of more obvious changes. The approach can be divided into the following four basic categories: joint surface and bone contour changes, bone density, abnormalities in osseous alignment, and soft tissue changes. Radiographs of the hands are generally considered the most fundamental and informative part of imaging in the setting of arthritis. We will use the hand to outline our recommended approach for assessing suspected joint disease. Figure 1.1 is a normal radiograph of the hand. We will begin by demonstrating some of the important changes in the hands using the framework of the four basic categories.

A. Basu (✉)
Cook County Health, Department of Radiology, Chicago, IL, USA
e-mail: abasu@cookcountyhhs.org

R. S. Katz, A. Basu (eds.), *Diagnostic Radiology of the Rheumatic Diseases*,
https://doi.org/10.1007/978-3-030-25116-1_1

Fig. 1.1 Normal AP hand radiograph

Articular Surface and Bone Contour Abnormalities

Pathologic changes centered at the joint, including joint space narrowing and erosive changes, are a common feature of most arthropathies and therefore, a good place to begin. The joint space represents radiolucent cartilage, and narrowing of this space implies some level of concomitant cartilage destruction. Joint space assessment typically is descriptive in clinical practice in contrast to assessment in clinical trials, in which formal scoring systems, such as the Larson, Sharp, and Sharp modified van der Heijdes methods are used to assess radiographic progression and possible treatment response. As a general rule of thumb, inflammatory arthropathies cause uniform joint space narrowing, whereas degenerative arthropathies will typically result in asymmetric joint space narrowing.

The joint spaces in the hand should be compared to the neighboring joint using a horizontal scanning pattern. Rheumatoid arthritis is well known for appearing symmetric and bilateral (Fig. 1.2), whereas degenerative and crystalline arthropathies typically manifest in an asymmetric joint involvement (Fig. 1.3).

The end-stage manifestation of cartilage and joint space narrowing is osseous bridging or "ankylosis." The presence of bony ankylosis may indicate an aggressive inflammatory arthropathy, most commonly seen in psoriatic arthritis and juvenile idiopathic arthritis in the peripheral joints, and seen in ankylosing spondylitis in the spine. Bony ankylosis is occasionally seen in rheumatoid arthritis, but is seen in neither primary osteoarthritis nor crystalline arthropathies.

Fig. 1.2 PA view of both hands demonstrates asymmetric joint space narrowing and marginal osteophyte formation (arrows) in this former basketball player

Fig. 1.3 Posteroanterior view of both hands demonstrates symmetric narrowing of the radiocarpal joints bilaterally with relative sparing of the remaining joint spaces

The contours of the bone may also provide important clues. While assessing bony contour, assess for the presence, morphology, and location of erosions. Active inflammatory arthropathy typically results in erosions which are absent of sclerotic borders. Erosions occur in up to 80% of patients with rheumatoid arthritis, up to 70% within the first 2 years in the natural history of disease. An early erosion will appear as focal discontinuity of the subchondral bone. Early inflammatory erosions occur in the juxta-articular or marginal region, as this area is relatively devoid of overlying hyaline cartilage, therefore making the cortex prone to destructive changes associated with active synovitis. Active inflammatory arthropathy typically results in erosions which are absent of sclerotic borders, often within 6–12 months of onset of the disease. An erosion with a sclerotic border, often described as an indolent erosion, may indicate an inflammatory or infectious arthropathy in remission. An erosion with corticated margins can represent a manifestation of gout. A gouty tophus may result in adjacent periosteal elevation. This periosteal elevation may result in bone formation, resulting in a hallmark "over-hanging edge" which is nearly pathognomonic for gout (Fig. 1.4).

Fig. 1.4 AP radiograph of the distal hand demonstrates numerous randomly distributed areas of erosive changes (arrow heads). These erosions demonstrate sclerotic borders. Adjacent soft tissue swelling (arrows) is also evident

Fig. 1.5 AP view of the hand demonstrates periostitis arising from the distal shafts of the second and fourth proximal phalanges

Additional osseous contour abnormalities should also be assessed, for example the presence of periosteal new bone formation or the presence of osteophytes. In psoriatic arthritis or reactive arthritis, periosteal new bone is deposited along the shaft of the phalanx or in the metaphysis in close proximity to an erosion (Fig. 1.5), resulting in "fluffy periostitis." It is an important radiographic feature, which can distinguish rheumatoid arthritis from seronegative spondyloarthropathies.

The presence of osteophytes, which are bone extensions from a normal articular surface, also indicates the presence of a reparative response, characteristic of osteoarthritis. Reparative changes can also manifest as subcortical cystic changes. Subcortical cysts can occur in virtually all arthropathies, therefore is often not beneficial in differentiating between them. A preponderance of subcortical cystic changes can indicate the diagnosis of calcium pyrophosphate dihydrate crystal deposition disease (CPPD), although large subcortical cysts can also be seen in rheumatoid arthritis or pigmented villondular synovitis (PVNS).

When articular surface or bony contour changes are identified, it is beneficial to compare the findings with prior radiographs. The time course of radiographic changes can provide important clues to the nature of the process. Radiographic manifestations of an infectious or neuropathic arthropathy can progress over a few weeks, inflammatory arthropathy can occur in several months, whereas a degenerative or crystalline-induced process such as gout may take several years to manifest.

Abnormalities in Bone Mineral Density

Bone density is another important variable in initial radiographic evaluation. Osteopenia is a nonspecific but early radiographic change of active inflammatory disease. Radiographs can detect early osteopenia which neither ultrasound nor MRI can visualize. In evaluation of the hand, overall mineralization can be made more objectively by assessing the relative ratio of the cortex compared to the overall width of the shaft. The sum of the two cortices of the shaft should equal at least one half the width of the overall shaft in a normally mineralized digit. Age-related osteoporosis is the most common cause of diffuse loss of bone mineral density. It can also be seen as a sequela of steroid therapy, renal failure of infiltrative marrow process. Juxta-articular demineralization can be a sign of an underlying inflammatory arthropathy, though has no objective criteria, and is therefore prone to high inter-observer variability (Fig. 1.6).

Focal osteoporosis may indicate active inflammation which leads to hyperemia and focal decrease in calcium, often indicative of septic arthritis when involving a single joint. Conversely, there may also be areas of increased bone mineral density, either in a focal or diffuse distribution. Increased mineralization in the subchondral areas, often referred to a subchondral sclerosis is a reparative response often seen in the setting of osteoarthritis. Central areas of increased density can be seen in the setting of metastatic disease, Paget's disease, bone infarcts (Fig. 1.7), or multiple bone islands, known as osteopoikilosis.

Fig. 1.6 AP views of both hands demonstrate diffuse periarticular osteopenia

Fig. 1.7 AP view of the hand demonstrates patchy sclerosis within the third and fourth phalanges (arrows)

Abnormalities in Osseous Alignment

Malalignment in the setting of joint disease indicates joint damage often as a result of untreated or poorly controlled inflammatory activity. It is an imaging and clinical hallmark of inflammatory arthropathies, particularly rheumatoid arthritis. Defects in bony alignment occur as a result of chronic synovitis and complex biomechanical forces from the supporting tendons and ligaments which are exacerbated by the patient's attempts to avoid pain by keeping the joint in the least painful position. The pattern of deformity may be specific for a particular disease and the severity of the may also give clues to the extent of the process. The common deformities are illustrated in Figs. 1.8, 1.9, and 1.10.

Soft Tissue Changes

The surrounding soft tissues can provide important clues as to the presence of the type of underlying joint disease. Diffuse swelling of a digit is most commonly seen in the setting of psoriatic or reactive arthritis, referred to as a "sausage digit". The term sausage digit refers to the clinical and radiological appearance of diffuse fusiform swelling of a digit due to soft tissue inflammation from underlying arthritis. Symmetrical soft tissue swelling around a specific joint is a manifestation of synovitis that accompanies inflammatory arthropathies. This may be the earliest radiographic manifestation of an inflammatory arthropathy and should prompt a closer examination of the bony contours around that joint. Asymmetrical soft tissue swelling around a joint, in contrast, is a less specific finding. It may be a manifestation of localized soft tissue masses, such as rheumatoid nodules or gouty tophi (Fig. 1.11).

Fig. 1.8 AP view of the hand demonstrates prominent ulnar deviations centered at the second and third MCP

Fig. 1.9 Lateral view of the hand depicts swan neck deformity- characterized by DIP flexion (arrows) and PIP hyperextension

Fig. 1.10 Hitchhiker's thumb depicts flexion of the metacarpophalangeal joint and extension of the interphalangeal joint of the thumb

Fig. 1.11 Numerous prominent focal areas of periarticular soft tissue swelling demarcating areas of gouty tophi

Fig. 1.12 Prominent coarse calcifications surrounding within the soft tissues of several digits most notably surrounding the first and third phlanges. In addition, there are distal erosive changes of the 2nd–fourth distal phlanges, described as distal acro-osteolysis

Alternatively, it may be due to the presence of an osteophyte or suggest the presence of a focal subluxation, such as in the setting of lupus. Loss of soft tissues is an important observation. Note the combination of loss of distal soft tissue, known as acro-osteolysis and the randomly distributed deposits of dense calcium within the soft tissues. This is a common manifestation of scleroderma. Calcium deposits are commonly seen in the soft tissues of patients with scleroderma (Fig. 1.12) or CREST syndrome but may also be seen in patients with acute bursitis, or dermatomyositis.

The presence of soft tissue calcifications and their distribution also help narrow the differential diagnosis. The presence of calcifications in hyaline and fibrous cartilage, as shown in Fig. 1.13, in the triangular fibrocartilage of the wrist is an important observation.

When seen in multiple distinct joints, for example in the wrist and knee, the diagnosis of calcium pyrophosphate deposition disease (CPPD) can be made. Vascular calcifications are often seen in the hands and feet in patients with long-standing diabetes or renal failure (Fig. 1.14).

Once these observations are made, one can use the following framework to help determine which category the imaging findings most favor (Fig. 1.15).

Fig. 1.13 AP radiograph of the wrist demonstrates amorphous calcifications (white arrow) in the expected region of the triangular fibrocartilage complex (TFCC)

Fig. 1.14 AP view of the hand demonstrates extensive stippled linear calcifications within the soft tissues of the digits consistent with vascular calcifications)

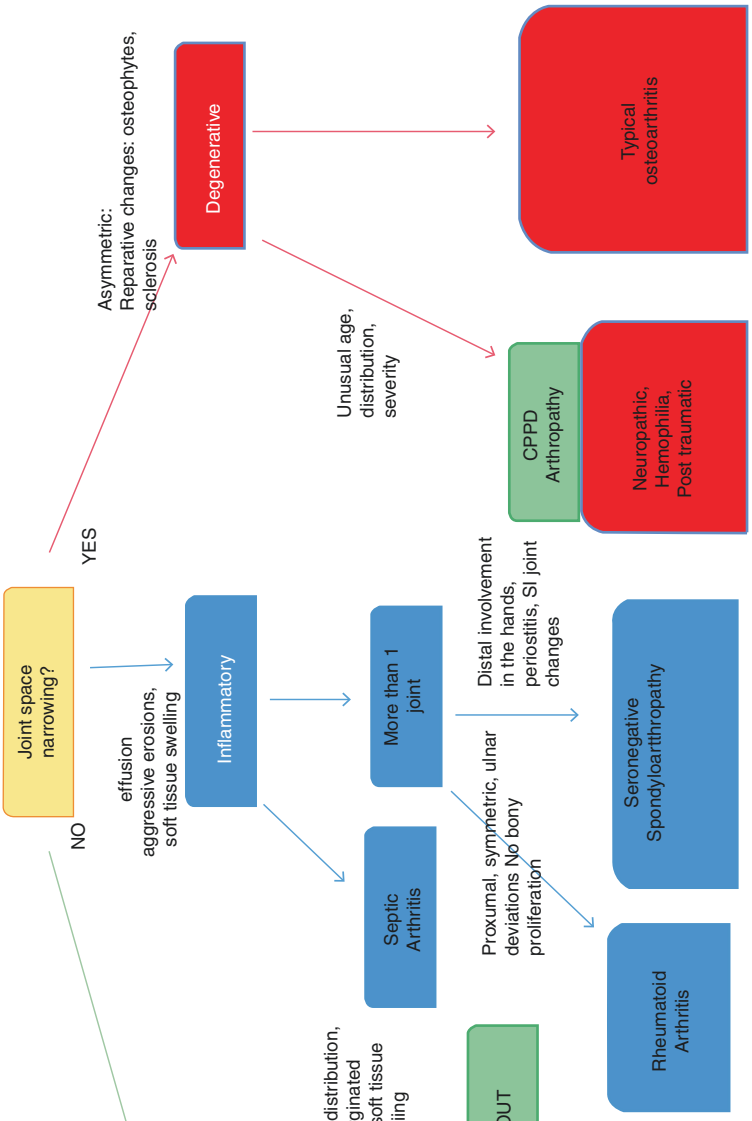

Fig. 1.15 A basic roadmap to differentiate the most common arthropathies encountered in clinical practice. The colors subcategorize the most common arthritides into inflammatory (blue), degenerative (red), and crystalline (green). This is not an exhaustive guide but can serve as a framework for approaching radiographs of patients with suspected joint disease

Further Reading

Brower AC, Flemming DJ. Arthritis in black and white. 3rd ed. Philadelphia: Saunders; 2012. p. 226–30.
Campion EW, Glynn RJ, DeLabry LO. Asymptomatic hyperuricemia: risks and consequences in the Normative Aging Study. Am J Med. 1987;82:421–6.
Huang M, Schweitzer ME. The role of radiology in the evolution of the understanding of articular disease. Radiology. 2014;273(2):S1–S22.
Jacobsen JA, Girish G, Jiang Y, et al. Radiographic evaluation of arthritis: inflammatory conditions. Radiology. 2008;248(2):378–89.
Klippel JH, Crofford LJ, Stone JH, Weyand CM. Primer on rheumatologic diseases. 12th ed. Atlanta: Arthritis Foundation; 2001. p. 307–19.
Layfer L, Petasnick J, Katz RS. Advanced exercises in diagnostic radiology: rheumatologic disorders. Philadelphia: Saunders; 1988. p. 3–48.
Manaster BJ, et al. Diagnostic imaging; musculoskeletal non-traumatic disease. 2nd ed. Philadelphia: Amirsys; 2016.
O'Neill J. Essential imaging in rheumatology. New York: Springer; 2015.
Resnick D, Kransdorf MJ. Bone and joint imaging. 3rd ed. Philadelphia: Elsevier Saunders; 2005. p. 531–7.
Schumacher HR. The pathogenesis of gout. Cleve Clin J Med. 2008;75(5):S2–4.

Chapter 2
Advanced Imaging Modalities

Anupam Basu and Sobia Hassan

Basics of MR Image Acquisition

Magnetic resonance imaging (MRI) uses a magnet measured in Tesla (T) to view the composition of various tissues. A key advantage of MRI over CT is the absence of ionizing energy, which can have cumulative long-term deleterious effects to the body. Clinical magnets typically range from 1.5 to 3 T, thousands of times stronger than the earth's magnetic field. The key to MRI is its excellent soft tissue contrast, which is the ability to discern tissue of one composition, apart from adjacent tissue, for example muscle and fat, fat and fluid, or fluid and bone (Fig. 2.1).

While these tissues vary in their fundamental molecular composition, the main difference that MR measures are subtle differences in the hydrogen atoms associated with the water and fat molecules present throughout the body. Each type of soft tissue results in unique MR "signatures." Radiofrequency energy is also used to help create the MR image. Radiofrequency (RF) is a type of energy, similar to light, sound. The main targets of signals emitted from this radiofrequency energy are the hydrogen atoms which each have tiny magnetic fields associated with the protons in their nuclei. The hydrogen proton normally is spinning around its own axis, similar to the Earth. When initially placed in the main magnetic field, the protons behave like mini-magnets and align themselves with the magnetic field in a low energy, "baseline" state. The homogeneity of these protons within the baseline state is an important characteristic and differentiator between unique tissue compositions. Specialized RF coils associated with the main magnet are responsible for either transmitting RF pulses or receiving the signal, known as the echo, given off by these altered protons. The radiofrequency pulse is sent at a

A. Basu (✉)
Cook County Health, Department of Radiology, Chicago, IL, USA
e-mail: abasu@cookcountyhhs.org

S. Hassan
Department of Rheumatology, Rush University Medical Center, Chicago, IL, USA
e-mail: Sobia_hassan@rush.edu

R. S. Katz, A. Basu (eds.), *Diagnostic Radiology of the Rheumatic Diseases*,
https://doi.org/10.1007/978-3-030-25116-1_2

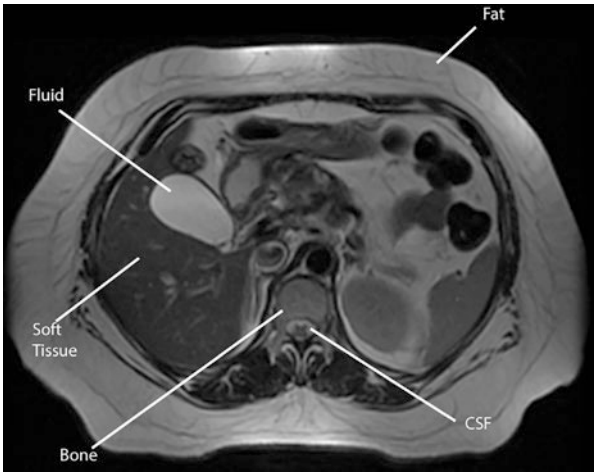

Fig. 2.1 This axial t2-weighted MRI through the upper abdomen depicts various normal structures labeled

particular frequency that changes the orientation of the protons. When the RF pulse is turned off, the spinning nuclei release energy as they return to their baseline state. The longer the pulse is active, the more energy it imparts. The subtle differences in the spin rate and variations as the protons return to their baseline state can be tracked, measured, and mapped using a complex mathematic model in three dimensions to create a two-dimensional image on a gray scale, a process known as Fourier transform.

What is often confusing to those who are not familiar with the detailed interpretation of MRI is identifying T1- and T2-weighted images. While a detailed discussion of the physics associated with image acquisition is beyond the scope of this discussion, one key to understanding the differences in scanning parameters is understanding repetition time (TR) and echo time (TE), typically measured in milliseconds. TR is the amount of time between two successive RF pulses acquired to the same slice of tissue. A TR time of less than 500 msec is considered short, a TR time of greater than 1500 msec is considered long. TE is the time between delivery of the RF pulse and the receipt of the echo signal. A TE time of less than 30 msec is considered to be short and that of greater than 80 msec is considered to be long. A T1-weighted image features a short TR, whereas a T2-weighted image features a long TE. Tissues that have a short T1 will be bright. Tissues that have a long T2 will be bright. Water is T1-dark and T2-bright. In general, liquids have a long T1 and long T2.

When getting oriented on an image and deciding if the image is T1- or T2-weighted, it is often of benefit to seek out fluid-filled structures such as cerebrospinal fluid, or fluid in the bladder, which will appear bright on a T2-weighted image, and dark on T1. Only a few structures are bright on T1-weighted images, primarily fat, blood products, and proteinaceous fluid. IV contrast can result in alterations in specific tissues which can be important. Gadolinium is the most common intravenous contrast agent used in clinical MRI. Gadolinium will shorten the T1 relaxation times of hydrogen atoms which results in brighter signal on T1-weighted images, described as enhancement.

Another key concept in musculoskeletal MR imaging is fat suppression. Suppression cancels out the signal of a particular tissue, most often fat, causing that tissue to appear dark on the image. Fat suppression is essential for evaluation of tissues in the context of joint disease.

Fig. 2.2 Ball catchers view of both hands in a 43-year-old male with diffuse joint pain demonstrating subtle erosive changes at the piso-triquetral joint on the right side (arrow)

MR imaging is a valuable and commonly used imaging modality for musculoskeletal imaging and has been well established as an effective method for early detection of the findings associated with rheumatologic conditions, particularly due to its sensitivity to alterations in marrow signal. The advantages of MRI are depicted below. There are relatively subtle changes on the radiographs of a patient suspected of having rheumatoid arthritis (Fig. 2.2).

Rheumatoid Arthritis

Hallmark imaging features of rheumatoid arthritis in the hands and wrists on MRI include:

- *Erosions*: Sharply marginated bone defects seen in two planes, with clear cortical break demonstrated on at least one plane, best seen on T1-weighted images (Fig. 2.3).
- *Marrow edema*: Alteration in the water content within the marrow of the bone, resulting in an ill-defined focus of high T2 signal (Fig. 2.4).
- *Bursitis*: A common early finding in rheumatoid arthritis patients, often located in the region of the metatarsal heads of the foot.
- *Synovitis*: Best illustrated by prominent asymmetric gadolinium enhancement within a joint. The thickness of the synovium should be greater in width than normal synovium. Enhancement is judged by comparison between the T1-weighted images obtained before and after the administration of IV gadolinium.

Detection of these imaging features can lead to early treatment with newer disease-modifying medications that can prevent irreversible cartilage damage and

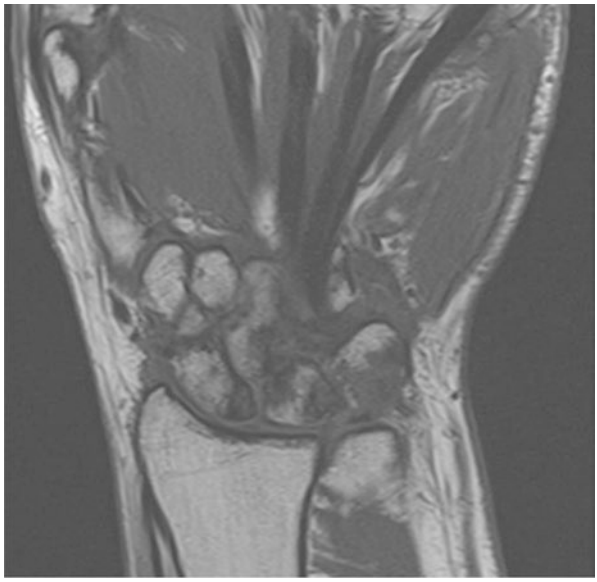

Fig. 2.3 MRI performed 2 weeks after the image depicted in Fig. 2.2, demonstrating erosive changes within multiple carpal bones

Fig. 2.4 Coronal T1-weighted fat saturation image demonstrates focal synovial thickening at the radiocarpal joint with numerous areas of abnormal high signal in numerous carpal bones

reduce morbidity. In addition, it is possible to monitor efficacy of various therapeutic interventions, as changes may occur on MRI within 3–6 months. The rheumatologist can quickly assess efficacy of a certain treatment regimen and titrate it as needed.

In addition to early detection of changes associated with inflammatory arthropathy, the greater soft tissue contrast resolution in MRI makes it a valuable tool in

detection of several other rheumatologic conditions, examples of which are illustrated below.

Seronegative Spondyloarthropathies

MRI is the test of choice for diagnosis of seronegative spondyloarthropathies both in the acute and chronic phase of the disease. This modality is particularly useful in detecting acute inflammatory lesion of the sacroiliac joints. Imaging hallmarks on MRI include bone marrow edema located at the periarticular or subchondral surfaces of the sacroiliac joints (Fig. 2.5). Stronger signal hyperintensity correlates with higher disease activity. Synovitis, capsulitis, and enthesitis may also be detected in the SI joints on MRI in the acute phase. The presence of both bone marrow edema and erosions has a 94% specificity and 75% sensitivity for the diagnosis of sacroiliitis. If present bilaterally, this is highly suggestive of ankylosing spondylitis. If the signal changes involving the SI joints are unilateral, it typically indicates other forms of spondyloarthritis, most often psoriatic arthritis.

Acute inflammatory lesions of the spine may also be present, and aid in diagnosis. Focal marrow edema in the anterior or posterior corners of the vertebral bodies indicates spondylitis (Fig. 2.6). When present in a patient under 40 years of age in more than three corners, and in the absence of osteophytes or Schmorl's nodes, it is 97% specific for the diagnosis of spondyloarthropathy. Additional areas of marrow edema include the posterior elements of the facet joints (Fig. 2.7), the costovertebral and costotransverse articulations.

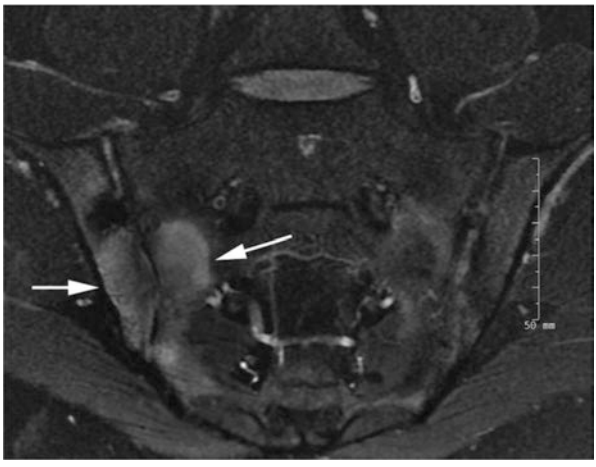

Fig. 2.5 Coronal oblique T2 fat saturation image depicts focal marrow edema surrounding the right SI joint in a patient with psoriasis

Fig. 2.6 Sagittal STIR image demonstrates areas of high signal at the anterior aspects of the L1, L2, L3, and L4 vertebral bodies (arrowheads)

Avascular Necrosis

MR imaging is 98% specific and 85% sensitive in diagnosing avascular necrosis and is considered the gold standard for diagnosis. Avascular necrosis occurs due to disruption of blood supply to the bone, resulting in bone death in the subchondral region of the bone. MRI demonstrates early findings of AVN which are not visible on radiographs. Hallmark feature on MRI include peripheral serpentine rim of low signal intensity on T1 (Fig. 2.8) and T2 images. Over time, serpiginous

Fig. 2.7 Sagittal STIR image demonstrates facet edema (arrows) at T12/L1 and focal soft tissue edema surrounding the posterior elements at L4/5 (arrowheads)

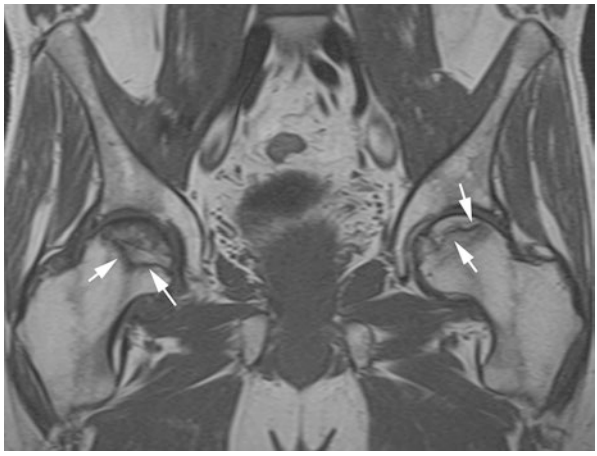

Fig. 2.8 Serpentine abnormal low T1 signal in the subchondral regions of both femoral heads (white arrows)

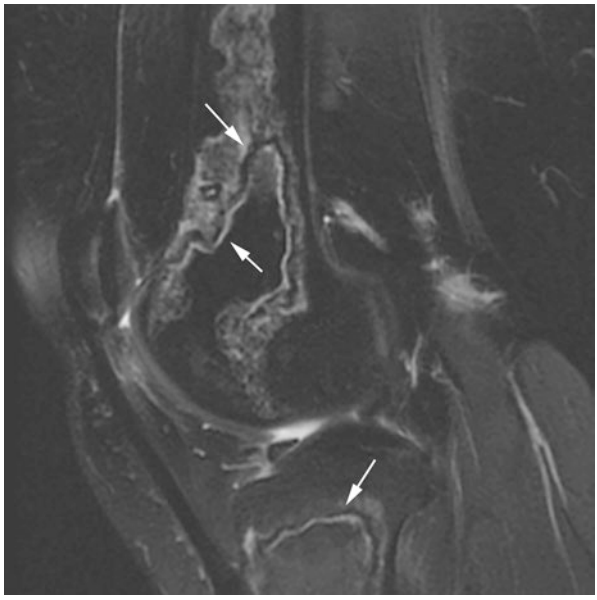

Fig. 2.9 A 25-year-old female with SLE and diffuse joint pain Sag T2 fat sat image demonstrating multiple intramedullary foci of abnormal serpiginous signal. This "double line" sign is pathognomonic for bone infarct and is characterized by contiguous linear low and high signal intensity areas (white arrows)

or amorphous sclerosis will develop on radiographs. The hip is the most common site of v necrosis. Fractures or dislocations of the hip can predispose to avascular necrosis. Numerous atraumatic etiologies are also known, including alcoholism, chronic steroid therapy, sickle cell disease, pancreatitis, and chronic renal failure. A bone infarct is similar in appearance to avascular necrosis except that bone infarct occurs in the metphyseal or diaphyseal regions (Figs. 2.9 and 2.10). Bone infarcts may cause dull pain, however more commonly are discovered incidentally on radiographs.

Acute Osteomyelitis

MRI is considered the gold standard in the diagnosis of acute osteomyelitis with sensitivity of 90% and specificity of 83%. Low signal intensity on T1-weighted images within the bone is considered the primary MR sign of osteomyelitis. Additional MR findings of include joint effusion, perisynovial, and marrow edema (Fig. 2.11a). The addition of gadolinium contrast is not always necessary for the diagnosis of osteomyelitis but has been reported to increase the specificity of findings (Fig. 2.11b). Contrast is contraindicated in patients with advanced renal failure due to the risk of nephrogenic systemic fibrosis. MRI facilitates not only the diagnosis of osteomyelitis, but complications associated with the bone infection, such as soft tissue abscess and tendinous involvement, and it is helpful in both initial treatment planning and follow up to therapy.

Fig. 2.10 Coronal T1-weighted image in the same 25-year-old patient depicted in the Fig. 2.9. This image demonstrates curvilinear areas of abnormal low signal in the distal tibial metaphysis and within the subchondral region of the talus (arrows)

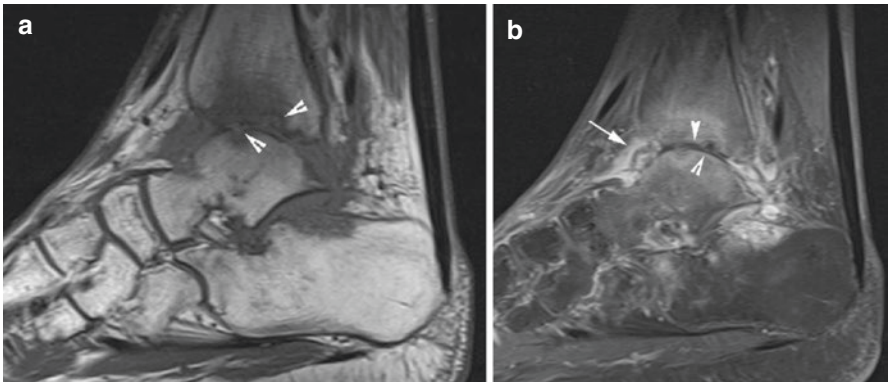

Fig. 2.11 (**a**) Sagittal T1-weighted ankle depict prominent erosions at the tibiotalar joint (arrowheads). (**b**) Sagittal T1-weighted postcontrast images depict marrow edema surrounding the tibiotalar articulation (arrow heads) and prominent synovial thickening (arrow)

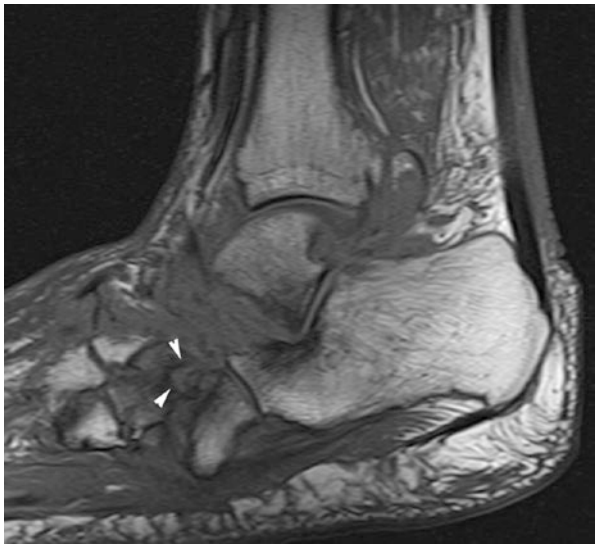

Fig. 2.12 Sagittal T1-weighted image depicts advanced neuropathic changes centered at the midfoot including diffuse tarsal-tarsal joint space narrowing and extensive areas of abnormal low T1 signal (arrowheads) within the tarsal bones

While MRI poses significant advantages over most other imaging modalities in the detection of osteomyelitis, it remains limited in specific instances, such as in patients with orthopedic hardware due to extensive associated artifact. In addition, in diabetic patients, the differentiation of osteomyelitis from neuropathic arthropathy can pose a particular challenge (Fig. 2.12). In these instances, correlation with the location of skin ulcerations and their proximity to marrow signal changes seen on MRI can be extremely beneficial.

Ultrasound Section

Due to advances in ultrasound (US) technology, high-resolution transducers are now able to image superficial structures such as joints, tendons, and nerves in great detail and with a lateral and axial resolution of 0.1 mm. This and the fact that US is a patient-friendly, cost-effective imaging modality available at the point of care has led to an expanding role for US in the assessment of rheumatological disorders. The disadvantages of US are its inability to penetrate through bone and its relatively small field of view. It is also a very operator-dependent imaging modality with a steep learning curve, and the ultrasonographer must also be aware of artifacts (anisotropy and Doppler artifacts) that should not be mistaken for pathology.

US machines generate sound waves that travel through the body until they encounter an acoustic interface (a change in density/stiffness between two adjacent tissues), at which point some sound waves are reflected back to the probe while others travel down deeper into the body. Signals returning to the probe are converted into an electric signal and displayed as a black and white two-dimensional image on the screen (Brightness "B" mode). The greater the difference between two acoustic

interfaces, the more sound waves that will be reflected back creating a "whiter" or "hyperechoic" image. An example of this would be at the interface between cartilage and bone where bone will appear as a hyperechoic signal. If there is no difference in the density of two tissues, the sound waves will travel straight through with no reflection of waves and the image will appear black or anechoic (such as fluid within a cystic structure.)

The joint spaces, bony contours, and tendons of patients with inflammatory arthritis can be interrogated with US looking for erosions, synovitis, tenosynovitis, rheumatoid nodules, tophi, and other signs of crystal deposition. The power Doppler capabilities of US machines can be used to detect the low flow states caused by dilated small blood vessels in inflamed joints.

Synovitis is identified as abnormal hypoechoic intra-articular tissue that is non-displaceable and which may exhibit power Doppler signal (Fig. 2.13). Erosions are seen as defects of the bone surface and should be identified in two orthogonal planes (Fig. 2.14). Multiple studies have demonstrated that US has a higher sensitivity than clinical examination for the detection of synovitis and a higher sensitivity for

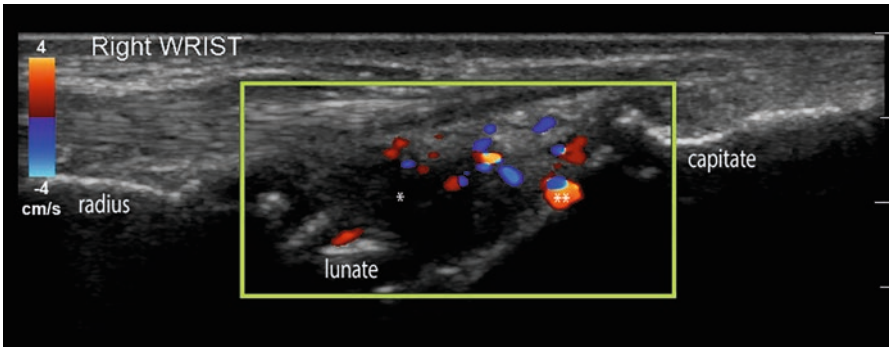

Fig. 2.13 US image showing the wrist of a patient with rheumatoid arthritis. (∗) synovial hypertrophy and (∗∗) positive power Doppler signal

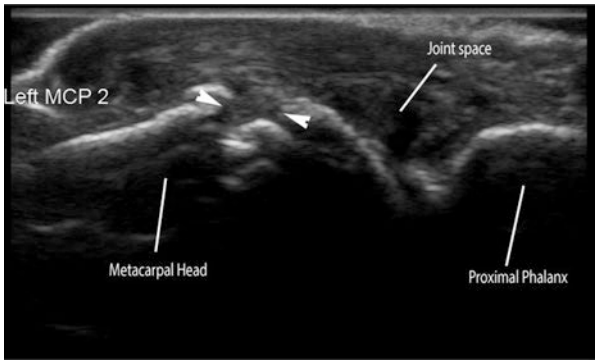

Fig. 2.14 Erosive changes at the second MCP (arrow heads)

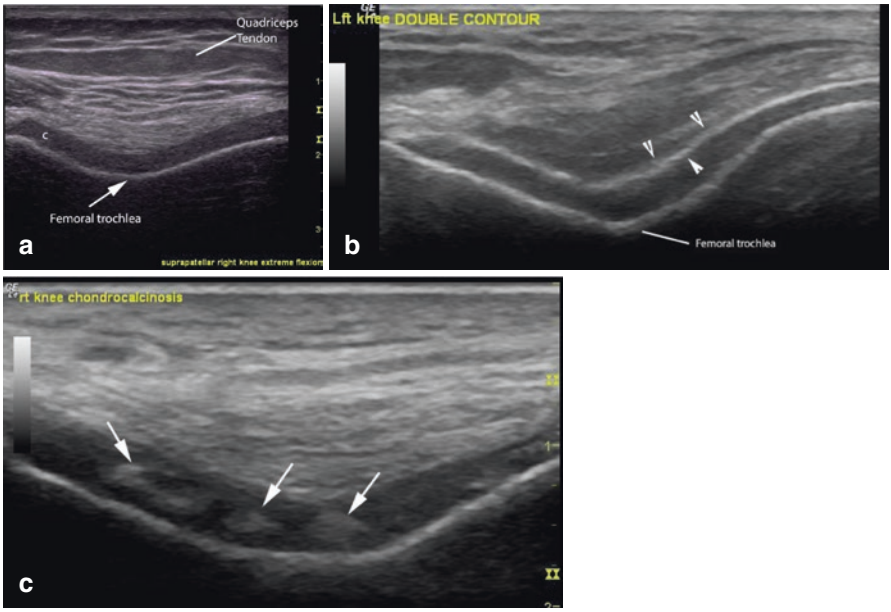

Fig. 2.15 (**a**) Normal knee US depicting patellofemoral cartilage (C). (**b**) Double countour sign: focal curvilinear hyperechoic irregular outline of the chondrosynovial margin. (**c**) Ovoid hyperechoic aggregates (arrows) within the patellofemoral compartment indicative of pyrophosphate crystal deposition

detecting erosions than conventional X-ray. Therefore, US has proven particularly useful in the detection of very early rheumatoid arthritis (RA) where findings can be subtle. Studies have found that erosions of >2.5 mm located in the distal ulna, second metacarpophalangeal, or fifth metatarsophalangeal joints help to increase the specificity for diagnosing early RA. In addition, US-detected tenosynovitis of the finger flexor and extensor carpi ulnaris tendons can be seen in patients with early RA and may predict erosive progression.

US is also useful in the assessment of the crystalline arthropathies, owing to the strong reflective properties of monosodium urate (MSU) and calcium pyrophosphate dihydrate (CPPD) crystals. MSU crystal deposits produce a "double contour sign" which is defined as a hyperechoic irregular outline of the chondrosynovial margin of the cartilage (Fig. 2.15b). Whereas MSU crystals are seen on the superficial surface of the joint cartilage, pyrophosphate crystals are identified as linear or oval aggregates lying within the substance of cartilage (Fig. 2.15c). Tophi can also be detected by US and appear as heterogeneous, hyperechoic aggregates with poorly defined margins and an anechoic halo (Fig. 2.16). Tophi can be detected in joints, tendons (patellar, triceps, quadriceps and achilles), and soft tissues and many US-detected tophi are not clinically apparent. The synovium in gouty joints can also

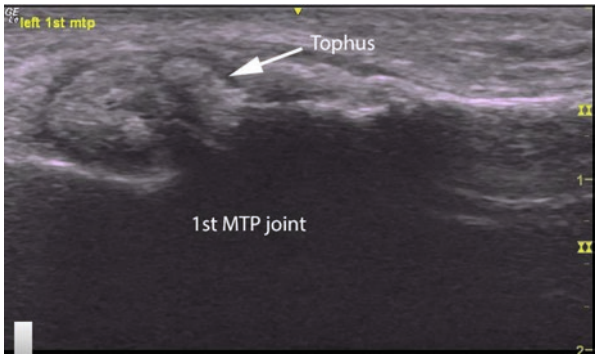

Fig. 2.16 Hyperechoic aggregates with poorly defined margins and an anechoic halo indicative of gouty tophi

lead to a characteristic "snowstorm" appearance which appears as hyperechoic dots swirling in the synovium.

In the evaluation of the spondyloarthopathies (SpA), the enthesis is an important site of pathology and US can be used to detect tendon or tendon insertion abnormalities many of which are subclinical. Tendon abnormalities seen in early SpA include entheseal thickening, hypoechogenicity, and fibrillar separation of the tendons due to intra-tendinous edema. Late changes include enthesophyte formation or the development of erosions at the site of tendon insertion to bone.

Finally, in addition to its role in the diagnoses of rheumatological conditions, US can also be used to guide procedures such as joint injections and aspirations. This is especially useful when accessing deep joints like the hip, for guiding injections in obese patients, and for identifying and accessing small pockets of fluid for aspiration.

Computed Tomography (CT)

CT is typically not indicated in first-line diagnosis of rheumatologic conditions due to its limited soft tissue contrast resolution compared to MRI. However, due to the speed of CT, advantages in patient comfort, and the ability to cover larger anatomical regions, it is used with increasing frequency in the ED. In particular, CT is utilized in acutely ill patients with acute joint and extremity pain, signs of soft tissue, joint, or osseous infection.

CT depicts bony architecture in exquisite detail and has shown to have high sensitivity in detecting cortical erosions, particularly those which may not be readily evident on radiographs. In septic arthritis, for example, CT may reveal the presence of erosions and joint effusion which can guide arthrocentesis (Fig. 2.17).

In the setting of necrotizing fasciitis, CT is the most sensitive modality for soft-tissue gas detection and can better evaluate the extent of osseous or soft tissue involvement than radiographs (Fig. 2.18).

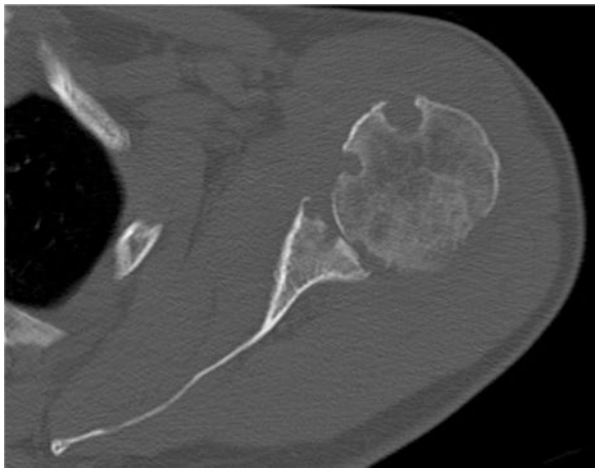

Fig. 2.17 Axial CT of the shoulder depicting prominent erosions at the humeral head and the glenoid in this 65-year-old patient with acute shoulder pain. Arthrocentesis was subsequently performed and confirmed the presence of *Staphylococcus aureus* septic arthritis

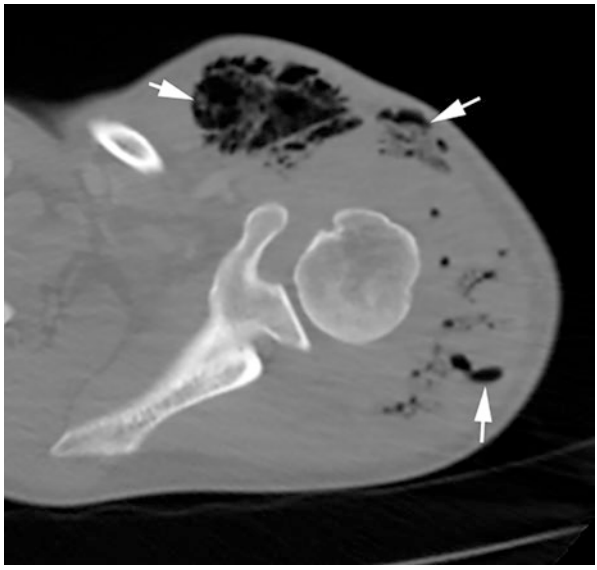

Fig. 2.18 Axial CT of the shoulder in bone window demonstrates numerous foci of air within the soft tissues surrounding the left shoulder (arrows) of this patient with necrotizing fasciitis

Further Reading

Alcalde M, D'Agostino MA, Bruyn GA, OMERACT Ultrasound Task Force. A systematic literature review of US definitions, scoring systems and validity according to the OMERACT filter for tendon lesion in RA and other inflammatory joint diseases. Rheumatology (Oxford). 2012;51(7):1246–60.

Averill LW, Hernandez A, Gonzalez L, Peña AH, Jaramillo D. Diagnosis of osteomyelitis in children: utility of fat-suppressed contrast-enhanced MRI. AJR. 2009;192:1232–8.

Canella C, Schau B, Ribeiro E, Sbaffi B, et al. MRI in seronegative spondyloarthritis: imaging features and differential diagnosis in the spine and sacroiliac joints. Am J Roentgenol. 2013;200:149–57.

Fayad LM, Carrino JA, Fishman EK. Musculoskeletal infection: role of CT in the emergency department. Radiographics. 2007;27:1723–36.

Gutierrez M, et al. A sonographic spectrum of psoriatic arthritis: "the five targets". Clin Rheumatol. 2010;29(2):133–42.

Herring W. Learning radiology; recognizing the basics. 3rd ed. Philadelphia: Elsevier; 2016. p. 220–6.

Howell GA. Osteomyelitis; MRI Web Clinic, Radsource-October 2017. Accessed April 2018.

Lillegraven S, et al. Tenosynovitis of the extensor carpi ulnaris tendon predicts erosive progression in early rheumatoid arthritis. Ann Rheum Dis. 2011;70(11):2049–50.

Noguerol TM, Alcala AL, Beltran LS, Cabrera MG, et al. Advanced MR imaging techniques for differentiation of neuropathic Arthropathy and osteomyelitis in the diabetic foot. Radiographics. 2017;37:1161–80.

O'Neill J. Essential imaging in rheumatology. New York: Springer; 2015. p. 305–39.

Polster JM, Winalski CS, Sundaram M, Liever ML, Schils J, Ilaslan H, Davros W, Husni ME. Rheumatoid arthritis: evaluation with contrast enhanced CT with digital bone masking. Radiology. 2009;252(1):225–31.

Salaffi F, et al. A clinical prediction rule combining routine assessment and power Doppler ultrasonography for predicting progression to rheumatoid arthritis from early-onset undifferentiated arthritis. Clin Exp Rheumatol. 2010;28(5):686–94.

Salgado CJ, Colen LB. Radiographic imaging in osteomyelitis: the role of plain radiography, computed tomography, ultrasonography, magnetic resonance imaging, and scintigraphy. Semin Plast Surg. 2009;23(2):80–9.

Szkudlarek M, et al. Ultrasonography of the metatarsophalangeal joints in rheumatoid arthritis: comparison with magnetic resonance imaging, conventional radiography, and clinical examination. Arthritis Rheum. 2004;50(7):2103–12.

Tins BJ, Butler R. Imaging in rheumatology: reconciling radiology and rheumatology. Insights Imaging. 2013;4(6):799–810.

Van der Ven M, et al. Absence of ultrasound inflammation in patients presenting with arthralgia rules out the development of arthritis. Arthritis Res Ther. 2017;19(1):202.

Vyas S, Bhalla AS, Ranjan P, Kumar S, Kumar U, Gupta AK. Rheumatoid arthritis revisited-advanced imaging review. Pol J Radiol. 2016;81:629–35.

Zayat AS, et al. The specificity of ultrasound-detected bone erosions for rheumatoid arthritis. Ann Rheum Dis. 2015;74(5):897–903.

Chapter 3
Clinical Issues in the Arthritis Patient

Robert S. Katz, Sobia Hassan, and Ben Small

Rheumatic diseases can be divided into several categories such as inflammatory arthritis, which includes rheumatoid arthritis (RA), psoriatic arthritis, ankylosing spondylitis, and crystal-induced arthritis, and noninflammatory arthritis for which osteoarthritis (OA) is the most common disorder. Although inflammation does play some role in OA, the problem is primarily mechanical with cartilage loss. There are also a number of other systemic rheumatic diseases such as systemic lupus erythematosus, scleroderma, inflammatory myopathy, and vasculitis that present with a myriad of multisystem signs and symptoms and can be associated with unique radiographic findings. Finally, there are various regional pain syndromes and diffuse pain syndromes such as fibromyalgia. Although laboratory tests and imaging are important, the patient's history and physical examination remains the cornerstone for diagnosis of any rheumatologic disorder.

History

Clues that point to an inflammatory arthritis include the presence of prolonged morning stiffness (lasting more than 30 minutes), pain that is worse in the morning and improved with activity. Pain from noninflammatory arthritis tends to worsen as the day progresses and with activity.

R. S. Katz (✉)
Rush University Medical Center, Section of Rheumatology, Department of Internal Medicine, Chicago, IL, USA

S. Hassan
Department of Rheumatology, Rush University Medical Center, Chicago, IL, USA
e-mail: Sobia_hassan@rush.edu

B. Small
Northwestern Memorial Hospital, Section of Rheumatology, Department of Medicine, Chicago, IL, USA

R. S. Katz, A. Basu (eds.), *Diagnostic Radiology of the Rheumatic Diseases*,
https://doi.org/10.1007/978-3-030-25116-1_3

The evaluation of autoimmune disorders requires a thorough review of all organ systems including specific inquiries about signs and symptoms such as rashes, oral ulcers, sicca symptoms, serositis, Raynaud's phenomenon, inflammatory eye conditions, recurrent sinus disease, and central nervous system symptoms.

Physical Examination

When examining a joint, the presence of swelling, warmth, pain on motion, range of motion, and joint tenderness should be assessed. Periarticular regions should also be evaluated. In the case of the spondyloarthropathies, the presence of heel pain or enthesitis can be one of the first manifestations of the disease.

A complete rheumatologic exam includes evaluation of all organ systems, not just the musculoskeletal system, and can provide important diagnostic clues. For example, careful inspection of the skin can detect vasculitic, psoriatic, or lupus-related rashes, as well as tophi and rheumatoid nodules.

Ancillary Laboratory Tests

Synovial Fluid Analysis

Synovial fluid can be sent for cell count, crystal analysis, and culture. A high synovial white blood cell count (over 2,000) helps to separate inflammatory arthritis from noninflammatory arthritis. Polarizing light microscopy is used to evaluate for the presence of uric acid and calcium pyrophosphate dihydrate crystals which occur in gout and pseudogout, respectively. Finally, cultures should be sent when suspecting septic arthritis.

Other Laboratory Tests

CBC – acute inflammatory arthritis can be associated with leukocytosis while diseases like lupus are associated with leukopenia. Patients with chronic inflammatory conditions can develop the anemia of chronic disease.

The erythrocyte sedimentation rate (ESR) and C-reactive protein (CRP) are nonspecific markers of inflammation, elevated in many rheumatic disease conditions.

Rheumatoid factor and cyclic citrullinated peptide (CCP) antibodies are present in the majority of RA patients.

Antinuclear antibodies (ANA), anti-double-stranded DNA and Smith antibodies, anti-chromatin antibodies, anti-Sjogren's A and Sjogren's B antibodies, anti-ribonuclear protein antibodies, and anti-centromere and Scleroderma-70

antibodies are useful in the evaluation of lupus, Sjogren's, mixed connective tissue disease, and scleroderma.

Low levels of C3 and C4 complement and elevated double-stranded DNA antibodies sometimes indicate a flare of activity in SLE patients.

Antineutrophil cytoplasmic antibodies (ANCA) are useful in the evaluation of granulomatosis with polyangiitis, microscopic polyangiitis, and eosinophilic granulomatosis with polyangiitis.

Specific rheumatic diseases are discussed in more detail below:

Osteoarthritis (OA) or degenerative joint disease is characterized by deterioration of articular cartilage with subsequent formation of reactive new bone at the articular surface. Commonly affected are the distal and proximal interphalangeal joints in the hands (bony enlargement of a distal interphalangeal (DIP) joint is termed a Heberden's node and similar enlargement of the proximal interphalangeal (PIP) joint is called a Bouchard's node), the first carpal metacarpal joint at the base of the thumb, and the joints of the knees, hips, first metatarsophalangeal (MTP) joints and mid-tarsal joints in the feet, and cervical and lumbar spine.

Osteoarthritis of "unusual" sites such as the metacarpophalangeal (MCP) joints, elbows, and shoulders should prompt evaluation for causes of secondary OA. Patients usually complain of pain and stiffness in the affected joints. Morning stiffness typically lasts less than 30 minutes and pain worsens with activity.

Osteoarthritis of the lumbar spine can lead to spinal stenosis when narrowing of the central canal occurs. Spinal stenosis is associated with paresthesias and pain in the lower extremities that is often worse with walking (pseudoclaudication) and relieved with sitting or lying.

Pharmacological agents including NSAIDs and intraarticular corticosteroid injections are not disease modifying but aimed at reducing pain.

Diffuse idiopathic skeletal hyperostosis or DISH is often an asymptomatic form of osteoarthritis that causes significant radiographic changes especially in the thoracic spine with flowing ossification along the anterolateral aspect of vertebral bodies, particularly the anterior longitudinal ligament.

Rheumatoid arthritis (RA) is a symmetrical polyarthritis. The joints become swollen and painful and there is significant morning stiffness, usually lasting over 1 hour. Synovitis, or swelling and inflammation of the synovial membrane, can be detected on examination as "boggy" swelling. Over time, these swollen joints can lead to permanent damage and deformities, including ulnar deviation, swan neck, and boutonniere deformities. The characteristic sites of RA include the PIP and MCP joints of the hands, the wrists, elbows, knees, ankles, MTP joints, cervical spine, shoulders, and hips. The DIP joints and the lumbar and thoracic spine are typically not involved.

Examination may also reveal the presence of rheumatoid nodules which are usually periarticular and commonly occur on the proximal forearm. Diagnosis is usually confirmed by imaging and the presence of RF and CCP antibody positivity, but a third of patients with RA may be seronegative.

In addition to traditional oral disease-modifying agents like methotrexate and leflunomide, there are now an increasing number of biologic modifying drugs that have a variety of therapeutic targets. There are inhibitors of tumor necrosis factor, interleukin-1, interleukin-6, interleukin-17, CD 20-positive B-cells, and T-cell co-stimulation. Biologic agents are generally well tolerated, although uncommon infections can occur. Newer options also include the kinase inhibitors which are oral agents. These agents are called disease modifying because they are effective at reducing inflammation and preventing joint damage in RA.

Crystal-Induced Arthritis

Gout is caused by the inflammatory reaction to monosodium urate crystal deposition in synovial tissue and tendon sheaths. Hyperuricemia is the biggest risk factor for gout. In acute gouty arthritis, there is generally an excruciating attack of pain in a single joint, often the first MTP joint, foot, ankle, or knee. Over time, if hyperuricemia is not treated, gout attacks can become more frequent, and occasionally polyarticular and chronic arthritis can occur with the development of tophi.

Monosodium urate crystals are identified from synovial fluid as needle-shaped and negatively birefringent crystals using fluorescent microscopy. Anti-inflammatory therapy, including short-term corticosteroid use and nonsteroidal anti-inflammatories as well as colchicine, can be effective for treating acute attacks. Long-term management of gout necessitates the use of medications such as allopurinol or febuxostat that reduce uric acid levels by inhibiting xanthine oxidase. If uric acid levels are maintained below 6 mg/dL, further acute gout attacks should occur less frequently.

Pseudogout is associated with calcium pyrophosphate dihydrate (CPPD) crystals. Patients can present with acute attacks of joint inflammation that most commonly affect the knee and/or wrist, or rarely a more chronic inflammatory arthritis that can mimic RA. CPPD deposition can also contribute to the development of secondary OA. CPPD crystals can be identified from synovial fluid as positively birefringent rhomboid-shaped crystals. The finding of chondrocalcinosis visible on radiographs of the hands, knees, and other joints can also aid diagnosis.

Seronegative Spondyloarthopathies (SpA)

The seronegative SpAs are a group of disorders which share similar clinical manifestations. Ankylosing spondylitis is the prototypic SpA, but psoriatic arthritis, reactive arthritis, and inflammatory bowel disease associated arthritis are all considered SpAs. Ankylosing spondylitis and reactive arthritis are associated with the HLA-B27 gene.

Inflammation of the axial joints, in particular, the sacroiliac (SI) joints, is a distinguishing feature of some of the SpAs. With time, ossification occurs leading to fusion of the SI joints and spinal ligaments. If axial joints are involved, the patient

classically describes lower back pain or buttock pain which is associated with prolonged morning stiffness and improvement with exercise. Stiffness, rigidity, and loss of ROM can occur with progressive fusion of the spine.

Generally, the process starts in the sacroiliac joints, and abnormalities of these joints can be detected by radiographs. However, it can take several years for changes to show up on plain film radiographs, and therefore there has been an increasing role for MRI to assess early changes of inflammation in the sacroiliac joints.

Peripheral involvement in spondyloarthritis is usually characterized by an asymmetric oligoarthritis (fewer than 5 joints) affecting the lower extremity joints, sausage-appearing digits termed dactylitis, and enthesitis which refers to inflammation at sites of tendon attachment to bone, such as heel pain where the Achilles tendon attaches to the calcaneus.

Biological modifying agents are helpful in reducing symptoms and may even slow down ossification of the spine if they are started early.

Patients with *psoriatic arthritis* can also present with similar peripheral and axial manifestations although peripheral symptoms are more predominant. When present, psoriasis appears as a thick, silvery scale on a well-demarcated red patch. The scale on psoriatic lesions is quite adherent, and attempting to peel it off can produce mild bleeding. Psoriasis typically occurs over the extensor surfaces such as the elbows, knees, and also on the scalp, but it can be even more extensive. It is important to inspect the patient thoroughly for psoriasis paying particular attention for hidden lesions behind the ears, in the umbilicus, and in the gluteal region. Nails should also be carefully examined for the presence of pitting.

Treatment is similar to rheumatoid arthritis with the use of methotrexate, leflunomide, and also TNF inhibitors and other biologic modifiers, which can be extremely effective for both the psoriasis and the inflammatory arthritis. Newer biologic therapies in psoriasis and psoriatic arthritis target the interleukin-17 and interleukin-23 cytokines. In addition, kinase inhibitors are effective treatments to reduce joint inflammation and prevent permanent damage.

Reactive arthritis refers to an inflammatory oligoarthritis that occasionally follows certain GI or genitourinary infections or appears spontaneously. Occasionally, the classic triad of arthritis-conjunctivitis-urethritis can be present. The arthritis is typically asymmetric, oligoarticular and intensely inflammatory.

The peripheral arthritis of *inflammatory bowel disease (IBD)*, which encompasses both Crohn's disease and ulcerative colitis, typically presents as an asymmetric oligoarthritis affecting large joints. However, a small subset of IBD patients will develop a more symmetrical polyarthritis that resembles RA, but the arthritis is usually less severe and is nonerosive and nondeforming. A smaller number of patients develop axial involvement. All the forms of SpA can be complicated by similar extra-articular manifestations including uveitis.

Systemic lupus erythematosus (SLE) is a multisystem disease associated with joint pain, fatigue, rashes, especially on sun-sensitive areas such as the butterfly-shaped malar rash on the face, nephritis, serositis (pericarditis and pleuritis), and central nervous system involvement. Musculoskeletal involvement is common and includes polyarthralgias and the development of a symmetrical polyarthritis in some patients. Rarely, SLE patients can develop a deforming arthritis with swan neck deformities similar to

patients with rheumatoid arthritis. SLE arthritis is typically considered nonerosive; however, advanced imaging modalities such as ultrasound and MRI have demonstrated erosions as well as tenosynovitis and synovial proliferation in SLE patients.

Various laboratory abnormalities can be seen including cytopenias, positive antinuclear antibodies, anti-DNA antibodies, and other autoimmune antibodies, of which anti-Smith and anti-Sjogren's syndrome A (SSA) are more specific. It is important to obtain a urinalysis, as the presence of microscopic hematuria and proteinuria may indicate lupus nephritis and the need for a renal biopsy. Central nervous system involvement can sometimes be detected with MRI imaging and by analyzing the cerebrospinal fluid for WBCs, a high IgG/albumin ratio and the presence of oligoclonal bands.

Hydroxychloroquine is an antimalarial medication that appears to inhibit antigen processing and is widely used as treatment for patients with lupus. Many patients require additional steroids or other immunosuppressive therapies including mycophenolate mofetil, azathioprine, methotrexate, leflunomide, and cyclosporine. The newest agent approved for SLE is belimumab, an anti-CD20 treatment, which inhibits B-lymphocytic stimulator signaling, decreasing B-cell survival and differentiation into immunoglobulin-producing plasma cells.

Sjogren's syndrome is a systemic inflammatory autoimmune condition that typically affects the lacrimal and salivary glands, causing dry eyes and dry mouth. Sjogren's can be primary or associated with other autoimmune conditions such as lupus, rheumatoid arthritis, or scleroderma. Patients often have increased fatigue and joint pain. It can be diagnosed by measuring decreased tear production (Schirmer test) or by lip/salivary gland biopsy. Labs often reveal positive SSA and SSB Abs.

Scleroderma or systemic sclerosis (SSc) is characterized by skin tightening and thickening. Progressive skin thickening occurs starting distally with the involvement of fingers (termed sclerodactyly) but can extend proximally to affect arms, face, trunk, and legs.

Vascular involvement is a prominent feature of SSc, and vasoconstriction and obliterative vasculopathy contribute to the development of Raynaud's phenomenon in the majority of patients, which manifests as repeated episodes of color change over the digits after cold exposure. In severe cases, patients can develop digital ulcers and digit-threatening ischemia.

Internal organ manifestations such as interstitial lung disease and pulmonary hypertension can occur and are a major cause of morbidity and mortality in scleroderma patients. Renal crises were previously the major cause of mortality in scleroderma patients but can now be more effectively treated with ACE inhibitors. Gastrointestinal involvement includes gastroesophageal reflux, dysphagia, and decreased gut motility that can lead to bacterial overgrowth.

Antinuclear antibodies are generally positive, and many, but not all, patients with scleroderma will have anti-Scl-70 antibodies.

CREST syndrome is a subset of systemic sclerosis associated with anticentromere antibodies and characterized by calcinosis, Raynaud's phenomenon, esophageal dysmotility, sclerodactyly, and telangiectasias.

Vasculitis In various types of necrotizing vasculitis, the blood vessels become inflamed leading to tissue damage and necrosis. This can also give rise to stenosis

and aneurysm formation. Classification of the vasculitides is predominantly based on vessel size and divided into large, medium, or small vessel disease:

- Large vessel involvement occurs in giant cell arteritis and Takayasu's arteritis.
- Medium vessel involvement is associated with polyarteritis nodosa.
- Small vessel involvement includes granulomatosis with polyangiitis, microscopic polyangiitis, eosinophilic granulomatosis with polyangiitis, cutaneous leukocytoclastic vasculitis, and Henoch-Schonlein purpura.

The signs and symptoms a patient will develop depends on the organs supplied by the affected vessels. Imaging vessels is useful in the evaluation of large and medium size vessel vasculitis, whereas ANCA testing and biopsy of affected tissue is helpful diagnostically in small vessel vasculitis. Patients often require aggressive treatment to induce remission with corticosteroids, cyclophosphamide, or rituximab, followed by maintenance therapy with other immunosuppressants such as mycophenolate, methotrexate and azathioprine.

Polymyosits and dermatomyositis are inflammatory myopathies that present as weakness of the proximal upper and lower extremity muscles. A characteristic rash, including a heliotrope purple rash on the eyelids and Gottron papules over the joints of the hands may be seen. Elevated creatine kinase levels are usually present. Muscle biopsy and electromyograms can establish the diagnosis. Patients are treated with oral steroids with the majority requiring steroid-sparing agents such as methotrexate or mycophenolate mofetil.

Polymyalgia rheumatica (PMR) presents in patients above the age of 50 with the fairly acute onset of bilateral shoulder and hip girdle pain and prolonged morning stiffness. The name of the condition is misleading as symptoms occur due to involvement of articular and peri-articular structures (bursitis, synovitis) rather than due to muscle disease.

There is no specific diagnostic test for PMR but patients are diagnosed based on a compatible history, significantly elevated acute phase reactants (sedimentation rate is generally above 50) and an immediate and dramatic response to corticosteroids.

Patients are managed with a prolonged course of oral steroids that are slowly tapered over the course of one or two years.

Fibromyalgia is associated with widespread, subjectively intense musculoskeletal pain. Poor sleep, fatigue, and cognitive symptoms ("fibrofog") are typically present. This is a nonarticular disorder in which joints are not swollen, and it tends to be chronic. A loss of lordotic curve of the cervical spine (straight neck) is often seen on lateral views, but otherwise there are no radiographic abnormalities.

Sometimes *pain is regional*, such as De Quervain's tenosynovitis with pain in the proximal thumb due to tendinitis of the abductor pollicis longus and extensor pollicis brevis tendons. Pain is elicited by wrapping the fingers around the thumb and ulnar deviating the wrist (positive Finkelstein test); trochanteric bursitis of the hip with tenderness and pain over the lateral hip; stenosing tenosynovitis of the hand with a trigger finger; rotator cuff tendinitis; and adhesive capsulitis (frozen shoulder) with pain, stiffness and limited range of motion of the shoulder upon examination.

Chapter 4
Hands and Wrists

Anupam Basu

Case 1

A 62-year-old former auto mechanic with persistent, progressive hand pain.

Fig. 4.1 The frontal image of the hand demonstrates asymmetric joint space narrowing at the thumb carpometacarpal joint with small marginal osteophytes and marginal sclerosis. Additional areas of joint space narrowing at the third and fourth PIP joints (arrows)

A. Basu (✉)
Cook County Health, Department of Radiology, Chicago, IL, USA
e-mail: abasu@cookcountyhhs.org

R. S. Katz, A. Basu (eds.), *Diagnostic Radiology of the Rheumatic Diseases*,
https://doi.org/10.1007/978-3-030-25116-1_4

Answer Thumb CMC and PIP osteoarthritis.

Discussion
The adverse effects of excessive repetitive loading on the joints, for example in specific occupational activities in workers using machinery such as vibrating tools, has been recognized as a predisposing factor in the development of osteoarthritis, most commonly in the first carpometacarpal joint. The thumb CMC is a common location for osteoarthritis of the hand (Fig. 4.1).

Case 2
A 62-year-old male with long-standing diffuse bilateral hand pain.

Fig. 4.2 AP view of both hands demonstrates relatively symmetric bilateral radiocarpal joint, carpal-carpal and metacarpo-phalangeal joint space narrowing, periarticular osteopenia, and relative paucity of productive changes suggesting rheumatoid arthritis. There are productive changes evident at the ulnar styloid process, seen in a minority of patients with rheumatoid arthritis

Fig. 4.3 Ball-catchers view of both hands in the same patient as above, again depicts relatively symmetric joint space narrowing, most notably at the metacarpophalangeal joints with relative paucity of productive changes

Answer Rheumatoid arthritis.

Discussion

The hand is involved in nearly all patients with the rheumatoid arthritis. The earliest manifestations of rheumatoid occur at the metacarpophalangeal and the proximal interphalangeal joints. Distal interphalangeal joints are much less commonly involved. Hand radiographs for the assessment of rheumatoid arthritis are crucial not only to identify the presence of the disease (Fig. 4.2) but also to assess the progression and monitor the effect on therapeutic intervention. The Norgard, also known as the "ball-catchers" view (Fig. 4.3), is ideal to assess erosions between the pisiform and triquetrum which can occur early in the disease process.

Case 3

A 43-year-old with hand pain and back pain progressing over several months.

Fig. 4.4 Single frontal view of the hand demonstrates soft tissue swelling of the fourth digit centered at the PIP. There is subtle periosteal reaction along the distal shaft of the fourth proximal phalanx (arrows) and "pencil in cup" deformity of the fifth DIP (arrowhead)

Answer Psoriatic arthritis.

Discussion

The destructive joint space narrowing of the distal interphalangeal joints of the hands are the most well-known and characteristic radiographic feature of psoriatic arthritis. The hands are most commonly involved in psoriatic arthritis, followed by the feet and the sacroiliac joints, although virtually any joint may be affected. The clinical presentation of the articular disease is variable as a monoarticular or polyarticular distribution may be encountered. Radiographic features of the process in the hands include fusiform soft tissue swelling of the entire digit, known as dactylitis, aggressive appearing erosive changes which can involve the central portion of the joints and result in "pencil-in-cup" deformities (Fig. 4.4) and rarely distal tuft resorption, acro-osteolysis. Another important radiographic feature is the bony proliferation which can result in the frayed or spiculated appearance, often called "fluffy periostitis" mentioned in Chap. 1.

Case 4
A 49-year-old male with history of alcoholism presents with hand pain and swelling over several months.

Fig. 4.5 AP view of both hands with scattered areas of predominantly periarticular and juxta-articular soft tissue swelling (white arrows) randomly distributed in both hands, many of which are associated with prominent underlying erosions with overhanging edges and sclerotic borders (arrowheads)

Answer Gout.

Discussion
Radiographic hallmarks of gout are the presence of tophi, soft tissue masses created by the deposition of urate crystals. These tophi are distributed in a random fashion typically periarticular, although may be intra-articular or remote from a joint. Additional imaging features include punched out erosions which result in overhanging edges (Fig. 4.5) with relative preservation of the joint space and of bony mineralization until late in the disease process. These imaging features usually occur after prolonged periods of hyperuricemia, on average 7–10 years.

Case 5

A 45-year-old with history of IV drug abuse presents with atraumatic wrist pain, discharged after initial visit to the ED and returns 2 weeks later with worsening swelling and erythema.

Fig. 4.6 Frontal view of the wrist demonstrates normal joint spaces without erosive changes. Nonspecific lucent focus (arrow) within the capitate bone, with sclerotic borders and overall nonaggressive features

Fig. 4.7 Lateral wrist; early septic. Lateral view of the wrist, windowed to accentuate the soft tissues, demonstrates mild bowing of the pronator quadratus fat pad (arrow) which is suggestive of the presence of an underlying joint effusion

Fig. 4.8 AP wrist radiograph; 2 weeks following the initial visit, there is dramatic disruption of normal carpal arcs, diffuse osteopenia, and prominent erosions within multiple carpal bones (arrows)

Answer Septic arthritis.

Discussion

The rapid onset of osseous erosive and destructive changes is a hallmark feature of septic arthritis. Radiographs may show a joint effusion, which in this case is suggested by bowing of the pronator quadratus fat pad (Fig. 4.6). The subsequent radiographic changes of septic arthritis are best depicted when comparing Figs. 4.7 and 4.8.

Case 6

A 15-year-old with short stature, long-standing hand, knee, and hip pain, establishing care as a new patient.

Fig. 4.9 AP view of the hand demonstrates diffuse osteopenia; the articular margins of the metacarpal heads are eroded (arrows) and there are carpal-carpal fusions (arrowheads)

Answer Juvenile idiopathic arthritis (Still's disease).

Discussion

Juvenile idiopathic arthritis (JIA) is a complex set of disorders that affect the articular structures in children, and is one of the more common causes of chronic childhood illness. JIA includes juvenile onset seronegative spondyloarthropathies, juvenile onset adult-type seropositive rheumatoid arthritis, and Still's disease (seronegative chronic arthritis). Still's disease makes up 70% of cases of JIA. Within this subgroup are certain clinical varieties, such as classic systemic disease, polyarticular disease, and pauciarticular or monoarticular disease. The hand and wrist are frequently involved. In the hand, any articulation may be affected. Radiographic features include diffuse osteoporosis, epiphyseal deformity, and ballooning and cupping of the proximal phalangeal ossification centers (Fig. 4.9). Growth disturbances and articular destruction can lead to significant wrist deformities.

Case 7
A 38-year-old female with diffuse, long-standing hand pain.

Fig. 4.10 AP view demonstrating placement of silastic arthroplasties at the MCPs (arrows)

Answer Long standing rheumatoid arthritis patient with post-operative changes.

Discussion
Metacarpal head surgeries (Fig. 4.10) have historically been performed in patients with advanced rheumatoid arthritis in an effort to improve grip strength. Although this procedure may temporarily restore alignment and improve patient's subjective feeling of well-being, the procedure has largely fallen out of favor due to high rate of failure, particularly with the advent of more effective means of medical management.

Case 8
A 61-year-old with diffuse hand pain.

Fig. 4.11 Frontal view of the wrist depicts severe radiocarpal joint space narrowing with widening of the scapholunate interval (arrow). In addition, there is downward displacement of the capitate (arrowheads)

Answer Pyrophosphate arthropathy.

Discussion
The structural joint changes associated with calcium pyrophosphate deposition have distinctive characteristics which allow an accurate diagnosis in the absence of chondrocalcinosis. In the wrist, the radiocarpal joint compartment is the most frequent site of disease. Joint space narrowing, sclerosis, and discrete subchondral radiolucent lesions are often observed between the distal end of the radius and the proximal carpal row. The image above demonstrates marked widening of the scapholunate space with downward displacement of the capitate (Fig. 4.11), resulting in disruption of the carpal arcs of Gilula. The overall features are consistent with scapholunate advanced collapse (SLAC) wrist, often seen in older patients with pseudogout.

Practice Questions

Q1. A 58-year-old with long-standing dry cough, referred by pulmonologist for intermittent hand pain. What is the most likely consideration?

A. Renal osteodystrophy.
B. Psoriasis.
C. Sarcoidosis.
D. Thermal injury.

Discussion
Sarcoidosis is a chronic multisystemic process characterized by the presence of noncaseating granulomas. The clinical and imaging manifestations are most often seen in the chest; however, rheumatologic involvement can be seen in 10–15% of patients with sarcoidosis. Patients present clinically with transient, migratory polyarticular joint pain. The fingers and toes are the most frequently involved. Radiographic features include the presence of lace-like lesions, destructive and cystic changes in the middle or distal phalanges of the hand (See fig above arrows) involving multiple digits.

Q2. A 35-year-old female with hand pain, history of hip replacement. What is the most likely diagnosis?

A. Juvenile Idiopathic Arthritis (JIA).
B. Erosive osteoarthritis.
C. Gout.
D. Lupus.

Discussion

The AP image of both hands (See fig above) depicts marked disruptions of the carpal arcs and relatively symmetric, extensive erosive changes of the radiocarpal, intercarpal, MCP, and PIP joints. Findings are consistent with the presence of an inflammatory arthropathy. In addition, flaring or ballooning of the distal aspects of the proximal phalanges is a finding often seen in JIA. JIA affects multiple large and small joints, and can result in joint replacement surgery at a relatively young age.

The distribution is not consistent with erosive osteoarthritis, which typically involves the DIP joints. Lupus causes subluxations without significant erosive changes. The morphology, distribution, and degree of erosive changes and relative absence of soft tissue abnormalities are not consistent with gout.

Q3. A 42-year-old homeless man with severe hand pain. What is the most likely diagnosis?

A. Psoriatic arthritis.
B. Thermal injury.
C. Rheumatoid arthritis.
D. Necrotizing fasciitis.

Discussion

This is a case of frostbite. See fig above reveals preservation of joint spaces and absence of erosive or productive osseous changes. There is diffuse soft tissue swelling of the second through fifth digits with relative thumb sparing. The thumb is often tucked into the palm and may be initially spared of the effects of frostbite. Frostbite is localized cold thermal injury that results when tissues are exposed to temperatures below their freezing point for extended periods, most commonly in the hands and feet. Radiographic features in the acute setting include soft tissue swelling, subcutaneous emphysema. Later stages of injury would manifest as osseous demineralization, periostitis, periarticular erosions, and acro-osteolysis. Alcohol consumption and psychiatric illness are the most common risk factors for frostbite injuries.

Q4. A 64-year-old female with worsening hand pain over several years. What is the most likely underlying diagnosis?

A. Rheumatoid arthritis.
B. Gout.
C. Erosive arthritis.
D. Lupus.

See fig above demonstrates joint space narrowing involving multiple DIP and PIP joints with relative preservation of the MCPs. The trapeziometacarpal joints are also involved. The distribution and presence of productive changes favors the diagnosis of erosive osteoarthritis. Erosive osteoarthritis and psoriatic arthritis are commonly included in the differential of DIP-predominant joint disease, and can be difficult to differentiate. Trapeziometacarpal arthritis is a common feature of erosive OA and is present in this patient. The distribution of joint disease make RA less likely.

Q5. Hand pain, palpable nodules. What is the most likely diagnosis?

A. Gout.
B. Scleroderma.
C. Rheumatoid arthritis.
D. Pyrophosphate arthropathy.

See fig above depicts diffuse symmetric, radiocarpal, carpo-carpal joints. Relative preservation of the MCPs, PIPs, and DIPs. In addition, there are areas of periarticular eccentric soft tissue swelling, adjacent to several PIP joints bilaterally. The top two considerations based on this image should be gout and rheumatoid arthritis. The best answer is rheumatoid arthritis. RA can result in soft tissue nodules near joints and prominent pressure points. These nodules may ulcerate, drain, and give rise to an infection. While soft tissue nodules are a hallmark feature of gout, the ancillary findings on this radiograph would be atypical, specifically the symmetric distribution of joint space narrowing and the degree of uniform joint space narrowing, making gout less likely.

Scleroderma typically results in acro-osteolysis and areas of coarse soft tissue calcifications. Pyrophosphate arthropathy can result in SLAC wrist as shown in Case 8.

Q6. A 47-year-old female has been a patient in your clinic for many years. Radiographs from 10 years prior are also shown. What is her most likely underlying diagnosis?

Fig. 4.12 AP view of the hand, initial presentation

Fig. 4.13 AP view of the hand 10 years after initial presentation

A. Systemic lupus erythematosus (SLE).
B. Rheumatoid arthritis.
C. Osteoarthritis.
D. Psoriasis.

Figures 4.12 and 4.13 depict marked progression of prominent subluxations in the 10-year interval which began at the second and third DIPs in 2005. There is marked ulnar subluxation centered at the MCPs. The best answer is SLE, and autoimmune disorder characterized by inflammation and immune complex deposition. Over 80% of SLE patients have symmetric, nonerosive polyarthritis affecting the small joints of the hands, wrists, knees, and shoulders. Approximately, 10% will have ulnar drift at the MCPs known as Jaccoud syndrome, or Jaccoud arthropathy. In Jaccoud arthropathy, muscle atrophy and contractures result in reversible subluxations eventually becoming fixed. Close inspection of the periarticular regions on both radiographs demonstrates periarticular osteopenia but relative absence of erosive changes or productive changes, making classic osteoarthritis or inflammatory processes such as psoriasis or RA less likely.

Answers to the Question

Q1: C. Sarcoidosis
Q2: A. Juvenile Idiopathic Arthritis (JIA)
Q3: B. Thermal injury
Q4: C. Erosive arthritis
Q5: C. Rheumatoid arthritis
Q6: A. Systemic lupus erythematosus (SLE)

Further Reading

Bieber EJ, Weiland AJ, Volenec-Dowling S. Silicone rubber implant arthroplasty of the metacarpophalangeal joints for rheumatoid arthritis. J Bone Joint Surg Am. 1986;68(2):206–9.
Brower AC, Flemming DJ. Arthritis in black and white, vol. 2012. 3rd ed. Philadelphia: Saunders. p. 226–30.
Farpour F, Maasumi K, Tehranzadeh J. Imaging of crystal deposition disease. Appl Radiol. 2012;41(8):18–25.
Kahn JE, Lidove O, Laredo JD, et al. Frostbite arthritis. Ann Rheum Dis. 2005;64(6):966–7.
Lalani TA, Kanne JP, Hatfield GA, Chen P. Imaging findings in systemic lupus erythematosus. Radiographics. 2004;24:1069–86.
Manaster BJ. Diagnostic imaging musculoskeletal: non-traumatic disease. 2nd ed. Philadelphia: Elsevier; 2016. p. 1044–7.
Martel W, Stuck KJ, Dworin AM, Hylland RG. Erosive osteoarthritis and psoriatic arthritis: a radiologic comparison in the hand, wrist and foot. AJR. 1980;134:125–35.

Millet JD, Brown RK, Levi B, Kraft CT, Jacobson JA, Gross MD, Wong KK. Frostbite: Spectrum of imaging findings and guidelines for management. Radiographics. 2016;36:2154–69.

Resnick D, Kransdorf MJ. Bone and joint imaging. 3rd ed. Philadelphia: Elsevier Saunders; 2005. p. 357–93.

Sommer OJ, Kladosek A, Weiler V, Czembirek H, Boeck M, Stiskal M. Rheumatoid arthritis: a practical guide to state of the art imaging, image interpretation, and clinical implications. Radiographics. 2005;25:381–98.

Chapter 5
Foot and Ankle

Anupam Basu

Case 1
A 58-year-old male with gradually increasing pain over his forefoot, centered at his great toe. No recent trauma.

A. Basu (✉)
Cook County Health, Department of Radiology, Chicago, IL, USA
e-mail: abasu@cookcountyhhs.org

R. S. Katz, A. Basu (eds.), *Diagnostic Radiology of the Rheumatic Diseases*,
https://doi.org/10.1007/978-3-030-25116-1_5

Fig. 5.1 Frontal radiograph of the foot demonstrates nonuniform first MTP joint space narrowing (arrowheads) with sclerosis and osteophyte formation (arrows). The location and marked surrounding productive changes are consistent with osteoarthritis

Diagnosis
Degenerative osteoarthritis.

Discussion
The first MTP is the most common location for osteoarthritis in the foot (Fig. 5.1). This is often seen in association with hallux valgus deformity and results in nonuniform joint space loss with osteophyte formation.

Case 2
A 45-year-old with foot and hand pain over several months.

Fig. 5.2 Joint space narrowing is noted of the left fourth and fifth MTP, left metatarsal-tarsal joint, and the right third through fifth MTP. There are erosive changes particularly of the right third through fifth metatarsal heads (arrows). In addition, there is fibular subluxation of the right proximal phalanges in relationship to the metatarsal heads

Diagnosis
Rheumatoid arthritis.

Discussion
The feet are involved in a majority of patients with rheumatoid arthritis, and in 10–20% of patients, may be the first site of manifestation. Rheumatoid arthritis of the foot is typically seen in the MTP and PIP joints with sparing of the DIP joints (Fig. 5.2). Rheumatoid arthritis often also involves the metatarsal-tarsal joints (MTT).

Case 3

A 58-year-old woman with long-standing, poorly controlled diabetes presents with increasing unilateral foot pain while walking. Previous radiographs are available from 1 year prior.

Fig. 5.3 Lateral radiograph of the left foot demonstrates essentially unremarkable foot radiograph aside from minimal midfoot joint space narrowing. No significant malalignment or soft tissue swelling

Fig. 5.4 Lateral image obtained one year after Fig. 5.3 in the same patient demonstrates loss of the plantar arch with joint space narrowing centered at the midfoot. There is downward displacement of the navicular (arrow), as well as the cuboid, which appears sclerotic and fragmented (arrowhead)

Discussion

Patients with insensitivity to pain, most often diabetic patients, may develop neuropathic arthropathy of their lower extremities, most frequently the tarsometatarsal, intertarsal, and MTP joints. There are a spectrum of imaging changes associated with neuropathic arthropathy which include atrophic, hypertrophic, and mixed pattern. In the lower extremities, the hypertrophic or mixed patterns predominate. Imaging hallmarks of the hypertrophic pattern include extensive sclerosis, bony fragmentation, dislocation, bony debris, and joint effusion. Compare the changes seen in Fig. 5.3 with the relatively normal radiograph of the foot seen in Fig. 5.4 only 1 year prior. Disruption of the Lis-Franc ligament, which spans from the medial cuneiform to the second metatarsal can occur with minimal trauma. Disruption of this ligament results in significant instability of the tarsometatarsal articulation.

Case 4
A 57-year-old male has had recent attacks of acute foot and knee pain for the last 5 years. He recently described soft tissue "bumps" around his elbows and his big toes.

Diagnosis
Topheacous gout.

Fig. 5.5 AP view of both feet demonstrates prominent, well-marginated peripheral erosions with "overhanging" edges at the medial aspect of the first metatarsal heads (arrows) and scattered periarticular areas of soft tissue swelling (arrow heads). The joint spaces are relatively well preserved. The morphology and location of the erosions are nearly pathognomonic for gout

Discussion
The first metatarsophalangeal joints are the most common areas affected by gout (Fig. 5.5). Other joints commonly involved are the ankles, knees, hands, and elbows. The hip, shoulder, and spine are typically spared.

Case 5

A 38-year-old male admitted for community-acquired pneumonia. Several days after admission, his ankle became acutely painful.

Fig. 5.6 Lateral radiograph of the ankle demonstrates diffuse periarticular osteopenia, erosive changes at the distal tibia (arrow), and prominent tibiotalar joint effusion (arrow head). This patient underwent subsequent MRI of the ankle as shown in Fig. 2.11a, b

Joint fluid cultures were positive for *Streptococcus pneumoniae*.

Diagnosis

Septic tibiotalar joint.

Discussion

Figure 5.6 depicts prominent osteopenia and erosive changes consistent with the presence of an inflammatory arthritis. In adults, the ankle is the third most common site of involvement of nongonococcal septic arthritis, following the knee and hip.

Case 6

71-year-old female who has known diagnosis of rheumatoid arthritis on biologic therapy presents to her regular clinic visit with more progressive ankle pain over the last several months (*courtesy of Dr. Mondira Sengupta*).

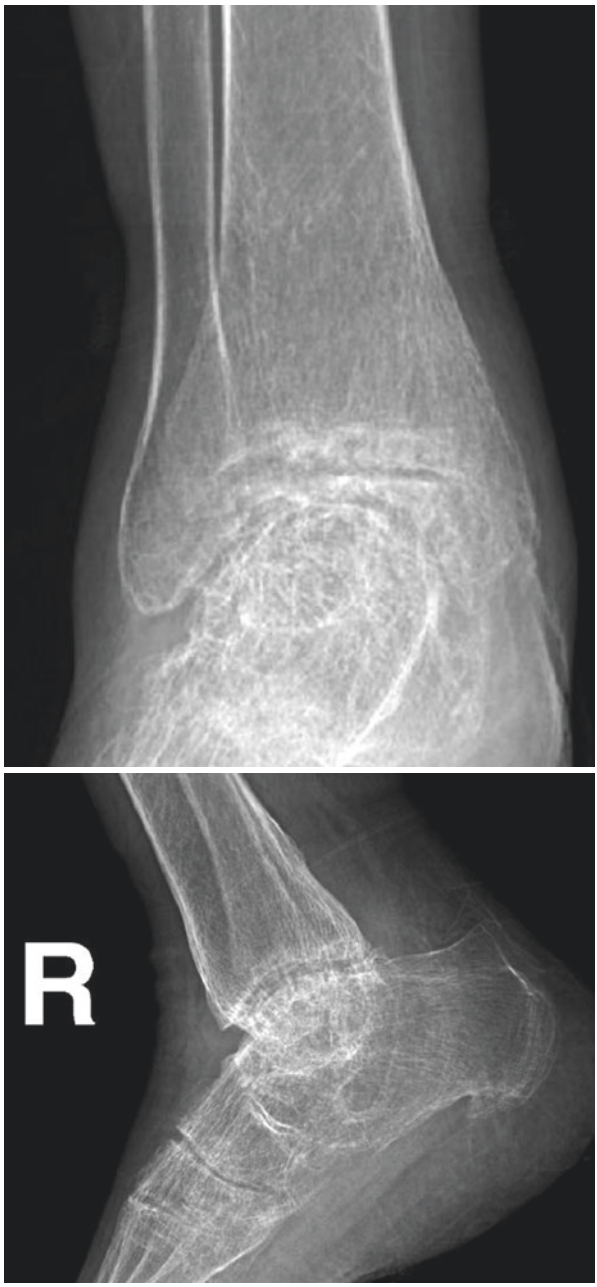

Figs. 5.7 and 5.8 Frontal and lateral views of the ankle demonstrate diffuse demineralization with marked, uniform tibiotalar joint space narrowing. Superimposed marginal sclerosis and subcortical cysts at the tibiotalar articulation

Diagnosis
Known rheumatoid arthritis with secondary osteoarthritis.

Discussion
Secondary osteoarthritis can occur in the setting of long-standing, quiescent inflammatory arthropathies, most commonly rheumatoid arthritis. Other conditions in which the articular cartilage is damaged including, trauma, infection, and CPPD, may also predispose the joint to develop osteoarthritis. The radiographic manifestations are similar to primary osteoarthritis (Figs. 5.7 and 5.8). The clinical history and superimposition of productive and reparative changes on rheumatoid erosions are the key features in this diagnosis.

Case 7
A 25-year-old with long-standing foot and hand pain.

Fig. 5.9 AP radiograph demonstrates diffuse osteopenia, tarsal ankylosis (arrow head), first MTP joint space narrowing, and epiphyseal widening of the base of the first proximal phalanx (arrow). In addition, there is diminutive appearance of the fifth metatarsal head, and fibular subluxations of the third through fifth proximal phalanges relative to the metatarsal heads

Diagnosis
Juvenile idiopathic arthritis.

Discussion
In general, radiographic manifestations of JIA may mirror adult rheumatoid arthritis with two notable exceptions; there is significant erosive disease with relatively late joint space loss, and there is often periostitis in the metaphyses of the metacarpals and metatarsals. Radiographic manifestations in the foot are similar to those seen in the hands. The tarsal bones may be fused as seen in this example (Fig. 5.9).

Case 8
A 48-year-old female with worsening foot pain and history of intermittent skin rash.

Fig. 5.10 The image demonstrates soft tissue swelling of the second toe with fibular subluxation of the second distal phalanx relative to the middle phalanx. There are erosive changes of the third, fourth, and fifth metatarsal heads (arrow heads) and pencil-in-cup deformity of the second and fifth DIPs (arrows)

Diagnosis
Psoriatic arthritis.

Discussion
The distribution of psoriatic arthritis in the foot can be similar to rheumatoid arthritis (involving the MTP and PIP joints) or may be limited to the DIPs and PIPs. But involvement of joints overall tends to be asymmetrical. Involvement of the MTP joints is more common than involvement of MCPs in the hands. Severe erosive changes and tapering of the proximal portion of the affected joint with bony overgrowth of the distal joint results in "pencil-in-cup" deformities (Fig. 5.10).

Case 9

A 58-year-old alcoholic patient with fever, fatigue, and dull lateral foot pain over the past several days. On physical examination, the patient was found to be tachycardic with moderate foot swelling laterally. The lateral forefoot was tender to palpation with moderate crepitus present.

Fig. 5.11 Marked soft tissue prominence within the lateral forefoot surrounding the fifth digit, with significant areas of soft tissue emphysema present (arrows)

Diagnosis

Necrotizing fasciitis.

Discussion

Necrotizing fasciitis is a progressive, often fatal soft tissue infection with reported levels of mortality as high as 70–80%. Clinical features may be nonspecific, including fever, malaise with often only vaguely localized symptoms. This entity

is most often a polymicrobial infection characterized by rapid soft tissue damage by liquefied necrotic tissue from bacterial endotoxins released into the deep fascial layers.

Necrotizing fasciitis is a clinical diagnosis although imaging may be of benefit to evaluate extent of disease and operative planning. The presence of soft tissue gas on imaging is characteristic for this process (Fig. 5.11); however this is seen in a minority of cases. CT is the most sensitive for detection of soft tissue gas (Fig. 1.18). Inflammatory edema involving the deep fascial layer separates necrotizing fasciitis from cellulitis and is best detected by MRI. However, particularly in patients who are severely ill, treatment should not be delayed for performance of cross-sectional imaging.

Patients at increased risk for necrotizing fasciitis include elderly or immunosuppressed patients. In addition, diabetics, HIV positive patients, patients undergoing chemotherapy, and alcohol or IV drug abusers are also at increased risk.

Case 10

A 39-year-old former college soccer player athlete with persistent ankle pain.

Fig. 5.12 AP image of the ankle demonstrates an ovoid lucency at the medial talar dome (arrow). The tibiotalar joint is well preserved

Diagnosis

Talar dome osteochondral defect.

Discussion

This is focal area of articular and osseous damage which can range in severity, often secondary to inversion or eversion injuries of the ankle. Talar dome osteochondral lesions (Fig. 5.12) may occur from impaction of the talus against the tibia, and are often associated with ligamentous injuries. The medial and lateral aspects of the dome of the talus are affected with equal frequency. MRI is often of benefit to demonstrate whether this fracture is unstable, in which case surgery is often indicated.

Practice Questions

Question 1 A 38-year-old male with foot pain.

What is the patient's most likely underlying diagnosis?

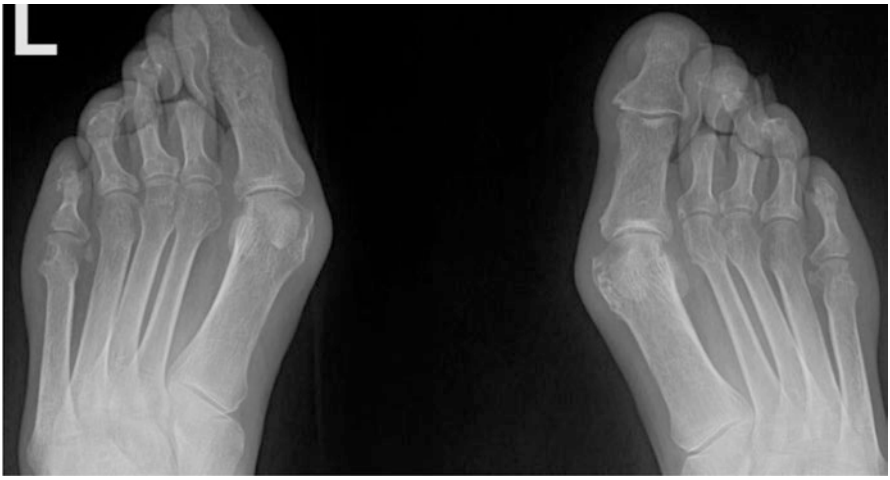

A. Rheumatoid arthritis.
B. Psoriatic arthritis.
C. Gout.
D. Osteoarthritis.

Discussion
Frontal images of both feet (See fig above) depict erosive changes within several metatarsal heads, pencil-in-cup deformity of the left fourth DIP, and partial bony ankylosis of the left first IP joint. The findings are indicative of an underlying inflammatory process. The distribution and presence of osseous ankylosis favors the diagnosis of psoriatic arthritis over rheumatoid arthritis.

Question 2 A 60-year-old patient with lateral foot pain. What is the most likely diagnosis?

What is the most reasonable imaging diagnosis?

A. Osteomyelitis.
B. Charcot arthropathy.
C. Osteoarthritis.
D. Gout.

Discussion

AP image of the foot (See fig above) depicts skin defect and focal swelling lateral to the fifth metatarsal head. There are erosive changes of the metatarsal head with relative preservation of the adjacent joint space. Soft tissue irregularities suggest skin ulceration. In addition, Extensive vascular calcifications are noted. The osseous destructive changes adjacent to the skin defect are most consistent with osteomyelitis. Osteomyelitis can arise from adjacent septic arthritis, from hematogenous

spread or direct inoculation from trauma or surgery. The presence of a skin ulcer, particularly in the presence of sinus tract or surrounding tissue necrosis, increases the risk infection of the underlying bone.

Question 3 Acute onset foot pain, swelling, redness.

What is the most likely underlying diagnosis?

A. JIA.
B. Gout.
C. Pyrophosphate arthropathy.
D. Neuropathic arthropathy.

Discussion

Lateral radiograph of the foot (See fig above) depicts extensive erosive and atrophic changes of the talus, calcaneus, and the tarsal bones of the midfoot which can be seen in the spectrum of neuropathic changes. JIA would not be expected to result in this degree of atrophic and erosive changes. Gout commonly affects the first MTP and would be expected to result in prominent well-marginated erosions with "over-hanging" edges. Pyrophosphate arthropathy is not often associated with the foot.

Question 4 A 50-year-old female with atraumatic medial foot pain, worsened when walking. Radiographs were unremarkable.

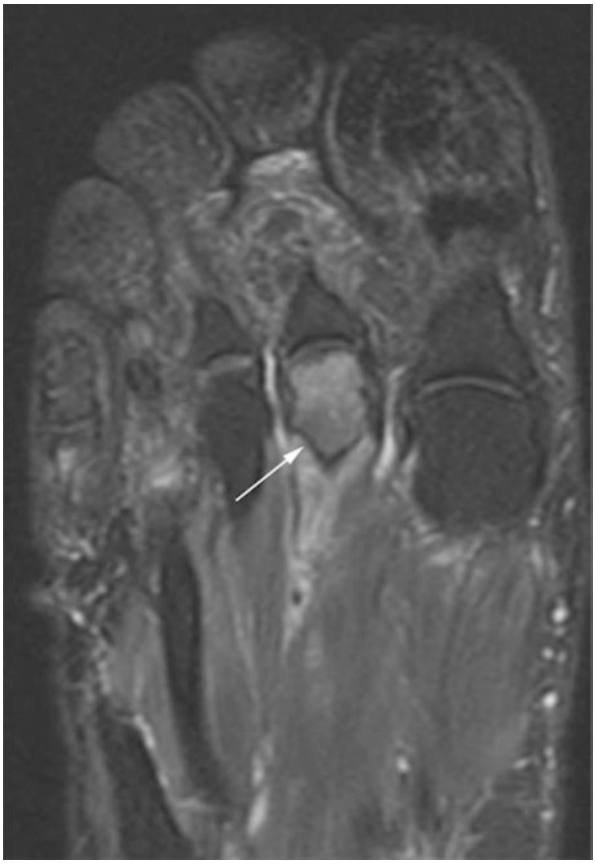

A. Gout.
B. Osteoarthritis.
C. Freiburg infraction.
D. Charcot arthropathy.

Discussion

This long-axis fat saturation MRI image (See fig above) demonstrates focal marrow edema (arrow) in the second metatarsal head with surrounding edema in the adjacent soft tissues. As discussed previously, MRI is a highly sensitive modality to detect marrow edema. Marrow edema carries a broad differential diagnosis, but in this specific location, suggestive of Frieburg infraction.

The term infraction refers to an incomplete fracture of the bone without displacement. This process is characterized by osteochondrosis of the metatarsal head with

subsequent subchondral collapse, secondary to vascular compromise, most often seen in the second metatarsal head, occasionally also seen involving the third metatarsal head. Studies suggest that the second and to a lesser extend the third metatarsal heads are relatively less mobile, and less able to disperse the associated biomechanical forces during weight bearing. The entity manifests predominantly in females (5:1 female to male ratio) but is relatively uncommon.

Answers to the Question

Q1: B. Psoriatic arthritis.
Q2: A. Osteomyelitis
Q3: D. Neuropathic arthropathy
Q4: C. Freiburg infraction

Further Reading

Chaudhry AA, Baker KS, Gould ES, Gupta R. Necrotizing fasciitis and its mimics; what radiologists need to know. Am J Roentgenol. 2015;204:128–39.

Chew FS, Bui-Mansfield LT, Kline MJ. Musculoskeletal imaging. Philadelphia: Lippincott Williams & Wilkins. 2003:p. 329–79.

Fugitt JB, Puckett ML, Quigley MM, Kerr SM. Necrotizing fasciitis, AFIP archives. Radiographics. 2004;24(5):1472–6.

Kaplan PA, Helms CA, Dussault R, Anderson MW, et al. Musculoskeletal MRI. Philadelphia: WB Saunders Co. Ltd. 2003:p. 422.

Klippel JH, Crofford LJ, Stone JH, Weyand CM. Arthritis Foundation. In: Primer on rheumatologic diseases. 12nd ed. Atlanta. 2003:p. 233–4.

Seetharaman M, Brent HL. Ankylosing Tarsitis; images in rheumatology. J Rheumatol. 2003;30(3):630–1.

Sommer OJ, Kladosek A, Weiler V, Czembirek H, Boeck M, Stiskal M. A practical guide to state-of-the-art imaging, image interpretation, and clinical implications. Radiographics. 2005;25:381–98.

Torriani M, Thomas BJ, Bredella MA, Ouellette H. MRI of the metatarsal head subchondal fractures in patients with forefoot pain. Am J Roentgenol. 2008;190:570–5.

Chapter 6
Knee

Anupam Basu

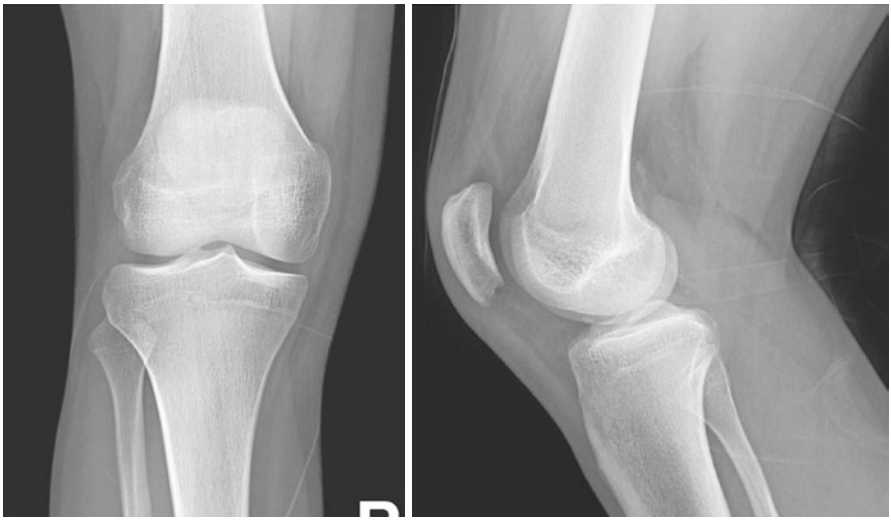

Figs. 6.1 and 6.2 Normal frontal and lateral radiographs of the knee

Standard views of the knee include AP standing view and lateral flexed view (Figs. 6.1 and 6.2). Standing view provides better assessment of the cartilage loss of the medial and lateral compartment. Lateral and "sun-rise" views allow evaluation of the patellofemoral joint. Each compartment should be analyzed individually and should demonstrate at least 3 mm of space.

A. Basu (✉)
Cook County Health, Department of Radiology, Chicago, IL, USA
e-mail: abasu@cookcountyhhs.org

R. S. Katz, A. Basu (eds.), *Diagnostic Radiology of the Rheumatic Diseases*,
https://doi.org/10.1007/978-3-030-25116-1_6

Assessment of knee radiographs begins with determination of the pattern of joint space narrowing which typically can be subdivided into three categories: processes that result in tricompartmental joint space loss, processes that specifically involve a specific compartment, or processes that initially do not result in joint space loss. Once the pattern of joint space loss is determined, often additional radiographic hallmarks discussed above in the "approach to the hand" section, in conjunction with physical exam and lab findings, can be used to further narrow the differential diagnosis (Table 6.1).

Table 6.1 Patterns of joint space narrowing in the knee

Total compartment involvement	Preferential compartment loss	Initial joint space preservation
Rheumatoid arthritis	Osteoarthritis	AVN
Psoriatic arthritis	CPPD arthropathy	Osteochondral defect
Reactive arthritis		
JIA		
Hemophilia		
Ankylosing spondylitis		
Septic arthritis		

Case 1

A 68-year-old male with worsening knee pain over several years, aggravated by walking or exercise.

Fig. 6.3 AP view of the knee demonstrates the radiographic hallmarks of osteoarthritis, including asymmetric joint space narrowing (arrows), sclerosis, and osteophyte formation (arrow heads)

Diagnosis Osteoarthritis.

Discussion

The knee is the most commonly involved joint in osteoarthritis. It is characterized by nonuniform joint space loss most commonly in the medial compartment (Fig. 6.3). In the knee, prior traumatic injury, particularly to the meniscus or the anterior cruciate ligament, can lead to accelerated onset of osteoarthritis (Table 6.2).

Table 6.2 Kellen and Lawrence radiographic scoring of knee OA

Grade	Description
0: Normal	
1: Questionable	Doubtful narrowing of the joint space and possible osteophyte lipping
2: Mild	Definite osteophytes and possible narrowing of the joint space
3: Moderate	Moderate multiple osteophytes, definite narrowing of the joint space, and some sclerosis with deformity of the bone ends
4: Severe	Large osteophytes, marked joint space narrowing, severe sclerosis, and definite deformity of the bone ends

Case 2

A 67-year-old male with knee pain, swelling.

Fig. 6.4 Lateral view of the knee demonstrates near complete loss of the patellofemoral joint space (arrow) with suggestion of subtle scalloping of the distal femur (arrow head) which is a result of repetitive movement of the patella as it abuts the femur when the knee is in extension

Diagnosis Calcium pyrophosphate deposition disease (CPPD).

Discussion
Calcium pyrophosphate deposition disease (CPPD) is the most common crystal arthropathy, and second in prevalence only to osteoarthritis. The changes very closely mirror osteoarthritis but in the knee are more pronounced in the patello-femoral compartment (Fig. 6.4). Chondrocalcinosis need not be present on imaging to raise suspicion for CPPD arthropathy. The knee is the most common joint involved in CPPD. Other joints affected include the hip, wrist, and spine.

Case 3
A 32-year-old male with long-standing knee pain, swelling, and diminished range of motion.

Fig. 6.5 AP view of the knee demonstrates widening of the intercondylar notch and overgrowth of the epiphyses (arrow). Prominent subchondral cysts are also evident (arrowhead)

Diagnosis Hemophilia.

Discussion
Rare, X-linked disorder that results in spontaneous bleeding into the synovial joints and resultant articular abnormalities. The most commonly affected joint is the knee, followed by ankle, elbow, shoulder, and hip in decreasing order of frequency. Recurrent intra-articular hemorrhage causes an inflammatory response within the

joint that is ultimately damaging to the cartilage. Radiographic hallmarks of this process include joint space narrowing, intermittent large joint effusion, epiphyseal "ballooning" or overgrowth (Fig. 6.5), soft tissue swelling, and erosions.

Differential considerations include: juvenile idiopathic arthritis, tuberculosis arthritis, and pigmented villondular synovitis (PVNS).

Case 4

A 35-year-old male with knee pain, swelling, locking, and diminished range of motion.

Fig. 6.6 Lateral radiograph of the knee demonstrates multiple relatively uniform lobulated calcified bodies within the suprapatellar bursa (arrows). Note the relatively preserved joint space, and normal mineralization, with are the radiographic hallmarks of primary synovial chondromatosis

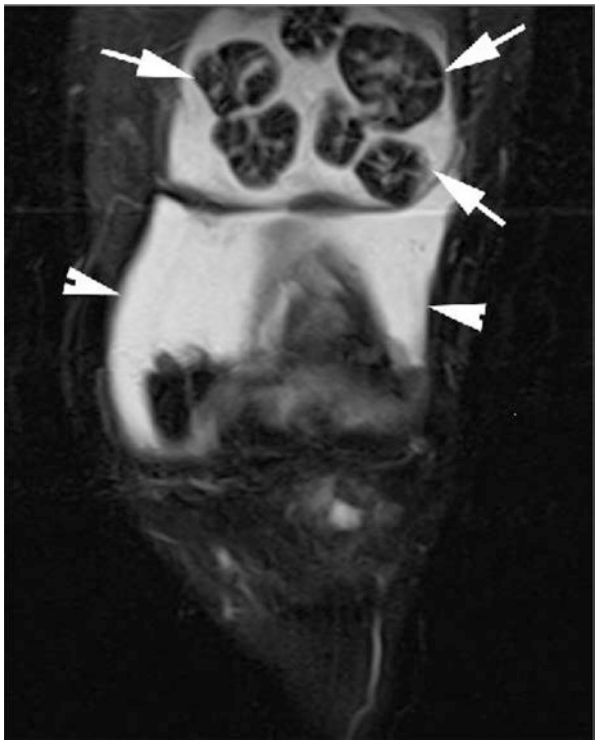

Fig. 6.7 Coronal T2 fat saturation image of the knee demonstrates relatively uniform low T2 signal masses (arrows) within a suprapatellar joint effusion (arrowheads). The MRI appearance of this entity can vary depending on the degree of ossification of the chondral bodies

Diagnosis Primary synovial osteochondromatosis.

This is a benign, relatively rare entity that typically affects patients in the third to fifth decade of life, most commonly affecting the knee. It is characterized by proliferation and sloughing of the synovium with intra-articular loose bodies that often subsequently calcify (Figs. 6.6 and 6.7). Reports suggest males are affected two to four times more often than women. It is often asymptomatic unless accompanied by osteoarthritis. Other joints involved include the hip, elbow, shoulder, and ankle. Reports of malignant transformation of primary synovial osteochondromatosis to chondrosarcoma exist in the literature, though this is considered extremely rare.

Case 5
A 45-year-old female with diffuse joint pain for several months, most pronounced in the wrists and knees bilaterally.

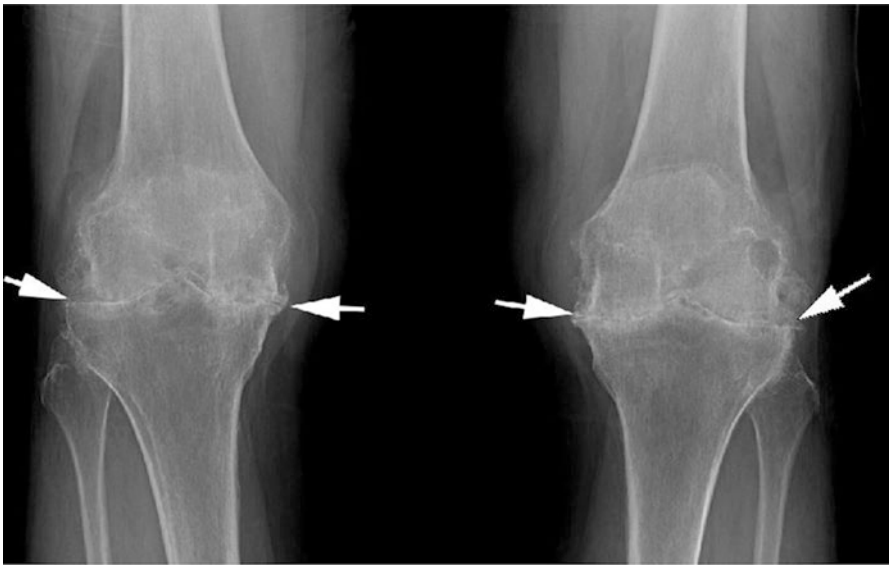

Fig. 6.8 Frontal standing views of both knees depict severe bilateral, *symmetric* joint space narrowing (arrows) with relative paucity of productive changes

Diagnosis Rheumatoid arthritis.

Discussion
The knees are affected in 75–80% of patients with rheumatoid arthritis, and typically affect both knees. Ideally, radiographs include standing AP and flexed lateral views to best assess alignment and joint spaces. This absence of productive change and symmetric joint space narrowing is the radiographic hallmark of rheumatoid arthritis in the knee (Fig. 6.8), and other larger joints, although erosions can also be seen.

Case 6

A 43-year-old man who presents with knee swelling, redness, and pain following arthroscopic procedure 2 weeks prior for meniscal repair.

Fig. 6.9 Lateral image of the knee depicts a large joint effusion (arrows), suggestion of periarticular osteopenia as depicted by subtle lucencies within the femoral condyles (arrowheads). No definite erosions or productive change are seen

Fig. 6.10 Axial STIR image of the knee demonstrates suprapatellar joint effusion (arrowhead), marrow edema (white arrow) and perisynovial edema (black arrow) suggesting the presence of an inflammatory process within the synovium

Diagnosis Septic knee.

Discussion

The knee is the most common site of septic arthritis. As stated previously, rapid diagnosis of septic arthritis requires a high degree of clinical suspicion, and a close level of interaction with the radiologist and the managing clinicians. The initial imaging manifestation is the presence of a joint effusion which is appreciated in the knee on the lateral radiograph (Fig. 6.9).

MRI can be helpful as an adjunct to diagnosis when clinical findings are equivocal. MR findings include marrow edema, erosions, synovial thickening, and perisynovial enhancement (Fig. 6.10).

Case 7

A 57-year-old female with worsening knee pain over several years.

Fig. 6.11 Lateral knee radiograph reveals broad-based calcific density arising from the posterior aspect of the proximal tibia (arrow). In addition, smaller excrescences arising from the distal femur (arrow heads), oriented perpendicular to the long axis of the native bone. The distal femur demonstrates a widened metadiaphyseal junction

Diagnosis Hereditary multiple exostoses (HME).

Discussion

This is a rare, hereditary condition transmitted in an autosomal dominant fashion resulting in multiple bony exostoses, or osteochondromas, throughout the skeleton, most often around the knee and shoulder. Males are affected 1.5 times more commonly than females, likely to a hypothesized incomplete penetrance in females, possibly a result of hormonal factors. Complications of the presence of these osteochondromas (Fig. 6.11) include growth disturbances and metaphyseal widening. The widening of this region results in the "Erlenmeyer flask" deformity which is one hallmark of this condition. Forty percent of the patients with HME manifest clinically with short stature. Local complications include fracture of osteochondroma, regional mass effect on adjacent nerves or blood vessels, and formation of neobursa. The joint space is not directly affected.

The most feared complication of osteochondroma is malignant transformation to chondrosarcoma, which reportedly occur in 3–5% of patients with HME.

Case 8

A 76-year-old female admitted for chest pain, rheumatology consulted for knee and thigh pain, history of prior car accident when the patient was very young.

Fig. 6.12 This lateral view of the knee demonstrates marked joint space narrowing between the femur and the tibia (white arrows), with anterior subluxation of the femur. In addition, there are calcific densities of varying sizes surrounding the remnant knee joint (black arrow heads). The quadriceps tendon (white arrowheads) and the patella (∗) are shown for orientation. (*Courtesy Dr. Aman Kugasia*)

Diagnosis Neuropathic joint.

Discussion

Neurosensory loss is the basic cause of a wide variety of diseases that result in eventual neuropathic arthropathy. The most common cause of neuropathic changes within the knee historically is related to tertiary syphilis, or tabes dorsalis which results in demyelination of the posterior columns of the spinal cord. Diabetes can also result in neuropathic changes at the knee. Recurrent joint effusions and subluxations occur and eventually become more pronounced with continued weight bearing. Radiographic findings (Fig. 6.12) which include malalignment, joint space narrowing, calcific debris, and sclerosis may overlap with findings of osteoarthritis and infection.

Case 9
A 38-year-old male with chronic knee pain over several years.

Fig. 6.13 Frontal image of the knee demonstrates a curvilinear lucency in the subchondral portion of the medial femoral condyle (arrow)

Diagnosis Osteochondral defect.

Discussion
As discussed in chap. 5, osteochondral defects, formerly called osteochondritis dessicans, typically arise from traumatic injury to the articular cartilage and the underlying bone. Sequelae of these injuries typically results in lucent defect within the articular bone (Fig. 6.13). The most common location for these lesions is the lateral portion of the medial femoral condyle. Differential considerations given the radiographic appearance include osteonecrosis, subchondral fracture, or osteoarthritis. MRI is typically obtained to better characterize osteochondral defects and assess the need for operative intervention.

Practice Cases

Question 1. A 34-year-old with known history of lupus and worsening dull knee pain over several months.

What is the most likely etiology of the patient's knee pain?

A. Osteoarthritis.
B. CPPD arthropathy.
C. Avascular necrosis.
D. Rheumatoid arthritis.

Discussion
Lateral and oblique views of the knee (See figs above) demonstrate linear sclerosis of the lateral joint compartment with subchondral surface irregularity (best seen on the lateral view). These serpiginous or linear areas of sclerosis imply disruption of blood supply to the bone, resulting in bone death. By convention, the term avascular necrosis is used to describe areas of subarticular involvement. When the diaphyseal or metaphyseal portions of the bone are involved, the term bone infarct is applied. The joint spaces are relatively well maintained initially in avascular necrosis.

Question 2. A 38-year-old female presents with long-standing bilateral knee swelling and pain most pronounced in the right knee.

The most likely diagnosis is?

A. Rheumatoid arthritis.
B. Psoriatic arthritis.
C. CPPD arthropathy.
D. Hemophilia.

Discussion

The knee is affected in the majority of patients with rheumatoid arthritis. The above image depicts marked, symmetric joint space narrowing in both the medial and lateral compartments with relative absence of productive changes. There are prominent erosive changes present. Psoriatic arthritis may involve the knee, but typically presents with enthesopathic changes at the extensor tendons, rather than the extensive erosive changes seen above. CPPD involves the patellofemoral compartment asymmetrically (Fig. 6.4) and does not typically result in such extensive erosive changes. Hemophilia can result in erosive changes secondary to the deleterious effects of recurrent intra-articular hemorrhage (Fig. 6.5), though the entity is X-linked, and therefore seen only in male patients. Note, septic arthritis was not listed as an option, and must always be considered in the setting of isolated erosive changes involving a single joint.

Question 3. Given the following lateral radiograph in a patient with atraumatic knee pain, the best next step in the management of the patient is which of the following?

A. Knee MR arthrogram.
B. CT angiogram.
C. Standing radiographs of both knees.
D. Arthrocentesis of the knee.

Discussion

The lateral knee radiograph depicts a large joint effusion with pockets of superimposed gas. The presence of a large effusion with areas of intra-articular gas is nearly pathognomonic for septic arthritis; therefore, further imaging should not precede an arthrocentesis (See fig above).

Question 4. This image best supports which diagnosis?

A. Pigmented villonodular synovitis (PVNS).
B. Synovial osteochondromatosis.
C. Tuberculous arthritis.
D. Scleroderma.

The lateral radiograph of the knee (See fig above) depicts numerous calcified foci grouped together posterior to the knee joint, which is a typical appearance of intra-articular bodies clumped within a Baker's cyst, confirmed on subsequent MRI (not shown). Pigmented villonodular synovitis (PVNS) is a synovial proliferative disorder which results in a joint effusion and possible erosive changes with preservation of the joint space. This entity rarely calcifies, thus is not the best answer choice.

Answers to the Question

Q1: C. Avascular necrosis
Q2: A. Rheumatoid arthritis
Q3: D. Arthrocentesis of the knee
Q4: B. Synovial osteochondromatosis

Further Reading

Jones EA, Manaster BJ, May DA, Disler DG. Neuropathic osteoarthropathy: diagnostic dilemmas and differential diagnosis. Radiographics. 2000;20:S279–93.

Manaster BJ. Diagnostic imaging musculoskeletal: non-traumatic disease. 2nd ed. Philadelphia: Elsevier; 2016. p. 1044–7.

Murphey MD, Choi JJ, Kransdorf MJ, Flemming DJ, Gannon FH. Imaging of osteochondroma: variants and complications with radiologic-pathologic correlation. Radiographics. 2000;20:1407–34.

Murphey MD, Vidal JA, Fanburg-Smith JC, Gajewski DA. Imaging of synovial chondromatosis with radiologic-pathologic correlation. Radiographics. 2007;27:1465–88.

Resnick D, Kransdorf MJ. Bone and joint imaging, 3rd ed. Philadelphia. Elsevier Saunders; 2005: 357–393.

Chapter 7
Hip

Anupam Basu

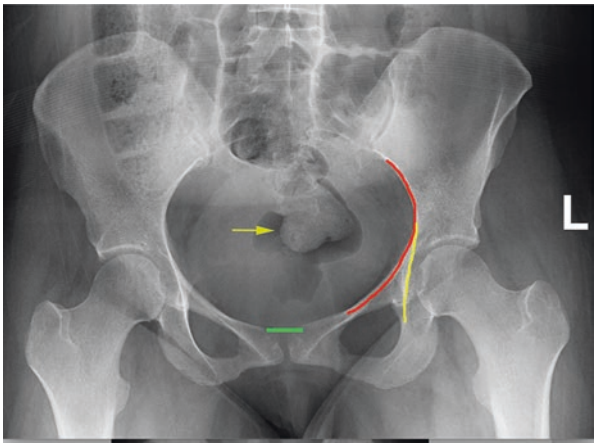

Fig. 7.1 Normal AP view of the pelvis; iliopectineal line (red) and ilioischial line (yellow). Sacrococcygeal junction (yellow arrow), upper border of the pubic symphysis (green line)

Assessment of suspected joint disease of the hip begins with properly positioned AP view of the pelvis (Fig. 7.1). A well-positioned AP view of the pelvis has little to no pelvic tilt. Pelvic tilt is assessed by measuring the distance from the sacrococcygeal junction to the upper border of the pubic symphysis. This should not exceed 4 cm on a well-positioned frontal view.

A. Basu (✉)
Cook County Health, Department of Radiology, Chicago, IL, USA
e-mail: abasu@cookcountyhhs.org

R. S. Katz, A. Basu (eds.), *Diagnostic Radiology of the Rheumatic Diseases*,
https://doi.org/10.1007/978-3-030-25116-1_7

Case 1
A 32-year-old male former college basketball player with worsening, atraumatic hip pain over several months.

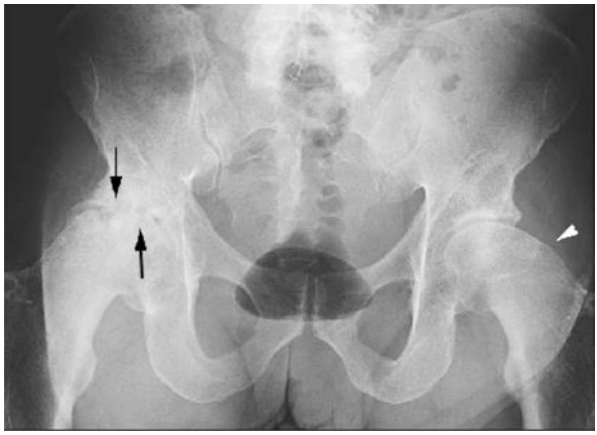

Fig. 7.2 Marked superior joint space narrowing of the right hip with marginal osteophyte formation and subchondral sclerosis (black arrows). The left hip demonstrates osseous protrusion at the femoral head/neck junction (white arrow), suggestive of femoroacetabular impingement

Diagnosis Femoral acetabular impingement with secondary OA.

Discussion
Classic imaging features of hip osteoarthritis include joint space narrowing and superolateral migration of the femoral head, although 20% of patients with osteoarthritis develop axial/circumferential femoral head migration. Productive changes and subcortical cyst formation are also typically seen. Many young patients with osteoarthritis of the hip have underlying morphologic disorder such as femoral acetabular impingement seen above (Fig. 7.2). Femoral acetabular impingement involves either acetabular over-coverage, Pincer deformity, or anterolateral femoral neck osseous bump, CAM deformity. Often these two deformities may coexist. Developmental dysplasia may also predispose to osteoarthritis. Developmental dysplasia manifests as under-coverage of the femoral head by the acetabulum. The presence of these morphologic deformities makes the acetabular labrum, the ring of cartilage that lines the outside rim of the socket of the hip joint, susceptible to damage. Damage to the acetabular labrum accelerates the destruction of the remaining underlying cartilage.

Case 2
A 42-year-old female with several years of back, hip, and hand pain.

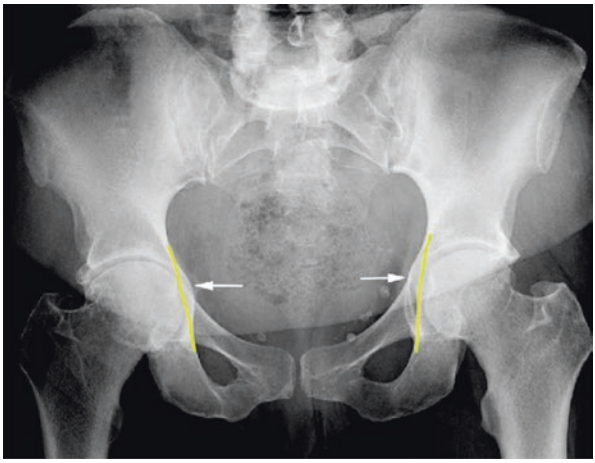

Fig. 7.3 AP view of the pelvis demonstrates relatively uniform axial migration of both femoral heads. The medial acetabular wall normally projects lateral to the ilioischial line (yellow lines). If the acetabular walls (white arrows) project medial to the ilioischial line, the patient has protrusio acetabuli. The generally accepted measurements for medial projection are 3 mm in men and 6 mm in women to qualify for protrusion

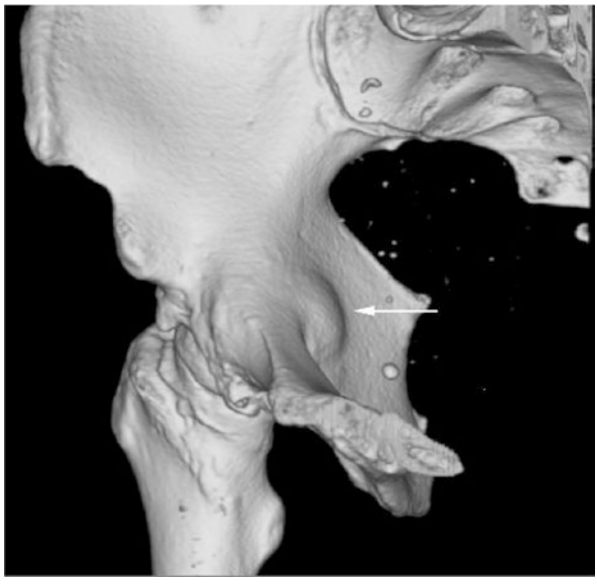

Fig. 7.4 Three-dimensional volumetric reconstruction of the pelvis demonstrates protrusion of the right medial acetabular wall resulting in bowing of the ischium (arrow)

Diagnosis Rheumatoid arthritis with protrusio acetabuli.

Discussion

The hips are affected in half of patients with rheumatoid arthritis. Imaging manifestations include osteopenia, bilateral uniform cartilage loss with axial migration of the femoral head within the acetabulum. Progressive axial migration can eventually result in protrusio acetabuli (Figs. 7.3 and 7.4). CPPD and ankylosing spondylitis may also demonstrate uniform cartilage destruction and axial migration of the femoral heads; these entities can also result in protrusio acetabuli, although typically to a lesser extent.

Erosive changes of the hips may be present in rheumatoid arthritis, but as with all inflammatory arthropathies, there is general absence of productive changes. Complications of long-standing rheumatoid arthritis of the hips include insufficiency fractures of the femoral neck and avascular necrosis of the femoral head due to prolonged steroid use.

Case 3

Gradually worsening hip pain over several weeks. History of long transcontinental flight approximately 7 months prior.

Fig. 7.5 AP view of the pelvis demonstrates left hip osteopenia. In addition, there are erosive changes of the femoral head (white arrows). Erosive changes are also evident within the medial acetabulum, resulting in apparent widening of the joint space (white arrow)

Fig. 7.6 CT coronal reformatted image of the pelvis (bone window) demonstrates erosive changes at the medial acetabulum (arrow) and the superior femoral head (arrow head)

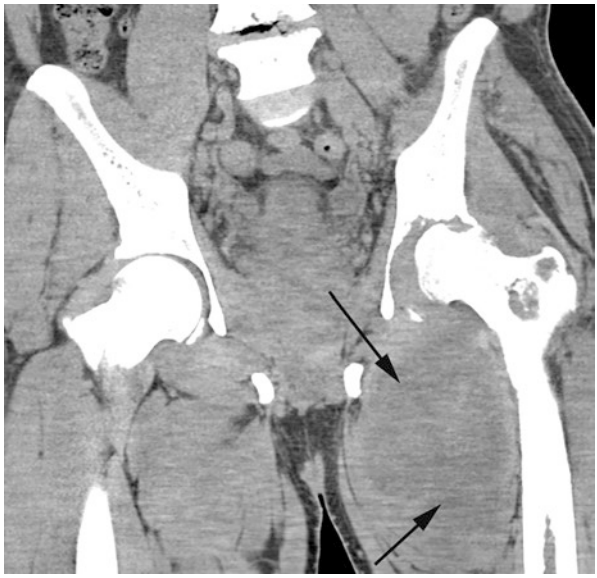

Fig. 7.7 CT coronal reformatted image of the pelvis (soft tissue window) demonstrates a large joint effusion and a large fluid density collection centered within the iliopsoas and adductor longus muscles consistent with intramuscular abscess (arrows)

Diagnosis TB septic arthritis.

Discussion

In developed countries, musculoskeletal manifestations of TB are typically seen in adults, and half of the cases involve the spine. The next most common sites are the hips and knees. The classic radiographic features have been described collectively as Phemister's triad, which includes juxta-articular osteoporosis, peripheral erosions, and late onset joint space narrowing (Fig. 7.5). Cross-sectional imaging

(Figs. 7.6 and 7.7) better depicts the soft tissue abscesses that are often associated with tuberculous septic arthritis.

Delay in diagnosis is common due to lack of clinical suspicion and relatively indolent onset of symptoms and imaging findings. As with pyogenic septic arthritis, definitive diagnosis requires either joint fluid sampling or synovial biopsy.

Case 4

A 32-year-old male with hip and back pain for several years presents as a new patient to establish care.

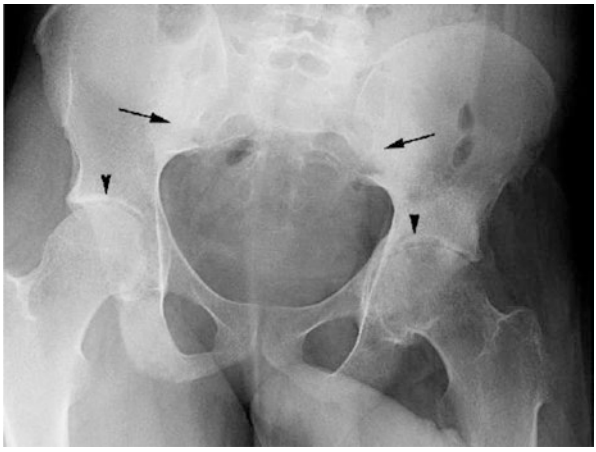

Fig. 7.8 AP image of the pelvis demonstrates bilateral sacroiliac joint fusion (arrows). There is circumferential hip joint space narrowing bilaterally (arrow heads). Note normal mineralization and normal contours of the femoral heads, without significant productive or erosive changes

Diagnosis Ankylosing spondylitis.

Discussion

Another cause of hip pain in the young adult is seronegative spondyloarthropathy. The hip is involved in 50% of patients with ankylosing spondylitis. Generally, hip involvement is correlated with more severe spine involvement. Classic imaging features include uniform joint space loss in the hips with axial migration of the femoral head (Fig. 7.8). Axial migration is typically less pronounced than that seen in the setting of rheumatoid arthritis. Advanced cases may manifest with frank bony ankylosis of the hips.

Case 5

A 62-year-old male with history of alcohol abuse with gradually worsening hip pain over several years.

Fig. 7.9 AP view of the pelvis demonstrates patchy sclerosis within both femoral heads. There is relative preservation of the femoral head contour and hip joint spaces

Diagnosis Bilateral hip avascular necrosis.

Discussion

Avascular necrosis is a primary abnormality of the femoral head, with subsequent secondary degenerative changes with sparing of the joint space until late in the process. The femoral head is the most common site of avascular necrosis. As discussed previously, MRI is more effective in detecting the early changes associated with avascular necrosis. The earliest radiographic manifestation is disruption of the normal trabecular pattern within the femoral head. Subsequently, subtle relative sclerosis of the femoral head occurs as a manifestation of reparative changes (Fig. 7.9). Risk factors include chronic steroid therapy, prior trauma, alcohol abuse, pancreatitis, and sickle cell anemia.

Case 6

A 55-year-old man presents to the ED after having severe hip pain for several days. Upon questioning, reveals he bumped his hip against the bannister yesterday.

Fig. 7.10 AP view of the pelvis reveals subtle relative osteopenia of the left hip. The hip joint spaces appear well maintained. No subchondral collapse. No significant productive or erosive changes are identified

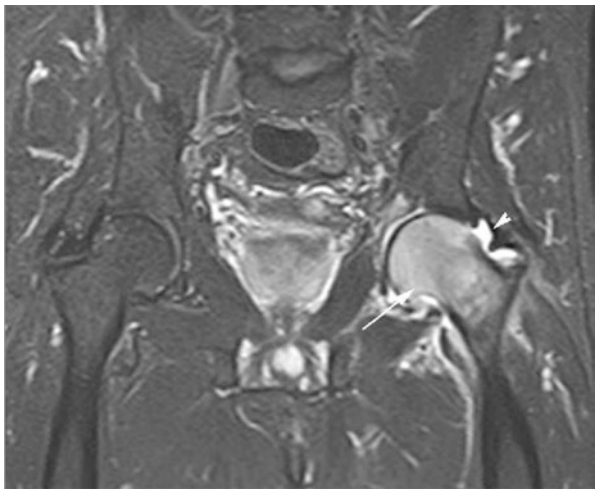

Fig. 7.11 Coronal STIR image of the pelvis demonstrates marked marrow edema (arrow) within the left femoral head and neck with small joint effusion (arrowhead)

Diagnosis Idiopathic transient osteoporosis.

Discussion

Subtle osteopenic changes may be present in the affected hip radiographically (Fig. 7.10), although changes on MRI are more convincing (Fig. 7.11). MR findings include diffuse marrow edema of the femoral head and neck which may extend to the intertrochanteric line. No subchondral sclerosis or fracture line was noted.

The history of trauma in this case prompted the ED to exclude early femoral neck fracture which can be occult on radiographs in older patients. Additional differential considerations include septic arthritis.

This entity is typically self-limited, more often seen in middle-aged men, although often described in women in their third trimester of pregnancy.

Practice Questions

Question 1 Which of the following conditions is most likely in this 55-year-old with gradually worsening bilateral hip pain?

A. Ankylosing spondylitis.
B. Avascular necrosis.
C. CPPD arthropathy.
D. Rheumatoid arthritis.

Discussion

AP image of the pelvis (See fig above) demonstrates significant circumferential hip joint space narrowing bilaterally resulting in axial migration of the femoral heads. In addition, there is significant productive change with prominent marginal osteophyte formation. Pyrophosphate arthropathy is the specific pattern of damage to the joints that results from deposition of crystal deposition within the cartilage. The chondrocalcinosis need not be visible to make the diagnosis of pyrophosphate arthropathy.

Manifestations of pyrophosphate arthropathy in the hip are commonly symmetrical. The imaging features of CPPD in the hip are a close mimic to osteoarthritis, including subchondral sclerosis, subcortical cystic changes, and osteophyte formation. Ankylosing spondylitis can also cause uniform joint space narrowing of the hips, but typically would also typically affect the SI joints, which appear normal in this case. Avascular necrosis can cause diffuse sclerosis of the femoral head, but

would be expected to result in predominantly superior joint space narrowing, and advanced AVN would be expected to result in prominent subchondral collapse.

Question 2 A 58-year-old female with acute onset of atraumatic lateral left-sided hip pain for the past 4 days. Mild pain when the hip is fully rotated.

Most likely diagnosis?

A. Avascular necrosis.
B. Hydroxyapatite deposition.
C. Rheumatoid arthritis.
D. Septic arthritis.

Discussion

AP image of the pelvis (See fig previous page) demonstrates subtle rounded calcification adjacent to the left greater trochanter, seen more clearly on the subsequent coronal reformatted CT of the hip (See fig previous page; white arrow).

Second to the rotator cuff muscles of the shoulder, the external rotator muscles of the hip, often described as the rotator cuff of the hip, manifest hydroxyapatite crystal deposition which can result in acute onset of pain. Findings are characterized by globular calcifications located within tendons or bursa. Small calcifications can be frequently overlooked on radiographs or MRI. Avascular necrosis would result in subchondral sclerosis within the femoral head. Rheumatoid arthritis and septic arthritis would result in circumferential joint space narrowing and medial migration of the femoral head with possible erosive changes.

Question 3 A 68-year-old male with persistent hip pain. Patient reportedly had "normal" radiographs at an outside hospital 2 months prior.

What is the most likely consideration in this patient?

A. Osteoarthritis.
B. Avascular necrosis.
C. CPPD arthropathy.
D. Rheumatoid arthritis.

Discussion

AP radiograph of the pelvis (See fig above) demonstrates a "hatchet" deformity with complete destruction of the femoral head. This, termed Postel OA, can be seen in rapidly progressive, destructive osteoarthritis, which can progress in a matter of weeks. Radiographic hallmark is the straight margin of the femoral neck and the rapidity of the process. Differential considerations include neuropathic and sequelae of previous septic arthritis.

Question 4 A 43-year-old with worsening hip pain for several weeks. Which of the following best explains the lucent focus seen in the intertrochanteric region of the right hip?

A. Osteosarcoma.
B. Aneurysmal bone cyst.
C. Osteochondroma.
D. Brodie's abscess.

Discussion

This AP image (See fig above) of the pelvis demonstrates a well-circumscribed lucent focus (between black arrow heads) within the intertrochanteric region of the right femur with narrow zone of transition and surrounding sclerotic rim. There is subtle lucent tract (black arrow) extending medially to the lesser trochanter. The surgical clips indicate operative intervention in this region. Though the radiographic findings are not completely specific, of the answer choices listed, the best answer is Brodie's abscess, which is subacute osteomyeltiits. Complete discussion of lucent bone lesions is beyond the scope of this text; however, osteosarcoma is an aggressive primary osseous malignancy most common on younger patients. The findings on radiographs typically include aggressive periosteal reaction surrounding a focal osseous lesion with wide zone of transition.

An aneurysmal bone cyst is an expansile lesion centered within the epiphysis, most often seen in long bones. An osteochondroma is a cartilage capped bony excrescence continuous with the cortex of a bone, most common in the femur and tibia.

Answers to the Question

Q1: C. CPPD arthropathy
Q2: B. Hydroxyapatite deposition
Q3: A. Osteoarthritis
Q4: D. Brodie's abscess

Further Reading

Boutry N, Paul C, Leroy X, Fredoux D, Migaud H, Cotten A. Rapidly destructive osteoarthritis of the hip: MR imaging findings. Am J Roentgenol. 2002;179(3):657–63.

Kim C, Linsenmeyer KD, Vlad SC, Guermazi A, Clancy MM, Niu J, Felson DT. Prevalence of radiographic and symptomatic hip osteoarthritis in an urban United States community: the Framingham osteoarthritis study. Arthritis Rheumatol. 2014;66(11):3013–7.

Manaster BJ. Diagnostic imaging musculoskeletal: non-traumatic disease. 2nd ed. Philadelphia: Elsevier; 2016. p. 1044–7.

Resnick D. Diagnosis of bone and joint disorders, vol. 5. 4th ed. Philadelphia: W.B. Saunders; 2002. p. 4870–919.

Resnick D, Kransdorf MJ. Bone and joint imaging, vol. 2005. 3rd ed. Philadelphia: Elsevier Saunders. p. p357–93.

Spicer PJ, Beaman F, Blomquist GA, Montgomery JR, Maxwell ME. Musculoskeletal imaging; a core review: Philadelphia: Wolters Kluwer; 2015. p. 206.

Chapter 8
Shoulder

Anupam Basu

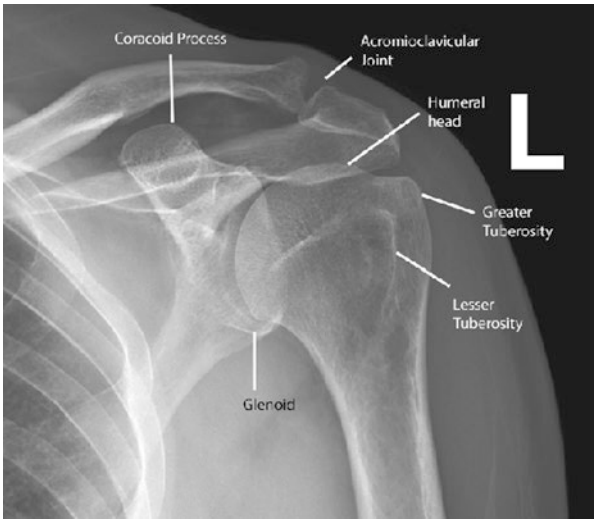

Fig. 8.1 Normal AP external rotation view of the shoulder

A standard shoulder series typically consists of AP internal, external rotation and scapular Y-views. Figure 8.1 provides the major osseous landmarks that are interpreted on a shoulder radiograph.

A. Basu (✉)
Cook County Health, Department of Radiology, Chicago, IL, USA
e-mail: abasu@cookcountyhhs.org

R. S. Katz, A. Basu (eds.), *Diagnostic Radiology of the Rheumatic Diseases*,
https://doi.org/10.1007/978-3-030-25116-1_8

Case 1
A 54-year-old male with progressive shoulder pain and decreased range of motion over several months duration.

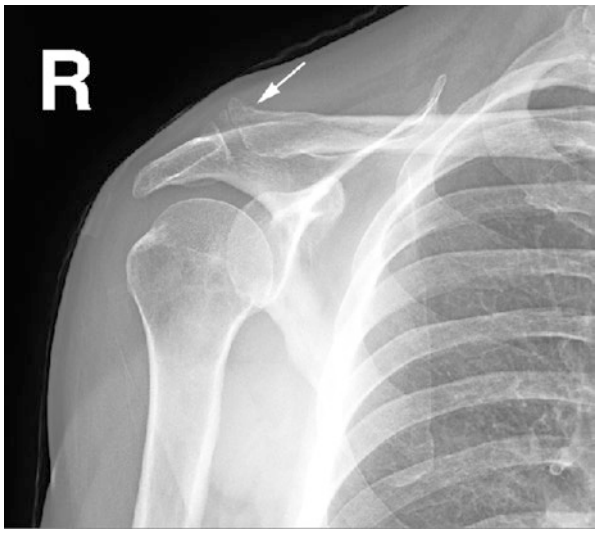

Fig. 8.2 AP view of the shoulder demonstrates moderate acromioclavicular joint space narrowing and osteophytes (white arrow)

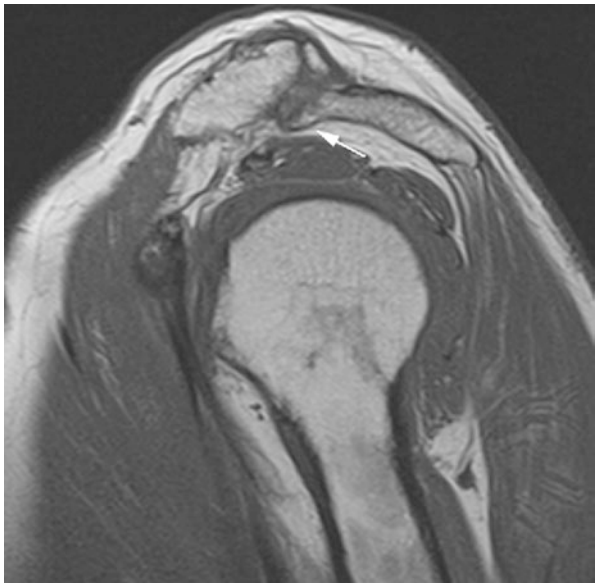

Fig. 8.3 Sagittal T1-weighted MR image demonstrates narrowing of the AC joint with formation of a bony excrescence (white arrow) arising from the site of osseous attachment of the coracoacromial ligament

Diagnosis Acromioclavicular osteoarthritis.

Discussion
Osteoarthritis is the most common type of arthropathy seen at the acromioclavicular joint, often secondary to prior trauma. Imaging (Figs. 8.2 and 8.3) reveals joint

space narrowing and marginal productive changes. Symptomatic acromioclavicular joint osteoarthritis is frequently associated with other pathologies of the shoulder including rotator cuff tears. It has been suggested that osteophytes at the acromioclavicular joint are an important contributor in the pathogenesis of supraspinatus tendon tears.

Case 2
A 50-year-old male with increasing shoulder pain over several months.

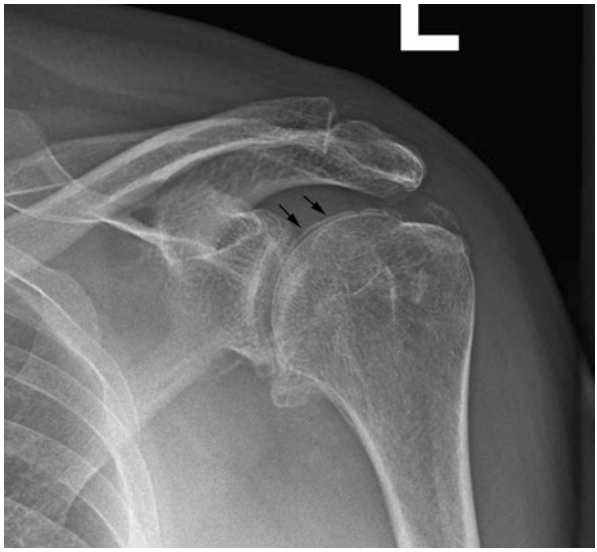

Fig. 8.4 Radiograph demonstrates mild narrowing of the glenohumeral joint space. The acromioclavicular joint space and the subacromial spaces are largely maintained. There are productive changes at the inferior aspect of the humeral head, and chondrocalcinosis is evident adjacent to the superior portion of the humeral head (arrows)

Diagnosis CPPD crystal deposition disease.

Discussion
Radiographically, pyrophosphate arthropathy resembles osteoarthritis. Hallmark imaging findings include joint space narrowing and osteophyte formation (Fig. 8.4). The presence of chondrocalcinosis is not necessary to make the diagnosis of pyrophosphate arthropathy. The glenohumeral joint is of course a nonweight-bearing joint; therefore, joint space narrowing and productive changes in the absence of prior injury raises the possibility of CPPD.

Case 3
A 48-year-old male computer specialist with acute onset shoulder pain.

Fig. 8.5 AP view of the shoulder demonstrates amorphous calcification superior to the humeral head in the expected region of the distal supraspinatus tendon (arrow)

Diagnosis Hydroxyapatite deposition disease (HADD).

Discussion
Hydroxyapatite deposition disease (HADD) is a broad spectrum of pathology due to hydroxyapatite crystals, which include calcific tendonitis and bursitis. The shoulder is the most common site of involvement of HADD, occurring most commonly within the supraspinatus tendon. On radiographs, homogeneous calcification is identified over the greater tuberosity seen best on external rotation (Fig. 8.5). Other tendons of the rotator cuff musculature may also be affected. This condition is generally monoarticular.

Other potential sites of involvement include hip, elbow, wrist, and neck. Differential consideration for the radiographic appearance includes CPPD, however hydroxyapatite typically involves the tendons, bursae and periarticular tissues, whereas CPPD deposition typically occurs in the hyaline and fibrocartilage the radiographic appearance is often linear, though may be lobulated.

Case 4
A 69-year-old female with progressive shoulder pain and limited range of motion and diffuse shoulder swelling.

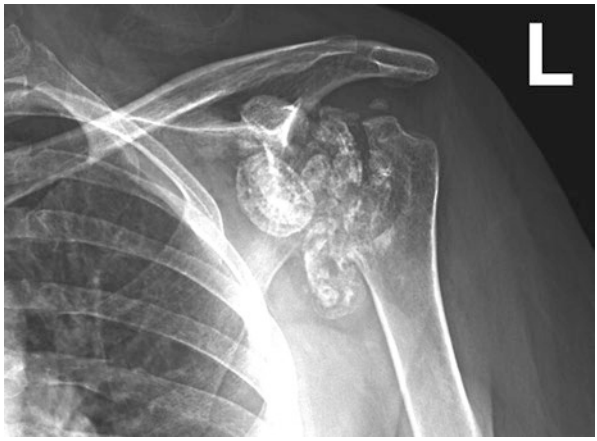

Fig. 8.6 AP shoulder radiograph; prominent lobulated calcifications of varying sizes within the joint with destructive changes and scalloping of the humeral head and apparent osteolysis of the glenoid

Diagnosis Milwaukee shoulder syndrome.

This is a destructive arthropathy first described in a group of elderly women from Milwaukee, characterized by hydroxyapatite in the synovial fluid. The pathophysiology is thought to be the intra-articular rupture of calcification with triggers the release of collagenase and protease enzymes that destroy the articular cartilage and eventually the rotator cuff. There is a 4:1 female to male ratio, and typically occurs in patients over 60 years of age.

Differential considerations, given the abundant degree of osseous destruction (Fig. 8.6), include septic arthritis and a neuropathic joint.

Case 5
A 42-year-old male with gradually worsening shoulder pain and stiffness over several months. No reported history of trauma. No fever or leukocytosis.

Fig. 8.7 AP view of the shoulder demonstrates extensive glenohumeral joint space narrowing (white arrow)

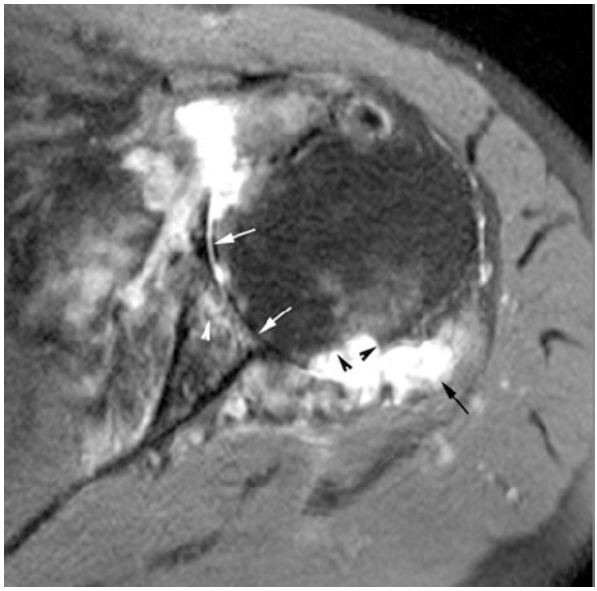

Fig. 8.8 Axial T2-weighted fat-saturation MRI image demonstrates moderate joint effusion (black arrow), extensive glenohumeral joint space narrowing (white arrows), subchondral marrow edema (white arrow head), and prominent erosive changes (black arrow head) along the humeral head

Diagnosis Rheumatoid arthritis.

Discussion

60% of patients with rheumatoid arthritis have shoulder involvement. Uniform glenohumeral joint space narrowing (Fig. 8.7) and generalized osteoporosis with a general lack of osteophyte formation are the primary imaging hallmarks of the condition. Effusion and erosions (Fig. 8.8) may also be present. Imaging differential considerations must include other types of inflammatory arthritis and septic arthritis if the process is monoarticular.

Case 6

A 55-year-old female with known history of rheumatoid arthritis, managed with methotrexate presents with 2 months of shoulder stiffness and pain worsened with overhead activities.

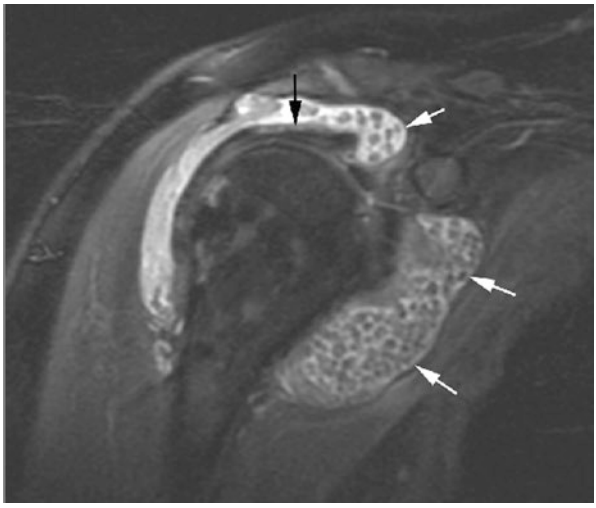

Fig. 8.9 Coronal T2 fat-saturation image demonstrates the supraspinatus tendon (black arrow) and numerous filling defects (white arrows) within the bright joint effusion

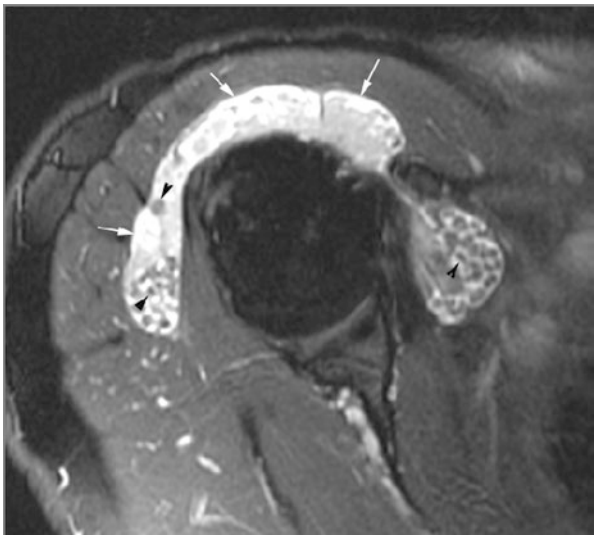

Fig. 8.10 Axial T2FS; Images demonstrate large amount of high signal joint fluid in the subacromial/subdeltoid bursa (white arrows) with numerous low signal, relatively uniform filling defects consistent with rice bodies (black arrow heads)

Diagnosis Subacromial/subdeltoid bursal rice bodies.

Discussion

Rice bodies are small nodules of fibrin that include a combination of collagen, reticulin, and elastin. It is believed that these bodies form as a result of shedding of the synovium due to microinfarctions with subsequent encasement by fibrin. If

mineralized, these bodies may appear on radiographs, but the diagnosis is more often made on MRI on which the small nodules will typically demonstrate low T1 and low T2 signal (Figs. 8.9 and 8.10).

Case 7
A 38-year-old weight lifter with dull shoulder pain over several weeks.

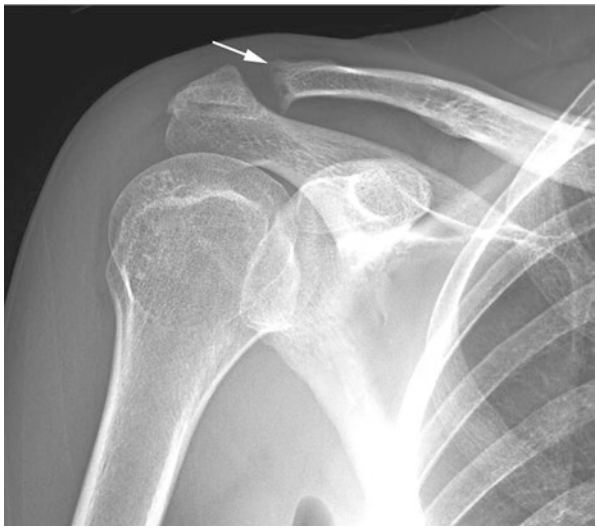

Fig. 8.11 Frontal radiograph of the shoulder in internal rotation demonstrates mild widening of the acromioclavicular joint space with erosive changes at the distal clavicle (white arrow)

Diagnosis Distal clavicular osteolysis.

Discussion
Clavicular osteolysis (Fig. 8.11) can be caused by acute trauma from falls or motor vehicle accidents. Frequently the traumatic insult is relatively minor. Posttraumatic osteolysis can occur bilaterally in those who experience repeated stress or microtrauma to the shoulder associated with athletic activities such as weightlifting or occupational activities. Osteolysis of the distal clavicle has been reported after spinal cord injury and on an idiopathic basis. True distal clavicular osteolysis should be differentiated from other causes of distal clavicular destruction including hyperparathyroidism, rheumatoid arthritis, and scleroderma. Additional considerations include lytic metastasis or osteomyelitis. Imaging findings include periosteal reaction, erosions, and osteopenia of the distal clavicle with widening of the AC joint.

Case 8

A 62-year-old male with acute onset of moderate shoulder pain gradually increasing over several days.

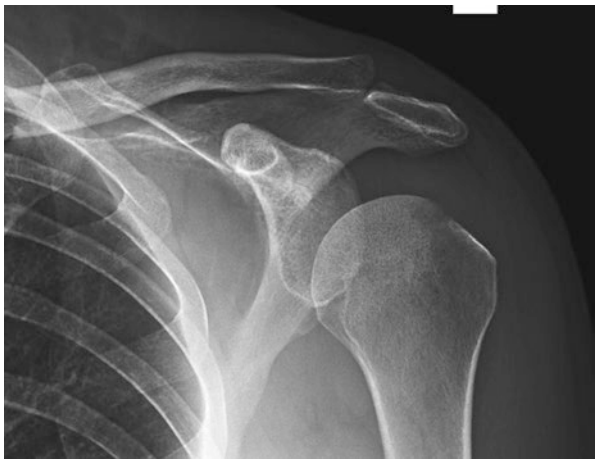

Fig. 8.12 AP shoulder radiograph demonstrates maintained joint spaces. Mild inferior subluxation of the glenohumeral joint can be seen in the setting of a joint effusion, often described as "pseudosubluxation"

Shoulder pain worsened over the next 3 months, and radiographic, CT, and MR imaging is performed.

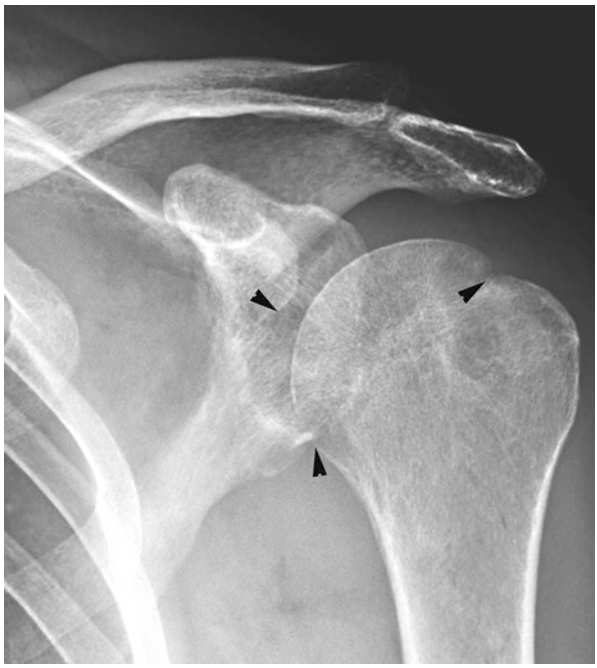

Fig. 8.13 AP shoulder radiograph obtained two months after Fig. 8.12 demonstrates erosive changes (black arrows) along the glenoid and humeral head

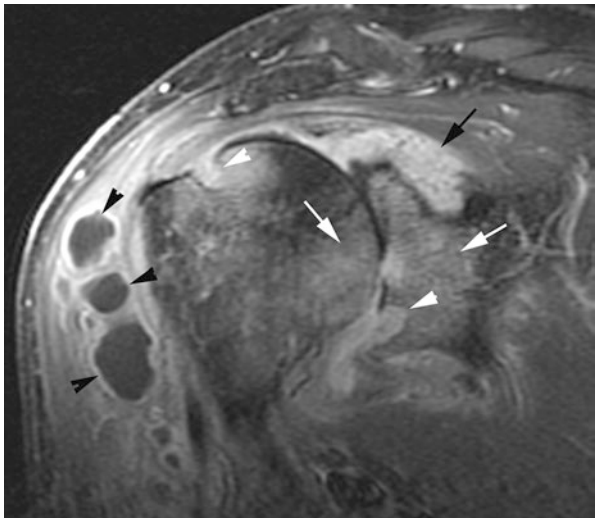

Fig. 8.14 Coronal T2FS image demonstrates a complex joint effusion (black arrow), marrow edema within the humeral head and glenoid (white arrows), erosive changes (white arrow head), and severe glenohumeral joint space narrowing. In addition, septated fluid collection within the deltoid was suspected to represent intramuscular abscess (black arrowheads)

Diagnosis Septic arthritis.

Discussion

Prompt diagnosis of septic arthritis requires collaborative effort between radiologists and clinicians. The diagnosis requires a high index of suspicion and prompt arthrocentesis. The initial radiographic sign is the presence of a joint effusion. This is often difficult or impossible to identify in the shoulder, as the glenohumeral joint is capacious and joint fluid may decompress into the subscapularis bursa, making it difficult to identify on radiographs. When present, joint effusion can often lead to widening of the glenohumeral joint and inferior displacement, known as pseudosubluxation, which can appear similar to glenohumeral dislocation (Fig. 8.12). Subsequent changes include joint space narrowing and erosive changes (Fig. 8.13).

MRI is typically abnormal within 24 h of the onset of septic arthritis and is the best modality for early diagnosis due to its high degree of sensitivity to marrow signal changes (Fig. 8.14). MR findings include synovial enhancement, erosive changes, abnormal marrow signal, and perisynovial edema. Although not as specific, ultrasound is highly sensitive to detect joint effusion and may be helpful to guide arthrocentesis.

Case 9
A 48-year-old female with loss of range of motion in the shoulder worsening over a period of weeks.

Fig. 8.15 AP radiograph demonstrates complete absence of the humeral head and the majority of the glenoid rim with surrounding calcific debris throughout the remnant glenohumeral joint space

Diagnosis Neuropathic joint.

Discussion
Imaging manifestations of neuropathic joint span a spectrum from hypertrophic and atrophic patterns. In the shoulder, the atrophic pattern predominates (Fig. 8.15). The most common cause of neuropathic joint in the shoulder is syringomyelia, which can be confirmed with a cervical spine MRI. Other causes of neuropathic arthropathy in nonweight-bearing joints include leprosy and diabetes mellitus. Imaging hallmarks include extensive osseous resorption giving the appearance of a surgical amputation, intra-articular osseous debris, cartilage destruction, and large joint effusion. The abnormal changes are centered within the joint, and involve both sides of the joint, excluding a primary osseous tumor. The rate of joint destruction can be rapid, rivaling that of septic arthritis, which must be included in the differential diagnosis.

Case 10

Fig. 8.16 AP image demonstrates amorphous periarticular calcifications surrounding the proximal humeral diaphysis and the lateral portion of the humeral head. The joint spaces appear maintained; no definite erosions are seen

Fig. 8.17 3-D reformated CT image demonstrates the glenohumeral joint with lobulated calcified masses (white arrow heads) surrounding the joint

Diagnosis Tumoral calcinosis.

Discussion
This is a hereditary dysfunction in body phosphate regulation resulting in the massive deposition of lobulated periarticular calcifications (Figs. 8.16 and 8.17) typically distributed around the extensor surface of large joints. Differential considerations include calcific tendonitis, gout, myositis ossificans, synovial osteochondromatosis, burn, and neurologic injury.

The most common sites of involvement in descending order are the hip, elbow, shoulder, foot, and wrist.

Practice Questions

Question 1. Which crystal is the most likely cause for the appearance in the above radiograph?

A. Calcium pyrophosphate dihydrate.
B. Calcium hydroxyapatite.
C. Monosodium urate monohydrate.
D. Amyloidosis.

The AP image (See fig above) of the shoulder depicts lobulated calcification in the supraspinatus tendon of the rotator cuff, classic for hydroxyapatite deposition disease. Deposition of calcium pyrophosphate dihydrate (chondrocalcinosis) typically conforms to regions of hyaline or fibrocartilage and manifests clinically as pseudogout. Monosodium urate is the crystalline form of uric acid which is associated with gouty arthritis. Amyloidosis is the end result of several different underlying processes in which proteinaceous material accumulates in the body. It is most associated with dialysis patients.

Question 2. What is the most likely diagnosis given the AP shoulder image provided?

A. Neuropathic joint.
B. Osteoarthritis.
C. Rheumatoid arthritis.
D. Scleroderma.

Discussion

AP radiograph demonstrates diffuse osteoporosis, severe glenohumeral joint space narrowing, elevation of the humeral head due to chronic rotator cuff tear, and erosions. These features are typical of manifestations of rheumatoid arthritis in the shoulder. Osteoarthritis is associated with bony productive changes (See fig above).

Question 3. Which is the best next imaging examination given the above AP shoulder radiographs in this patient with atraumatic shoulder pain?

A. C-spine MRI.
B. Lumbar spine MRI.
C. Chest radiograph.
D. Bone scan.

Discussion
AP image (See fig above) depicts joint space narrowing, fragmentation, and debris within the glenohumeral joint space. The findings suggest the presence of a neuropathic joint. As stated above, this is most often related to presence of a cervical syringomyelia and can be best confirmed with cervical spine MRI.

Question 4. What is the most likely underlying process present in this patient with atraumatic shoulder pain given the following radiograph?

A. Rheumatoid arthritis.
B. Sickle cell anemia.
C. Distal clavicular osteolysis.
D. Amyloidosis.

Discussion
The AP view of the shoulder (See fig above) demonstrates subtle sclerosis within the humeral head suggesting avascular necrosis without evidence of subchondral collapse. Joint space is well preserved. There are no distal clavicular erosive changes present to suggest clavicular osteolysis. In addition to sickle cell anemia, common etiologies for atraumatic avascular necrosis include alcoholism and chronic high dose corticosteroid therapy.

Answers to the Question

Q1: B. Calcium hydroxyapatite.
Q2: C. Rheumatoid arthritis.
Q3: A. C-spine MRI.
Q4: B. Sickle cell anemia.

Further Reading

Best C, Basu A, Sengupta M. Subacromial-subdeltoid bursal Rice bodies causing shoulder pain. J PM&R. 2015;7(9):1014–6.
Farpour F, Maasumi K, Tehranzadeh J. Imaging of crystal deposition disease. Appl Radiol. 2012;41(8):18–25.
Forse CL, Mucha BL, Santos ML, Ongcapin EH. Clin Rheumatol. 2012;31:1753–6.
Ha AS, Petscavage-Thomas JM, Tagoylo GH. Acromioclavicular joint: the other joint in the shoulder. Am J Roentgenol. 2014;202(2):375–85.
Kaplan PA, Resnick D. Stress induced osteolysis of the distal clavicle. Radiology. 1986;158(1):139–40.
Olsen KM, Chew FS. Tumoral calcinosis: pearls, polemics, and alternative possibilities. Radiographics. 2006;26:871–85.
Tan CHA, Rai SB, Chandy J. MRI appearances of multiple rice body formation in chronic subacromial and subdeltoid bursitis, in association with synovial chondromatosis. Clin Radiol. 2004;59:753–7.

Chapter 9
Elbow

Anupam Basu

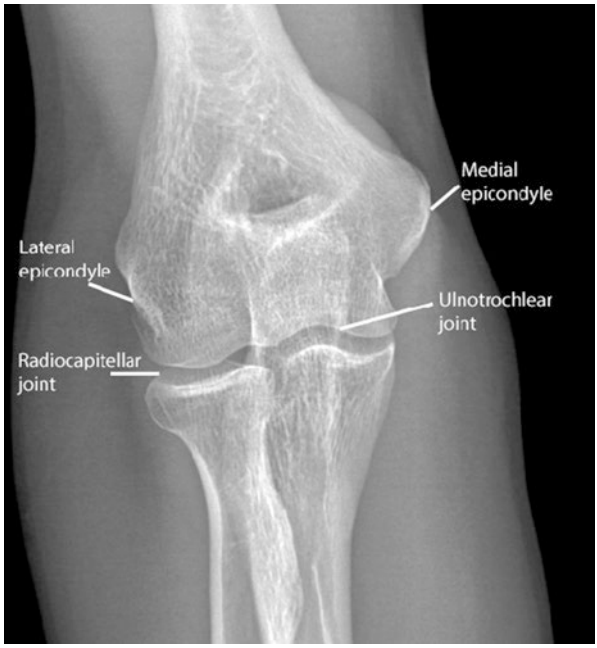

Fig. 9.1 Frontal view of the normal elbow joint with the ulnotrochlear and radiocapitellar joints labeled

A standard series of elbow radiographs consists of frontal, oblique, and lateral images. Figure 9.1 outlines major bony landmarks.

A. Basu (✉)
Cook County Health, Department of Radiology, Chicago, IL, USA
e-mail: abasu@cookcountyhhs.org

R. S. Katz, A. Basu (eds.), *Diagnostic Radiology of the Rheumatic Diseases*,
https://doi.org/10.1007/978-3-030-25116-1_9

Case 1
A 43-year-old female with bilateral elbow stiffness.

Fig. 9.2 Lateral elbow radiograph demonstrates generalized osteopenia, diffuse joint space, uniform narrowing at both the radiocapitellar (arrows) and the ulnotrochlear joints (arrow heads) with erosive changes, most pronounced at the ulnotrochlear articulation resulting in scalloped appearance of the ulnar articular surface. The striking lack of productive changes also indicates an underlying inflammatory arthropathy

Diagnosis Rheumatoid arthritis.

The elbow is involved in one-third of all rheumatoid arthritis patients, and when present, typically involves both elbows. The patient shown in Fig. 9.2 demonstrates many of the findings commonly associated with rheumatoid arthritis, mainly significant joint space narrowing with relative paucity of productive or reparative changes.

Case 2
A 19-year-old college pitcher with persistent elbow pain.

Fig. 9.3 Oblique view of the elbow demonstrates fragmentation of the capitellum (arrow) typical in location and appearance for osteochondral defect

Diagnosis Osteochondral defect.

Discussion
The most well-established theory on the formation of osteochondral lesions of the elbow is from a combination of injury related to repetitive trauma and tenuous regional blood supply. The anterior portion of the capitellum has limited vascular supply, making this region most prone to this defect. Although less frequent, similar defects have been described in the trochlea, radial head, and olecranon. The entity is most commonly seen in adolescent and young adult males with clinical history of overuse of the involved extremity.

Radiographic features include flattening and irregularity of the articular surface of the bone (Fig. 9.3). MRI is considered the most sensitive and reliable modality to assess osteochondral lesions and determine whether they are stable or unstable relative to the native bone from which they arise. Unstable lesions are often addressed surgically.

Case 3
A 57-year-old alcoholic with unilateral chronic swollen elbow.

Fig. 9.4 Lateral view of the elbow demonstrates amorphous calcifications and focal soft tissue prominence (arrow) in the expected region of the olecranon bursa. The joint space is relatively well preserved and no erosions or productive changes are seen

Diagnosis Olecranon bursitis secondary to gout.

Discussion
The elbow is involved in one-third of patients with gout, often manifesting as olecranon bursitis (Fig. 9.4). Gout is most often the diagnosis in a patient with bilateral olecranon bursitis. Other causes of olecranon bursitis include repetitive trauma and rheumatoid arthritis. Approximately one-third of all olecranon bursitis cases are superinfected.

Case 4
A 38-year-old with incidental finding on elbow radiographs.

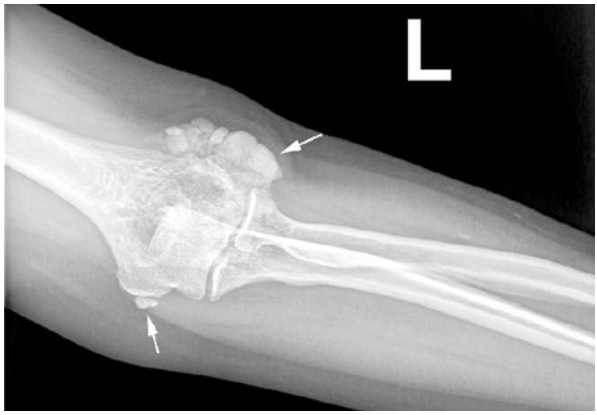

Fig. 9.5 AP view of the elbow demonstrates lobulated, calcified masses within the soft tissues adjacent to the lateral epicondyle and to a lesser extent adjacent to the medial epicondyle (arrows). The joint space appears maintained without erosions or productive changes present

Diagnosis Tumoral calcinosis.

Discussion
Tumoral calcinosis is characterized by the presence of large lobulated juxta-articular calcified masses in the soft tissues (Fig. 9.5). The most common locations are the hip, elbow, shoulders, and knees. Differential considerations include calcific tendinopathy, tophaceous gout, myositis ossificans, and synovial osteochondromatosis. Although rare, neoplastic processes such as surface osteosarcoma or synovial sarcoma may also appear similarly.

Case 5
A 28-year-old male with intermittent elbow swelling and chronic elbow and knee pain over many years.

Fig. 9.6 Lateral elbow radiograph reveals ballooning of the ulnar articular margin (arrow). There is hyperdensity in the region of the posterior fat pad, suggesting the presence of a hemorrhagic effusion. There is diffuse joint space with minimal productive change present

Diagnosis Hemophilia.

Rare X-linked disorder that results in bleeding into the synovial joints and resultant articular abnormalities. The joints affected are knee, ankle, elbow, shoulder, and hip in decreasing order of frequency. Radiographic hallmarks of this process include joint space narrowing, epiphyseal "ballooning" or overgrowth (Fig. 9.6), soft tissue swelling, and erosions.

Case 6
A 51-year-old with history of long-standing elbow pain and stiffness (Fig. 9.7).

Fig. 9.7 AP elbow radiograph demonstrates changes from prior ORIF of the proximal ulna. There is marked joint space narrowing of the ulnotrochlear and radiocapitallar joints with significant surrounding productive change noted

Diagnosis Posttraumatic osteoarthritis.

Discussion
Posttraumatic arthritis develops after acute trauma to the involved joint. It is estimated that 12% of the overall burden of disease of osteoarthritis is secondary to joint trauma, often with significant ligamentous or capsular injuries. Unlike other forms of osteoarthritis, posttraumatic OA often affects younger adults for whom joint replacement or joint fusion is not a desirable treatment. A variety of molecular and cellular events are involved in the progression of posttraumatic arthritis, and extensive research is ongoing to address and mitigate its effects.

Case 7
A 42-year-old immigrant from Sierra Leone presents with severe progressive elbow pain and stiffness over several weeks (Fig. 9.8).

Fig. 9.8 Lateral image depicts severe joint space narrowing and marginal erosions. No significant productive changes are seen

Diagnosis Tuberculosis septic arthritis.

Discussion
The incidence of extrapulmonary tuberculosis has been increasing over the past decades for a variety of factors including aging population, increasing travel and immigration, and increasing number of patients with chronic HIV. Radiographic features include periarticular osteopenia, marginal erosions, effusion, and joint space narrowing commonly seen in other causes of inflammatory arthritis. The differential diagnosis for the imaging appearance of tuberculous septic arthritis therefore includes pyogenic causes of septic arthritis as well as rheumatoid arthritis. Other less common considerations include pigmented villonodular synovitis, gout, and hemophilic arthropathy. A collaborative approach to the diagnosis, combining imaging and clinical features, is imperative.

Further Reading

Anderson DD, Chubinskaya S, Fuilak F, Martin JA, Oegema TR, Olson SA, Buckwalter JA. Post-traumatic osteoarthritis: improved understanding and opportunities for early intervention. J Orthop Res. 2011;29(6):802–9.

Chang EY, Chen KC, Huang BK, Kavanaugh A. Adult inflammatory arthritides; what the radiologist should know. Radiographics. 2016;36:1849–70.

Choi JA, Koh SH, Hong SH, Koh YH, Choi JY, Kang HS. Rheumatoid arthritis and tuberculous arthritis; differeniating MRI features. AJR Am J Roentgenol. 2009;193(5):1347–53.

Floemer F, Morrison WB, Bongartz G, Ledermann HP. MRI characteristics for olecranon bursitis. AJR. 2004;183:29–34.

Ho G Jr, Tice AD, Kaplan SR. Septic bursitis in the prepatellar and olecranon bursae; an analysis of 25 cases. Ann Intern Med. 1978;89:21–7.
Mihara K, Tsutsui H, Nishinaka N, Yamaguchi K. Non-operative management of osteochondnritis dessicans of the capitellum. Am J Sports Med. 2009;37(2):298–304.
Smith MV, Bedi A, Chen N. Surgical treatment for osteochondritis dessicans of the capitellum. J Bone Joint Surg Am. 2007;89(6):1205–14.
Stell IM. Septic and non-septic olencranon bursitis in the accident and emergency department; an approach to management. J Accid Emerg Med. 1996;13:351–3.

Chapter 10
Introduction to Spine Imaging and Sacroiliac Imaging

Merve Ozen, Mehmet Kocak, and Anupam Basu

The three main magnetic resonance imaging (MRI) sequences used when assessing the spine include T2-weighted (W) imaging (Fig. 10.1a), T1 W imaging (Fig. 10.1b), and a fat-suppressed sequence such as short tau inversion recovery (STIR) (Fig. 10.1c) depending on the scanner.

The cerebrospinal fluid (CSF) appears bright on T2W images. The intervertebral discs have a higher water content compared to the adjacent bone; therefore, they also look brighter than bone on T2W images. Please note that subcutaneous fat tissue is bright on T2W images (Fig. 10.1a).

The cerebrospinal fluid (CSF) (Arrow, Fig. 10.1b) appears dark on T1W images. The discs also appear darker than the adjacent bone on T1W images. Again, the subcutaneous fat tissue is bright on T1W images as well.

The STIR sequence is helpful in assessing the bone and/or marrow abnormalities. It allows us to suppress the high signal from fatty bone marrow (arrow, Fig. 10.1c), and therefore enabling to differentiate the abnormalities such as edema, infiltration, or mass. Examples of STIR signal abnormalities will be given in case discussions.

We mainly use the sagittal and axial planes for spine imaging with the optional coronal imaging. Both planes help to evaluate the bone, intervertebral discs, spinal canal, and foramina. Postcontrast T1W images are usually added for the investigation of tumors, infection, or inflammation.

With these images, the spinal alignment, vertebral body height, marrow, and disc spaces is assessed, as well as the patency of the spinal canal and foramina.

M. Ozen (✉) · M. Kocak
Department of Radiology & Nuclear Medicine, Rush University Medical Center, Chicago, IL, USA
e-mail: merve_ozen@rush.edu

A. Basu
Cook County Health, Department of Radiology, Chicago, IL, USA

R. S. Katz, A. Basu (eds.), *Diagnostic Radiology of the Rheumatic Diseases*,
https://doi.org/10.1007/978-3-030-25116-1_10

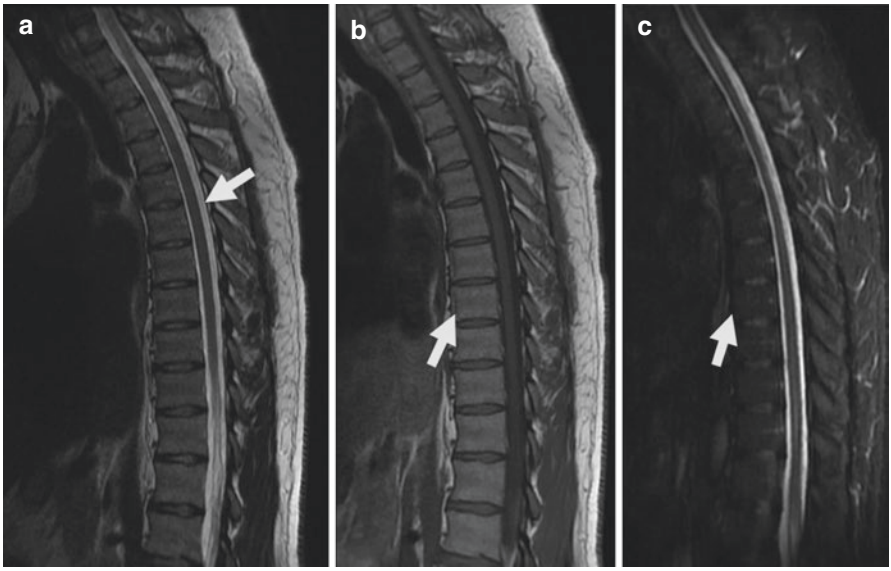

Fig. 10.1 A normal MRI of the thoracic spine (**a**) T2W; (**b**) T1W; (**c**) STIR

The alignment is evaluated on the coronal and sagittal images. Presence of scoliosis, any changes in normal kyphosis, and lordosis is evaluated.

Vertebral body height is assessed for any acute or chronic fracture, or compression deformity.

Bone marrow is assessed for edema or infiltration.

Spinal cord is evaluated on axial and sagittal images for the morphology and medullary signal including any compression or enhancement.

When foramina and recesses are evaluated, attention should be paid for any nerve root compressions.

Degenerative Disease of Spine

Case: A 55-year-old male presenting with neck pain

Three main changes occur in spine with the advanced age. Loss of bone mineralization and loss of water content of intervertebral discs with the osteophyte formation and subluxation.

Figure 10.2a is a T2W image as the CSF is bright. Multilevel disc bulging/protrusion causes varying degrees of spinal canal stenosis including a cord compression at C5–6 (arrow).

Figure 10.2b is an STIR sequence. We would expect to see brighter signals in case of bone edema. In this specific case, there is no signal abnormality on STIR images.

Figure 10.2c is a contrast-enhanced T1W sequence. We need to correlate the enhanced T1 images with nonenhanced T1W image (Fig. 10.2d) to see any pathologic enhancement. In this case, there is no abnormal contrast enhancement.

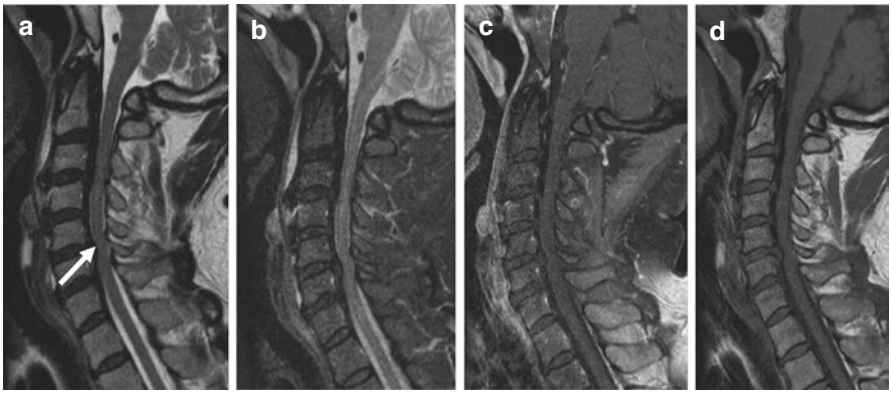

Fig. 10.2 Sagittal views of cervical spine. (**a**) T2W; (**b**) STIR; (**c**) contrast-enhanced T1W; (**d**) noncontrast T1W

Case: A 70-year-old female with back pain

Figure 10.3a is a T2W axial image at the level of the facet joints. Image demonstrates severe spinal canal stenosis with narrowing of the bilateral lateral recesses due to broad-based posterior disc protrusion and severe facet joint hypertrophy. There is minimal fluid in the left facet joint (Fig. 10.3a, arrow).

Figure 10.3b is a T1W image as the CSF is dark (gray arrow). Severe hypertrophy of the ligamentum flavum is present (white arrow). Please note the associated minimal contrast enhancement around the left facet joint (Fig. 10.3c, arrow).

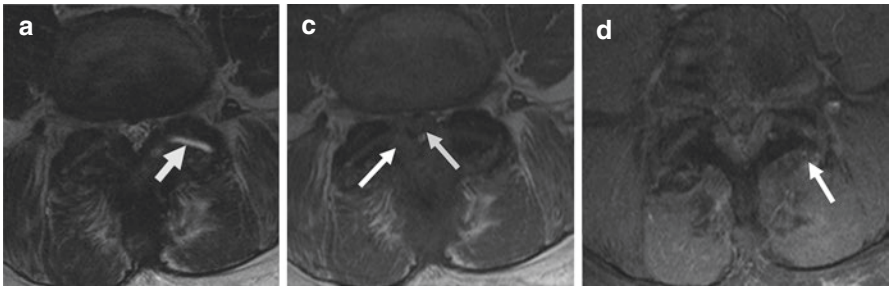

Fig. 10.3 Axial views of lumbar spine at the level of a facet joint. T2W (**a**), T1W (**b**), and contrast-enhanced T1W (**c**) images, respectively

Case: An 84-year-old female who presents with worsening dull right-sided headache with numbness and tingling, with loss of balance over the past 4 months

Figure 10.4 is a case of cervical synovial cyst. Marked degenerative changes are seen in the atlanto-odontoid joint. There is a large T2 bright and T1 dark lesion in the posterolateral aspect of the joint on the right compatible with a synovial cyst (as pointed with arrows in Fig. 10.4). The cyst causes moderate spinal canal stenosis with flattening of the ventral cord surface. There are no signal changes in the cord.

The synovial cysts are usually seen in the lumbar spine, are rare in the cervical spine. They are usually asymptomatic and they grow slowly. This is an unusual case that the patient required surgical intervention for cord decompression.

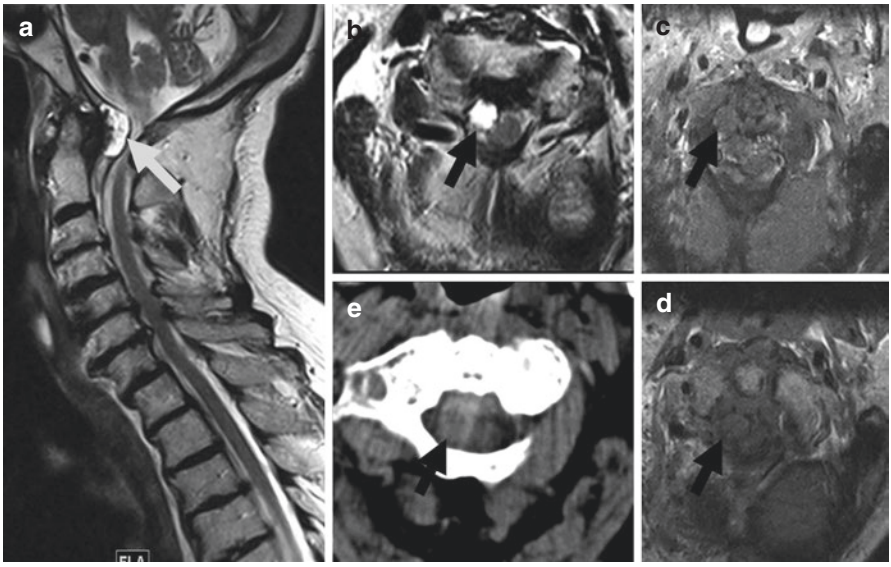

Fig. 10.4 (**a**) Sagittal T2W. (**b**) Axial T2W. (**c**) Axial postcontrast T1W. (**d**) Axial precontrast T1W. (**e**) Axial CT image

Case: A 37-year-old female with back pain
Figure 10.5 is a case of a pars defect. The figure demonstrates anatomical defects in the vertebral pars interarticularis with associated spondylolisthesis at L5-S1. Spondylolisthesis may be associated with the degeneration of the intervertebral disc or posterior facet joints or may occur in relation with spondylolysis which is the isthmic type. Isthmic spondylolisthesis most commonly occurs at the L5-S1 level.

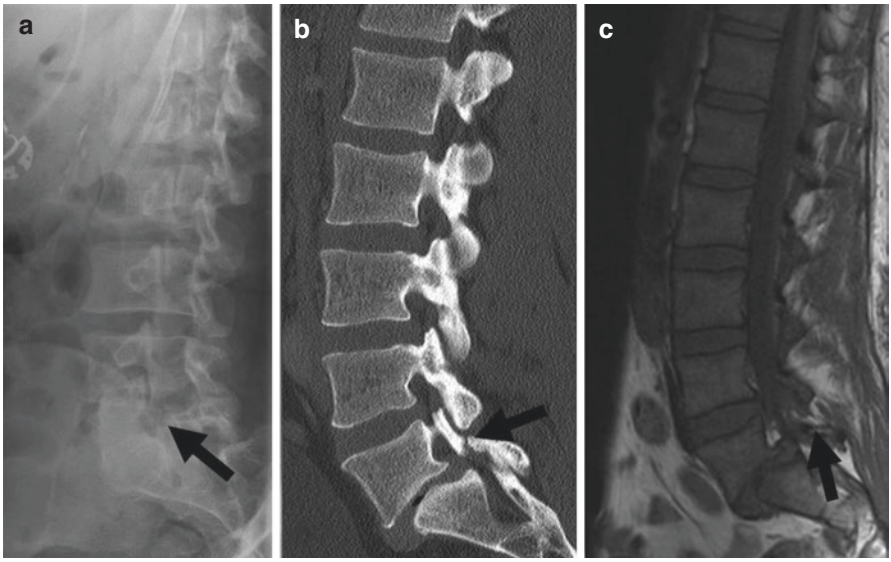

Fig. 10.5 (**a**) Oblique lumbar radiograph. (**b**) Sagittal CT image. (**c**) Sagittal T1W

Seropositive Spondyloarthropathy

Case: A 53-year-old female with past medical history of rheumatoid arthritis
Figure 10.6 is a case of rheumatoid arthritis with the mild cephalad migration of the odontoid process in the anterior foramen magnum. There is resultant mild narrowing at the foramen magnum. No intramedullary signal changes are noted. There is widening of the atlanto-dental space (Fig. 10.6d). Pannus formation is seen between the dens and left lateral mass of C1 (Fig. 10.6b).

Degenerative changes in the form of marginal osteophytes (Fig. 10.6c). The cervical vertebrae demonstrate normal height.

Rheumatoid arthritis usually involves cervical spine, typically the atlanto-axial region. Erosive changes with inflammation of synovium around the odontoid process causes pannus formation. In advanced stages, posterior transverse ligament is involved which results in instability with a potential risk of spinal cord injury.

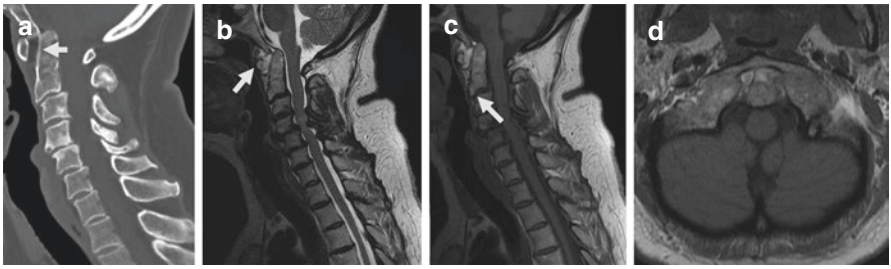

Fig. 10.6 (**a**) Sagittal CT image. (**b**) Sagittal T2W. (**c**) Sagittal T1W. (**d**) Axial T1W

Seronegative Spondyloarthropathy

Case: A 72-year-old male with past medical history of ankylosing spondylitis (AS) is presenting with neck pain

In Fig. 10.7, we see ossification throughout the anterior longitudinal ligament with extensive syndesmophytes creating bamboo spine appearance. No signs of posterior ligament calcifications. These findings are consistent with ankylosing spondylitis. The main mechanism of syndesmophytes is the formation of calcification, during healing process of erosive lesions.

Fig. 10.7 Lateral radiograph of cervical spine

Case: A 66-year-old male with significant past medical history of ankylosing spondylitis was admitted after a fall

Figure 10.8 demonstrates an acute fracture of the C7 vertebral body (Fig. 10.8a, white arrow). There is mild compression deformity of the C7 vertebral body with anterior height loss (Fig. 10.8a, white arrow). A fracture line with associated marrow edema is also noted as well as vertebral body of the C6 loss (Fig. 10.8c, white arrow). The bright signal on STIR image (which is a fat-suppressed sequence; please note that the normal bone marrow fat and subcutaneous fat is dark in this sequence) indicates edema. Moderate kyphotic deformity with it's apex at C6–C7 (Fig. 10.8b, white arrow). There is mild flattening of the ventral aspect of spinal cord without definite edema or contusion. In addition, there is a posterior epidural hematoma extending from C6–C7 to the level of T3 measuring approximately 4–5 mm in thickness contributing to moderate dural compression (Fig. 10.8a, gray arrow). Fracture is a common complication in AS. Major predisposing for spinal fractures is increased rigidity of spine with new bone formation.

Fig. 10.8 (**a**) Sagittal T2W. (**b**) Sagittal T1W. (**c**) Sagittal STIR

Case: A 65-year-old female with past medical history of psoriatic arthritis

Figure 10.9 shows marked levoscoliotic deformity with apex centered at L2–L3 and slight left lateral subluxation of L3. Degenerative disc/endplate changes multiple levels. Bridging right lateral osteophytes between T12 and L3 with mild right lateral wedging of L3, which is better seen on CT image (Fig. 10.9c). A CT scan may be able to better demonstrate osteophytes and endplate sclerosis.

The lateral bridging syndesmophytes and partial fusion of vertebrae which is caused by ossification of annulus fibrosus. This is a typical finding in psoriatic arthritis.

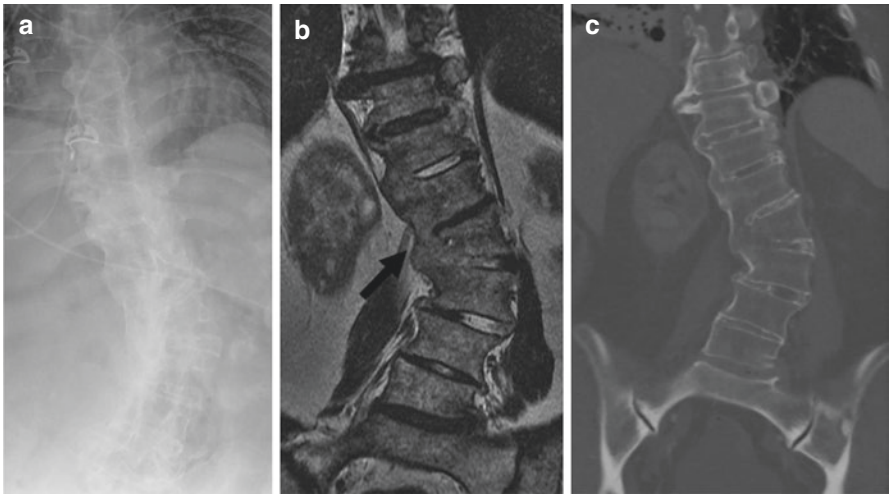

Fig. 10.9 (**a**) Frontal radiograph. (**b**) T2W. (**c**) CT image

Case: A 73-year-old male with a history of Crohn's colitis (diagnosed at age 18) presenting with back pain. Thoracic spine X-ray was obtained to exclude prevalent vertebral fractures

Anteroposterior and lateral radiographs of thoracic spine (Fig. 10.10) show bridging anterior and lateral syndesmophytes seen diffusely throughout the thoracic spine with the preservation of the intervertebral disc spaces. There is also fusion of the interspinous ligament in the thoracic spine. Findings, though nonspecific, are compatible with Crohn's spondyloarthropathy with the known past medical history. In Crohn's disease, one of the most common sites of enthesitis in axial spondyloarthropathy is annular ligament–vertebral body endplate attachments in the spine. However, these findings are indistinguishable from AS.

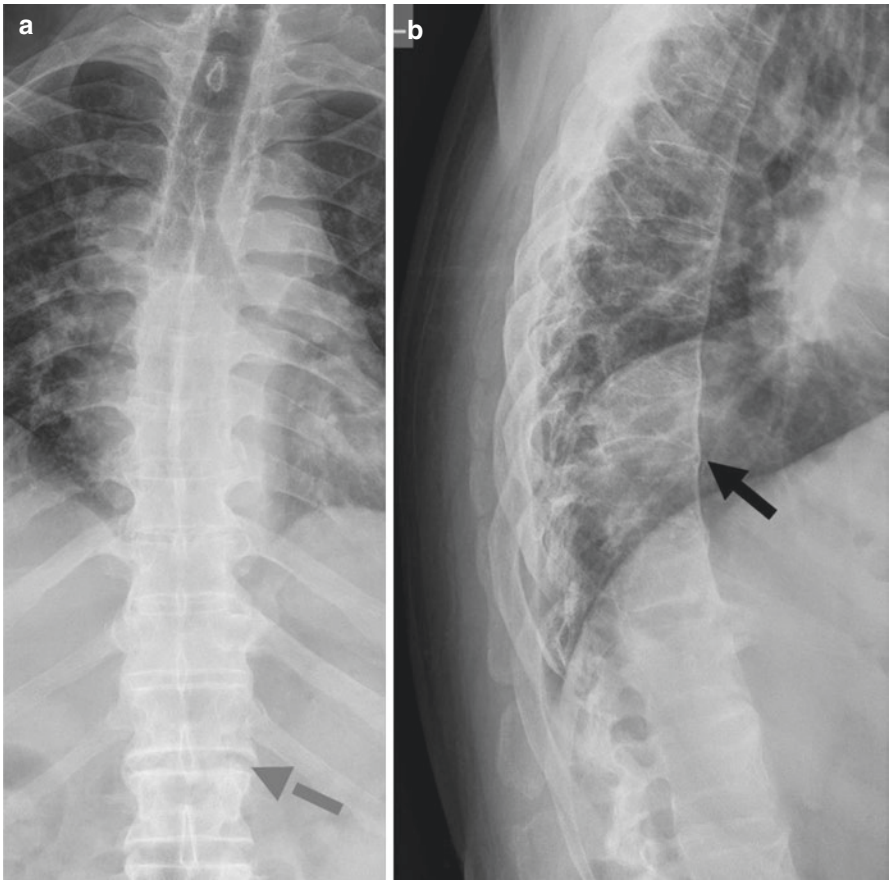

Fig. 10.10 Frontal (**a**) and lateral (**b**) radiographs of thoracic spine

Infection

Case: A 55-year-old female with 2 months history of back pain found to have discitis

Posterior discitis involving the L4–L5 (Fig. 10.11a, b-arrow) disc space with associated epidural enhancing soft tissue (Fig. 10.11d, arrow), likely phlegmon, circumferentially extending along the epidural space and contributing to marked thecal sac narrowing (Fig. 10.11c, gray arrow). Paravertebral extension of the inflammatory tissue also seen on both sides of the vertebrae as well as anteriorly (Fig. 10.11c, white arrow) with edema and enhancement (Fig. 10.11d, black arrow) of the adjacent iliopsoas muscles. MRI is essential for discitis diagnosis with its high sensitivity and specificity.

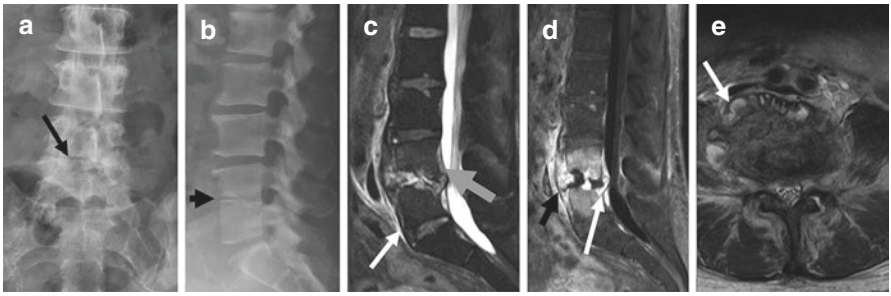

Fig. 10.11 (**a**) Anteroposterior radiograph. (**b**) Lateral radiograph. (**c**) Sagittal T2W. (**d**) Sagittal T1W post-contrast. (**e**) Axial T2W

Case: A 40-year-old female presenting with back pain

Figure 10.12 is a case of Pott's disease. Sagittal T2W (a) and contrast enhanced T1W (b) images show enhancing tuberculosis lesion with Gibbus formation. Spinal tuberculosis causes the destruction, collapse of vertebrae, and angulation of vertebral column. Pott's disease usually involves two adjacent vertebral bodies with the disc involvement. The infection first spreads within the vertebral body. Then, respectively to the endplate, to the disc space, to the vertebral arch, and beneath the anterior or posterior longitudinal ligaments, leading to extension of the infection to multiple adjacent or separate vertebral segments.

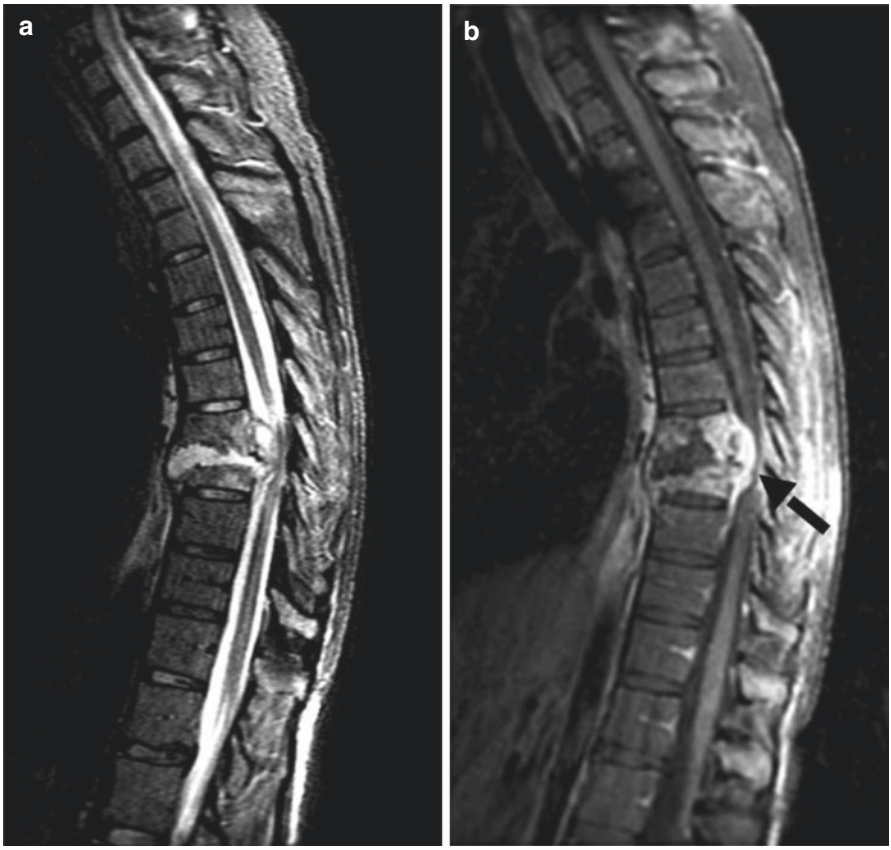

Fig. 10.12 (**a**) Sagittal STIR. (**b**) Sagittal T1W postcontrast

Renal Osteodystrophy

Case: A 65-year-old male with past medical history of end-stage renal disease is presenting with back pain

Figure 10.13 is a case of renal osteodystrophy. Sagittal reformatted CT images and MRI images show heterogeneous sclerotic appearance (arrow) of the lumbosacral osseous structures, related to renal osteodystrophy. Mild compression deformity is seen of the superior endplate of T11 (Fig. 10.13, white arrow). Multilevel endplate degenerative changes are present with Schmorl's node formation (Fig. 10.13c, arrow). Renal osteodystrophy usually occurs as the subperiosteal, subchondral, trabecular resorption in the axial skeleton.

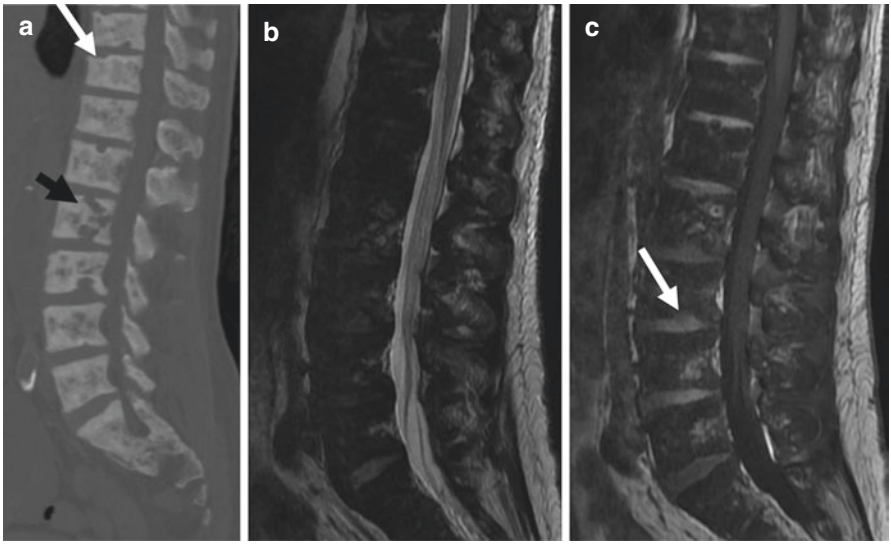

Fig. 10.13 Sagittal CT (**a**), MRI T2W (**b**), and T1W (**c**) images, respectively

Metastasis

Case: A 25-year-old male with significant past medical history of metastatic testicular cancer

In Fig. 10.14, there is a T1 hypointense (a), STIR hyperintense (b), enhancing (c) lesion in the L5 vertebral body consistent with metastasis. There is a smaller lesion in L2 vertebral body with the same imaging features (Fig. 10.14a, c). Figure 10.14d and e is obtained after the radiation treatment showing peripheral edema and contrast enhancement compatible with postradiation changes.

Metastases to the spine can involve the bone, epidural space, leptomeninges, and spinal cord. Metastatic lesions can be present in very different radiographic appearances. Even though some specific tumors have characteristic findings of bone metastasis, it is very difficult to diagnose the origin of the tumor from the appearance of the metastatic lesion. The combination of unenhanced T1-weighted and STIR sequences have shown to be most useful for the detection of bone marrow abnormalities.

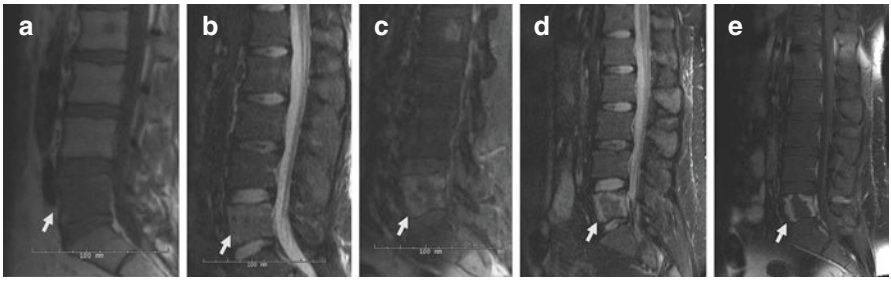

Fig. 10.14 (**a**) T1W. (**b**) STIR. (**c**) Postcontrast T1W. (**d**) STIR. (**e**) Postcontrast T1W

Miscellaneous (Kummels, DISH, OPPL, Degenerative Disease)

Case: A 66-year-old male is presenting with bilateral upper extremity weakness

Diagnosis:

1. Ossification of the posterior longitudinal ligament (OPPL)
2. Diffuse idiopathic skeletal hyperostosis (DISH)

Figure 10.15 (dashed circle) shows posterior longitudinal ligament ossification at the level of C2–C3 and diffuse idiopathic skeletal hyperostosis in the upper cervical spine. The signal intensity of ossification is similar in signal to that of the bone on conventional MRI sequences. Therefore, we expect to see multilevel hypointense thickening of posterior longitudinal ligament for OPPL diagnosis.

DISH is typically seen as flowing ossifications along the anterior or anterolateral aspects of the spine and involving at least four contiguous vertebrae with preserved disk spaces (Fig. 10.15a – circle and arrow, Fig. 10.15b – gray arrows).

OPPL and DISH usually are seen together. Most of the patients present with compression symptoms to adjacent structures. In the OPLL cases, examination on the whole spine is necessary for investigation of other levels, given the ligamentum flavum extends to the thoracolumbar region. The pathogenesis of OPLL and DISH is still unknown. There is some evidence that the ligament cells from OPLL patients have osteoblast-like characteristics.

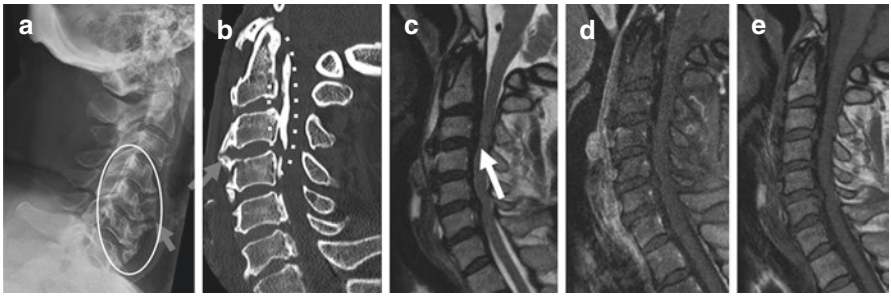

Fig. 10.15 Cervical spine. (**a**) Lateral radiograph. (**b**) Sagittal reformat CT. (**c**) Sagittal T2W. (**d**) Sagittal T1W postcontrast. (**e**) Sagittal T1W

Case: An 89-year-old female with severe back pain

Figure 10.16 is a case of Kummel's disease. There is diffuse edema involving the L4 vertebral body and adjacent disc on STIR image (a and b, arrow) with a cleft underneath the superior endplate (d, arrow). The appearance is compatible with the Kummel's deformity related to avascular necrosis. Kummel's disease is the avascular necrosis of a vertebral body presenting as vertebral osteonecrosis (c, arrow). Intravertebral vacuum cleft is the typical finding. This is an uncommon condition and is usually associated with osteoporosis.

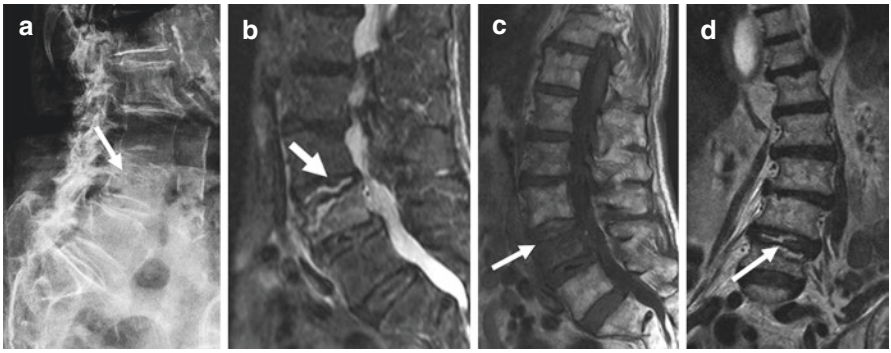

Fig. 10.16 Lumbar spine. (**a**) Lateral radiograph. (**b**) Sagittal T1W contrast enhanced. (**c**) Sagittal T1W. (**d**) Coronal T2W

Spinal Canal Stenosis

For the evaluation of the spinal canal, stenosis is defined as the anteroposterior diameter of the canal less than 10 mm in the cervical spine or 14 mm in the lumbar spine. Spinal canal stenosis subjectively can be graded as mild (Fig. 10.17b), moderate (Fig. 10.17c), or severe (Fig. 10.17d) if the canal is narrowed by less than a third, one-third to two-thirds, or greater than two-thirds of the original diameter, respectively. A similar grading system can be employed for the neural foramen.

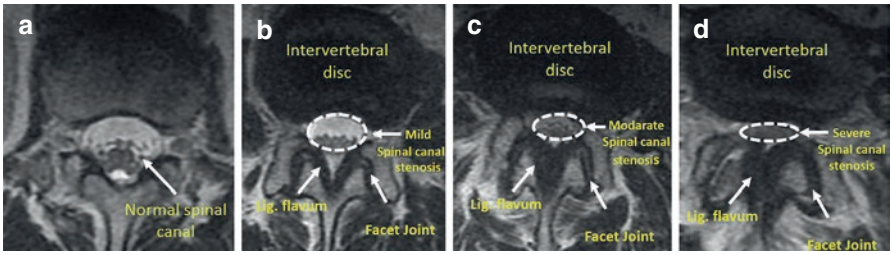

Fig. 10.17 Axial T2W (CSF is bright) images of lumbar spine. (**a**) No spinal canal stenosis. (**b**) Mild spinal canal stenosis. (**c**) Moderate spinal canal stenosis. (**d**) Severe spinal canal stenosis

Foraminal Stenosis and Intervertebral Disc Disease

Overall, we evaluate the foraminal narrowing with comparison to the normal levels and by looking at the surrounding fat (which will be seen bright on T2W images).

Foraminal stenosis subjectively can be graded as mild, moderate, or severe if the foramen is narrowed by less than a third, one-third to two-thirds, or greater than two-thirds of the original diameter, respectively. Figure 10.18 depicts progressive multi-level foraminal stenosis along the lumbar spine. The sagittal images are combined with the axial images at individual levels (Fig. 10.19) to assess the degree of stenosis present.

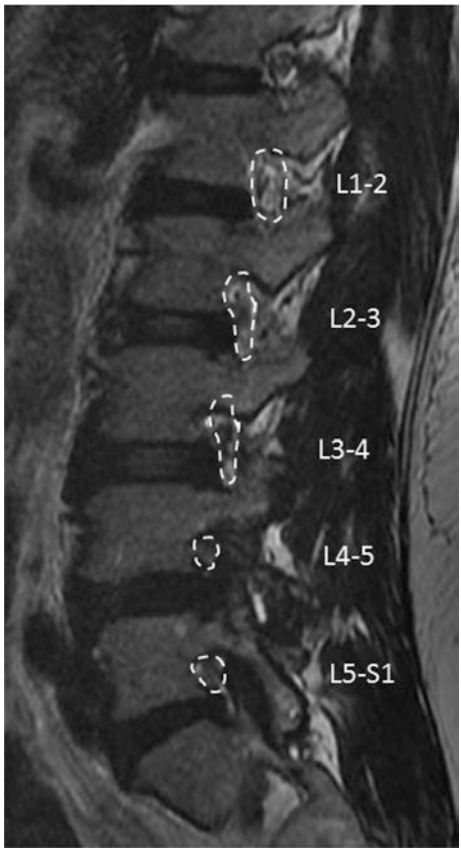

Fig. 10.18 Sagittal T2 image of the spine. L1–L2; normal foramina. L2–L3; mild foraminal stenosis due to stenosis. L3–L4; mild to moderate foraminal stenosis. L4–L5; severe foraminal stenosis. L5–S1; moderate foraminal stenosis

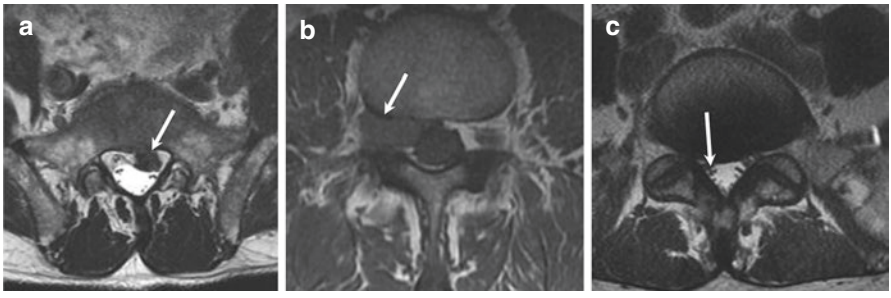

Fig. 10.19 (**a**) Mild spinal canal stenosis due to left posterior disc protrusion. (**b**) Severe right foraminal stenosis due to disc protrusion**.** (**c**) Mild spinal canal stenosis due to right asymmetric broad-based disc protrusion

Sacroiliac Joint Imaging and Pathology (By Anupam Basu, MD)

Normal Ferguson View of SI Joints

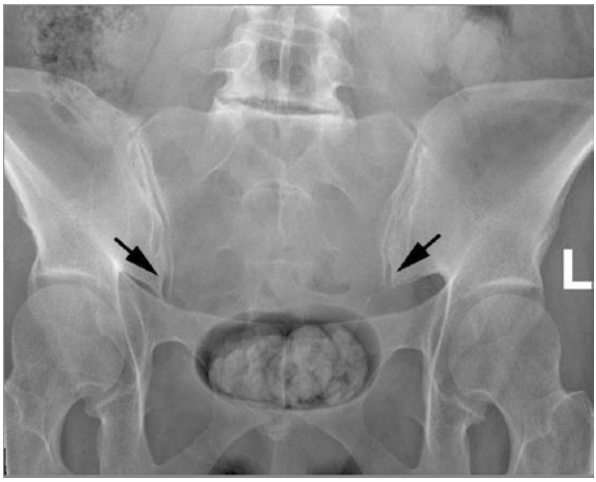

Fig. 10.20 Normal Ferguson view of the SI joints which is obtained with the patient placed supine. The X-ray tube is centered over L5/S1 and the tube is angled 25–30° towards the patient's head. This view best profiles the antero-inferior portion of the SI joints (black arrows)

Radiography is the most widely accepted imaging method for sacroiliitis because it is relatively inexpensive and readily available. However, SI joints are considered by many to be the most difficult joint to assess radiographically based on the complexity of the regional anatomy and variation in obliquity of the joint from person to person. In most instances, the synovial portion of the joint, which is the lower half or two thirds of the interosseous space between the sacrum and the ilium is affected to a greater degree than is the upper or ligamentous portion. The synovial portion of the joint is best imaged using an AP-modified Ferguson view (Fig. 10.20), in which the X-ray tube is angled 30° cephalad to better demonstrate the synovial portion of the joints. Radiographic assessment relies on determination of the width of the joint space, as well as the presence of erosions, sclerosis, and bony bridging. The modified New York criteria aids in categorizing the radiographic findings (see Table 10.1). The differential diagnosis is aided by determining the distribution of these abnormalities which can be categorized as bilateral and symmetrical, bilateral, and asymmetrical or unilateral. Radiographs are often the first imaging method for workup of suspected sacroiliitis. The unequivocal presence of SI changes at radiography is sufficient to establish the diagnosis. However, these radiographic changes usually require several years to become evident. Moreover, radiographs have relatively low intra- and interobserver correlation. MRI is therefore considered the gold standard imaging modality for assessment because of its superior ability to assess active inflammation (Fig. 10.21).

Table 10.1 Modified New York criteria for assessment of sacroiliitis3

Grade 0	Normal
Grade 1	Suspicious changes
Grade 2	Minimal abnormalities; small localized areas with erosion; sclerosis without alteration of the joint width
Grade 3	Unequivocal abnormality – moderate or advanced sacroiliitis with one or more of erosions, evidence of sclerosis, widening, narrowing, or partial ankylosis
Grade 4	Severe abnormality – total ankylosis

Case: A 28-year-old with intermittent back pain and skin rash

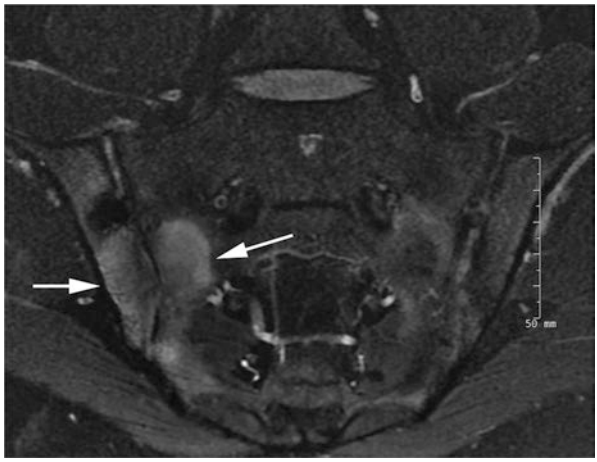

Fig. 10.21 Coronal oblique T2 fat-saturated image depicts focal marrow edema surrounding the right SI joint in a patient with psoriasis (arrows)

Answer Psoriatic arthritis

Discussion

MRI is the test of choice for diagnosis of seronegative spondyloarthropathies both in the acute and chronic phase of the disease. This modality is particularly useful in detecting acute inflammatory lesion of the sacroiliac joints. Imaging hallmarks on MRI (Fig. 10.21) include bone marrow edema located at the periarticular or subchondral surfaces of the sacroiliac joints. Stronger signal hyperintensity correlates with higher disease activity. Synovitis, capsulitis, and enthesitis may also be detected in the SI joints on MRI in the acute phase. The presence of both bone marrow edema and erosions has a 94% specificity and 75% sensitivity for the diagnosis of sacroiliitis. If present bilaterally, this is highly suggestive of ankylosing spondylitis. If the signal changes involving the SI joints are unilateral, it typically indicates other forms of spondyloarthritis, most often psoriatic arthritis.

Case: A 60 year-old with chronic back pain and recurrent, intermittent bouts of abdominal pain.

Fig. 10.22 Frontal view of the pelvis demonstrates nonvisualization of the SI joints consistent with complete ankylosis

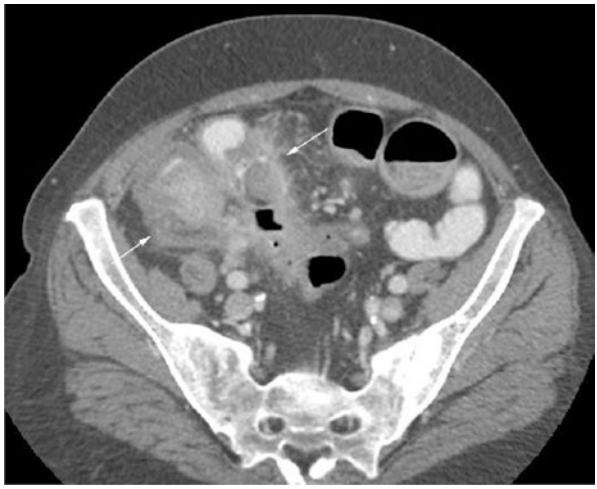

Fig. 10.23 Axial postcontrast soft tissue window image through the pelvis demonstrates marked inflammatory changes and bowel wall thickening in the region of the terminal ileum (between the arrows)

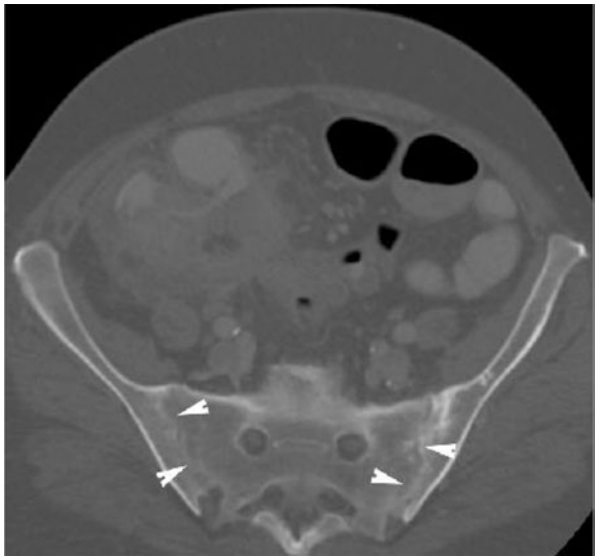

Fig. 10.24 Axial postcontrast bone window image through the pelvis demonstrates bilateral near complete fusion of the SI joints (arrow heads)

Answer Sacroiliitis related to inflammatory bowel disease

Discussion

Sacroiliitis and spondylitis occur in approximately 10% of patients with inflammatory bowel disease; they are more frequently seen in males. The clinical manifestations of spondylitis typically occur independent of the presence of active bowel inflammation. The imaging (Figs. 10.22, 10.23, and 10.24) and clinical features of IBD-associated spondylitis are not distinguishable from those of ankylosing spondylitis.

Case: A 35-year-old male with worsening back pain over several days.

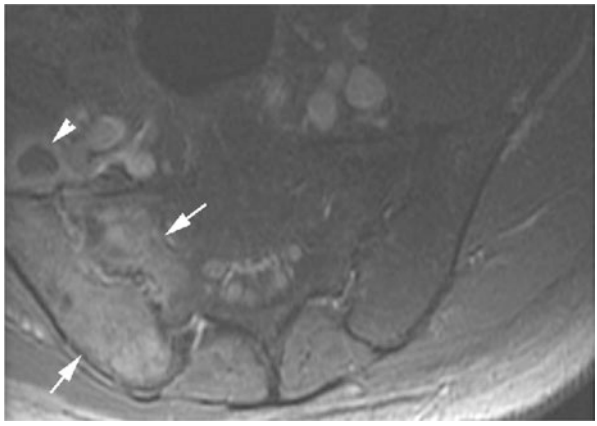

Fig. 10.25 Axial T1 fat-saturated postcontrast sequence demonstrates enhancement on both sides of the right SI joint (arrows) with a small peripherally enhancing collection (arrow head) immediately anterior to the joint consistent with extra-capsular fluid collection)

Answer SI joint septic arthritis.

Discussion

The differential for unilateral sacroiliitis includes septic arthritis, psoriatic arthritis, reactive arthritis, and early-stage ankylosing spondylitis. The adequate differentiation between infectious etiology and seronegative spondyloarthropathy is important to avoid delays in appropriate therapeutic management. MR findings which favor the diagnosis of infection include periarticular muscle edema, extracapsular fluid collection, and thick capsulitis (Fig. 10.25).

Case: A 64 year-old female with worsening hip pain for several weeks. Films obtained at an outside hospital were reportedly read as normal (not shown).

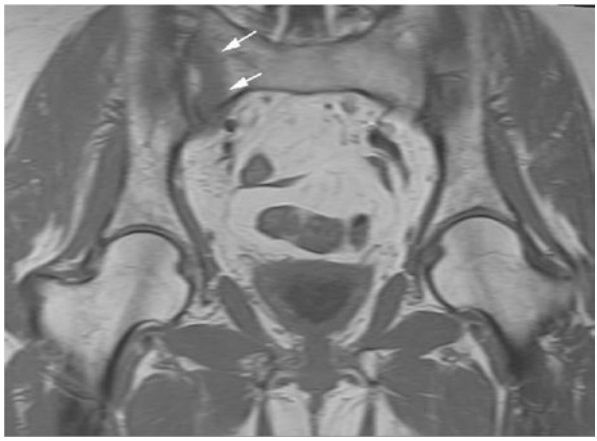

Fig. 10.26 Coronal T1 image demonstrates linear low T1 signal immediately medial to the right SI joint (arrows)

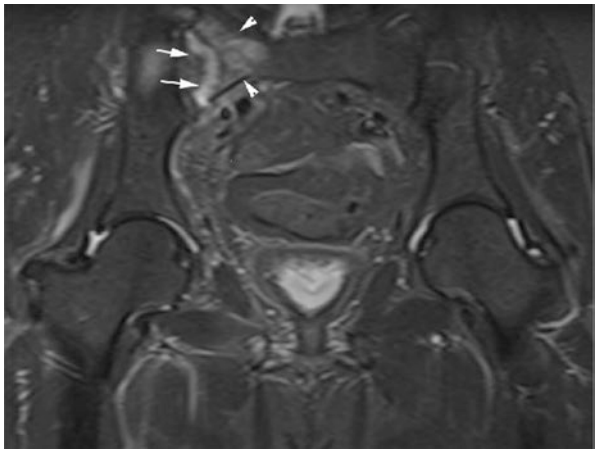

Fig. 10.27 Coronal STIR image demonstrates linear high T2 signal immediately medial to the right SI joint (arrows) with surrounding high T2 signal consistent with marrow edema (arrow heads)

Answer Insufficiency fracture of the sacrum

Discussion

Sacral insufficiency fractures are a common cause of debilitating back pain in the elderly, most commonly affecting elderly women with osteoporosis. Additional risk factors include prior pelvic radiation, chronic steroid therapy, renal osteodystrophy, and hyperparathyroidism. Studies suggest that only 20–38% of sacral insufficiency fractures are detected on radiographs. Bone scan and MRI (Figs. 10.26 and 10.27) are the most sensitive imaging modalities to detect sacral insufficiency fractures.

Further Reading

Brower AC, Flemming DJ. Arthritis in black and white. 3rd ed. Philadelphia: Elsevier Saunders; 2012.

Choi BW, Song KJ, Chang H. Ossification of the posterior longitudinal ligament: a review of literature. Asian Spine J. 2011;5(4):267–76.

Costa F, Menghetti C, Cardia A, Fornari M, Ortolina A. Cervical synovial cyst: case report and review of literature. Eur Spine J. 2009;19(Suppl 2):S100–2.

Golfieri R, Baddeley H, Pringle JS, Souhami R. The role of the STIR sequence in magnetic resonance imaging examination of bone tumours. Br J Radiol. 1990;63(748):251–6.

Jang JH, Ward MM, Rucker AN, et al. Ankylosing spondylitis: patterns of radiographic involvement--a re-examination of accepted principles in a cohort of 769 patients. Radiology. 2011;258(1):192–8.

Jurik AG. Imaging the spine in arthritis-a pictorial review. Insights Imaging. 2011;2(2):177–91.

Kang Y, Hong SH, Kim JY, Yoo HJ. Unilateral Sacroiliitis: differential diagnosis between infectious Sacroiliitis and Spondyloarthritis based on MRI findings. AJR. 2015;205:1048–55.

Khan SA, Sattar A, Khanzada U, Adel H, Adil SO, Hussain M. Facture of the pars interarticularis with or without spondylolisthesis in an adult population in a developing country: evaluation by multidetector computed tomography. Asian Spine J. 2017;11(3):437–43.

Klippel JH, Crofford LJ, Stone JH, Weywand CM, et al. Primer on rheumatic diseases. 12th ed. Atlanta: Arthritis Foundation; 2001.

Lyders EM, Whitlow CT, Baker MD, Morris PP. Imaging and treatment of sacral insufficiency fractures. Am J Neuroradiol. 2010;31(2):201–10.

Maataoui A, Vogl TJ, Khan MF. Magnetic resonance imaging-based interpretation of degenerative changes in the lower lumbar segments and therapeutic consequences. World J Radiol. 2015;7(8):194–7.

Matsumura M, Hara S. Crowned dens syndrome. N Engl J Med. 2012;367:e34.

Mihra S, et al. Imaging characteristics of diffuse idiopathic skeletal hyperostosis with an emphasis on acute spinal fractures: review. Am J Roentgenol. 2009;193(3_supplement):S10–9.

Modic MT, Ross JS. Lumbar degenerative disk disease. Radiology. 2007;245:45–61.

Navallas M, Ares J, Beltran B, Lisbona MP, et al. Sacroiliitis associated with axial spondyloarthropathy: new concepts and latest trends. Radiographics. 2013;33:933–56.

Nickell LT, Schucany WG, Opatowsky MJ. Kummell disease. Proc (Bayl Univ Med Cent). 2013;26(3):300–1.

Pathria M, Sartoris DJ. Osteoarthritis of the lumbar facet joints: accuracy of oblique radiographic assessment. Radiology. 1987;164:227–30. https://doi.org/10.1148/radiology.164.1.3588910.

Rivas-Garcia A, Sarria-Estrada S, Torrents-Odin C, Casas-Gomila L, Franquet E. Imaging findings of Pott's disease. Eur Spine J. 2012;22(Suppl 4):567–78.

Shah LM, Salzman KL. Imaging of spinal metastatic disease. Int J Surg Oncol. 2011;2011:769753.

Steurer J, Roner S, Gnannt R, et al. Quantitative radiologic criteria for the diagnosis of lumbar spinal stenosis: a systematic literature review. BMC Musculoskelet Disord. 2011;12(1):175–83.

Sudoł-Szopińska I, Matuszewska G, Kwiatkowska B, Pracoń G. Diagnostic imaging of psoriatic arthritis. Part I: etiopathogenesis, classifications and radiographic features. J Ultrason. 2016;16(64):65–77.

Taljanovic MS, Hunter TB, Wisneski RJ, Seeger JF. Imaging characteristics of diffuse idiopathic skeletal hyperostosis with an emphasis on acute spinal fractures: review. AJR. 2009;193:S10–9.

Index

R. S. Katz, A. Basu (eds.), *Diagnostic Radiology of the Rheumatic Diseases*,
https://doi.org/10.1007/978-3-030-25116-1